Oxidative Medicine and Cellular Longevity

Interplay between Oxidative Stress and Metabolism in Signalling and Disease 2016

Guest Editors: Eric E. Kelley, Antonio Marcus de Andrade Paes, Hariom Yadav, Celia Quijano, Adriana Cassina, and Andrés Trostchansky

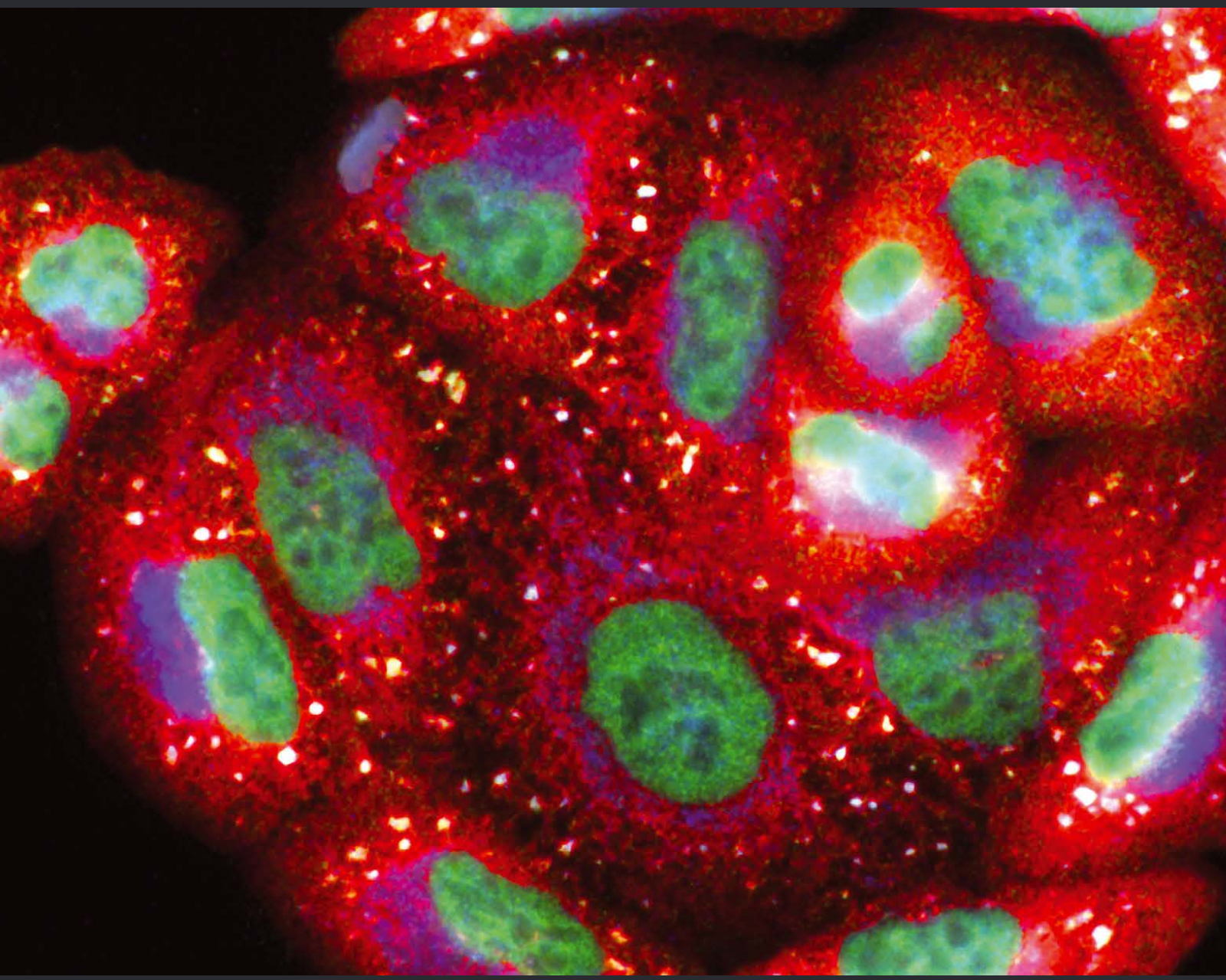

Interplay between Oxidative Stress and Metabolism in Signalling and Disease 2016

Oxidative Medicine and Cellular Longevity

Interplay between Oxidative Stress and Metabolism in Signalling and Disease 2016

Guest Editors: Eric E. Kelley,
Antonio Marcus de Andrade Paes, Hariom Yadav,
Celia Quijano, Adriana Cassina, and Andrés Trostchansky

Editorial Board

Contents

Hindawi Publishing Corporation
Oxidative Medicine and Cellular Longevity
Volume 2017, Article ID 7013972, 2 pages
http://dx.doi.org/10.1155/2017/7013972

Editorial

Interplay between Oxidative Stress and Metabolism in Signalling and Disease 2016

Eric E. Kelley,[1] Antonio Marcus de Andrade Paes,[2] Hariom Yadav,[3] Celia Quijano,[4] Adriana Cassina,[4] and Andrés Trostchansky[4]

[1]*Department of Physiology and Pharmacology, West Virginia University, Morgantown, WV, USA*
[2]*Laboratory of Experimental Physiology, Department of Physiological Sciences, Federal University of Maranhão, São Luís, MA, Brazil*
[3]*Diabetes, Endocrinology and Obesity Branch, NIDDK, NIH, Bethesda, MD, USA*
[4]*Departamento de Bioquímica and Center for Free Radical and Biomedical Research, Facultad de Medicina, Universidad de la República, Montevideo, Uruguay*

Correspondence should be addressed to Andrés Trostchansky; trocha@fmed.edu.uy

Received 5 December 2016; Accepted 6 December 2016; Published 22 January 2017

Being frequently present in insulin-sensitive tissues and the vasculature as well as critically linked to the inflammatory response, oxidative stress is a common component of metabolic dysfunction. However, despite much effort, it remains unclear to what extent oxidative stress contributes to metabolic abnormalities such as insulin resistance, steatosis/dyslipidemia, diabetes, and allied cardiovascular disease. While the identities of the specific oxidants or reactive metabolites, the sources thereof, and the associated redox-sensitive pathways that mediate the effects of oxidative stress remain elusive, progress has been made. A portion of this progress is represented in this special issue and reveals the identification of a specific source of ROS in the synaptosome and the contributory impact of thioredoxin-interacting protein (TXNIP) on inflammasome activation. These studies are complemented by comprehensive reviews of the role of mitochondria in the neuroinflammatory response and the potential participation of protein disulfide isomerase (PDI) in metabolic syndrome-induced platelet hyperactivation. Specific contributions to this special issue are summarized as follows.

E. A. Abdel-Rahman and colleagues describe the interplay between ROS-generating systems at the synapse. In freshly isolated synaptosomes, they differentiate mitochondrial-dependent consumption of molecular oxygen from that consumed through NADPH oxidase (NOX) while concomitantly defining H_2O_2 generation. While alteration of cellular redox homeostasis is implicated in pathology as well as aging, this process may be dependent upon the ratio of complete to incomplete oxygen reduction by the mitochondria in context of NADPH oxidase (NOX) enzymatic activity. Based on high-resolution respirometry coupled to fluorescence or electrochemical detection, the authors demonstrated that NOX and not the mitochondria is the dominant source of synaptic H_2O_2. As such, this study begins to more clearly elucidate the redox-related players that contribute to a variety of physiological and pathological processes in neurons.

L. Li and C. M. Stary also focused their work on mitochondria from microglia cells in the context of cerebral ischemia. Noting that microRNAs (miRs) function to regulate mitochondrial processes in astrocytes under oxidative stress, the active role for mitochondria in microglial activation, and regulation of the microglial neuroinflammatory response by miRs, the authors postulate that miR-targeted therapies represent a viable strategy for optimizing mitochondrial function and thus improve clinical outcome following cerebral ischemia. This is supported by extensive evidence of the participation of mitochondria in the glial response to injury as well as the contributory roles for miRs in regulating the glial mitochondrial response to cerebral ischemia.

H. Lee and T. Park endeavored to push beyond the associative relationship between elevated oxidant stress and metabolic syndrome by quantifying oxidative balance score (OBS) and subsequently assessing the resultant impact in the

context of genetic variation. Their study of over 6000 participants found that the highest OBS scores correlated with the lowest incidence of metabolic syndrome. Furthermore, GWAS-based pathway analysis demonstrated that the VEGF signalling pathway, glutathione metabolism, and the Rac1 pathway were contributory and thus potentially involved in the interplay between oxidant stress, genetic variation, and metabolic syndrome.

The other contributions to this special issue focused on chronic inflammation (obesity/diabetes) and the role of thiol-dependent enzymes. For example, Y. D. Xiao and colleagues describe the participation of thioredoxin-interacting protein (TXNIP) on inflammasome activation in diabetes in the context of allied ischemic acute kidney injury (AKI). The ROS sensor and endogenous inhibitor of the antioxidant thioredoxin, TXNIP, is assumed to be involved in pathogenesis of diabetes. Using a rat model of diabetes, the authors report higher expression of TXNIP in addition to an increased susceptibility to ischemia/reperfusion (I/R) injury, a process attenuated by Resveratrol. Moreover, diabetic rats subjected to renal I/R injury presented lower binding of TXNIP to NLRP3, decreasing inflammasome activation. The proposed mechanism of action, validated in cell culture experiments, is TXNIP-mediated inflammasome activation through oxidative stress and this process represents a seminal signalling mechanism driving susceptibility to AKI in diabetes.

R. S. Gaspar and collaborators comprehensively reviewed the worldwide epidemic metabolic syndrome and the contributory role for protein disulfide isomerase (PDI). Elevated rates of reactive species production are tied to enhancement of platelet hyperactivation and ischemic events in obese/metabolic patients. While PDI and peroxide tone at the platelet cell membrane have been demonstrated requisite for platelet aggregation, the relationship between PDI and platelet hyperactivation in the context of metabolic syndrome is unclear. Thus, the authors focus on the activity of PDI in metabolic syndrome in order to develop a more clear understanding of the potential participation of PDI in metabolic syndrome-induced platelet hyperactivation.

In the aggregate, this special issue enhances our understanding of the intricate interplay between metabolism and oxidative stress in metabolic diseases with particular focus on mitochondria- and inflammation-derived factors that may represent potential therapeutic targets for addressing crucial health issues.

Acknowledgments

The authors would like to thank all the reviewers that contributed during the peer-review process.

Eric E. Kelley
Antonio Marcus de Andrade Paes
Hariom Yadav
Celia Quijano
Adriana Cassina
Andrés Trostchansky

Hindawi Publishing Corporation
Oxidative Medicine and Cellular Longevity
Volume 2017, Article ID 6873197, 9 pages
http://dx.doi.org/10.1155/2017/6873197

Research Article

Pathway-Driven Approaches of Interaction between Oxidative Balance and Genetic Polymorphism on Metabolic Syndrome

Ho-Sun Lee and Taesung Park

Interdisciplinary Program in Bioinformatics and Department of Statistics, Seoul National University, Seoul 152-742, Republic of Korea

Correspondence should be addressed to Taesung Park; tspark@stats.snu.ac.kr

Received 17 August 2016; Revised 17 November 2016; Accepted 24 November 2016; Published 16 January 2017

Academic Editor: Victor M. Victor

Despite evidences of association between basic redox biology and metabolic syndrome (MetS), few studies have evaluated indices that account for multiple oxidative effectors for MetS. Oxidative balance score (OBS) has indicated the role of oxidative stress in chronic disease pathophysiology. In this study, we evaluated OBS as an oxidative balance indicator for estimating risk of MetS with 6414 study participants. OBS is a multiple exogenous factor score for development of disease; therefore, we investigated interplay between oxidative balance and genetic variation for development of MetS focusing on biological pathways by using gene-set-enrichment analysis. As a result, participants in the highest quartile of OBS were less likely to be at risk for MetS than those in the lowest quartile. In addition, persons in the highest quartile of OBS had the lowest level of inflammatory markers including C-reactive protein and WBC. With GWAS-based pathway analysis, we found that VEGF signaling pathway, glutathione metabolism, and Rac-1 pathway were significantly enriched biological pathways involved with OBS on MetS. These findings suggested that mechanism of angiogenesis, oxidative stress, and inflammation can be involved in interaction between OBS and genetic variation on risk of MetS.

1. Introduction

Oxidative stress is a complex and multifactorial process that results from an imbalance between antioxidant protection and reactive oxygen species produced by prooxidants [1]. Basic research has established a link between oxidative stress and pathogenesis of human illness, including cardiovascular disease and cancer with the process of aging [2]. Despite the solid molecular and mechanistic theory of oxidative stress and its role in chronic disease, most clinical trials and observational studies failed to provide a clear answer to the effects on chronic disease by individual prooxidant or antioxidant.

Studies of diet and health have demonstrated that combination of antioxidant factors can be more strongly associated with disease risk than any single nutrient [3]. In this way, it appears possible that a combination of oxidative stress-related factors may be more strongly associated with health outcomes than any individual exposure [4]. Therefore, several groups previously proposed an oxidative balance score (OBS) as a measure of combined pro- and antioxidant exposure status, indicating the role of oxidative stress in human chronic disease pathophysiology and found that OBS can be a comprehensive oxidative balance marker [5–7]. OBS has been shown to correlate inversely with several cancers including colorectal adenoma and prostate cancer and chronic kidney diseases [5, 8, 9]. Nevertheless, the exact mechanism of how the combination of pro- and antioxidants influences diseases is still not fully understood.

The number of individuals with metabolic syndrome (MetS) is increasing worldwide. It was reported that MetS affects 20% to 30% of the population in developed countries [10]. MetS is of substantial clinical relevance and concern because of its high prevalence and association with the development of more serious pathologies. Additional to the health issues directly associated with MetS, this condition contributes to a 5-fold increased risk of type 2 diabetes (T2D), 3-fold increased risk of cardiovascular disease, and also an increased risk of developing common cancers of liver, colorectal, bladder, and so on [10, 11]. Growing evidences suggest that the pathogenic role of oxidative stress causes cellular damage and dysfunction which are associated with

MetS and clinical complications [12]. The link between oxidative stress and MetS can be accepted because there is the association of the end-products of free radical-mediated oxidative stress with body mass index (BMI), insulin resistance, hyperlipidemia, and hypertension. In addition, a number of studies indicate that oxidative stress along with chronic inflammatory condition paves the way for the development of MetS-related manifestations, including atherosclerosis, hypertension, and T2D [13, 14]. Despite evidences of association between basic redox biology and MetS, few studies have evaluated combination of oxidative score or indices that account for multiple oxidative effectors with MetS.

It is well accepted that not only exogenous factors including diet and smoking but also endogenous factors like genetic variation contribute to the development of MetS. Genome-wide association studies (GWAS) have identified important susceptible loci [15] that are significantly associated with the risk of MetS. Nevertheless, these findings explain only a small portion of the heritability and clear association of genetic factors with causative effects on MetS requires further elucidation.

Genetic variation also modulates reactive oxidative stress, which may influence several diseases through their interaction with OBS components [16]. Slattery et al. pointed the importance of interaction between OBS and endogenous factors for risk of diseases [16, 17]. For better understanding of the comprehensive mechanism of oxidative balance for the risk of MetS, it has to consider interaction effect between OBS and genetic variation for development of diseases. The identification of genes-environment interaction related to oxidative stress has been studied for cardiovascular disease, atherosclerosis, diabetes, and so on [18, 19]. However, these studies focused on only a few SNPs or selective SNPs with environment factors and considered each of the identified SNPs independently; therefore, it was hard to explain comprehensive action of multiple genes or biological processes in complex diseases. As an alternative to GWAS-driven approaches to detect interaction effect, pathway approach may help identify potential biological pathways that might be missed by the standard GWAS approach [20, 21].

The purpose of this study is to investigate the relationship between OBS and risk of MetS. First, we used OBS as an oxidative balance indicator for estimating risk of MetS. OBS is multiple exogenous factor score for development of disease; therefore, we investigated interplay between oxidative balance and genetic variation for development of MetS. We focused on biological pathways by using gene-set-enrichment analysis (GSEA) for investigating how OBS affects development of MetS with genetic factors.

2. Material and Methods

2.1. Study Participants. This study was based on the Korea Association Resource (KARE) data included in the Korean Genome Epidemiology Study (KoGES). The details of the study design and procedures used in the KoGES have been described previously [22]. The population based cohort study included 10,030, aged ≥40 years, at baseline from 2001 to 2002. This present analysis used cross-sectional data from 2007 to 2008, the samples were scrutinized for quality control purposes, and 6,688 participants were remained. Study participants completed a questionnaire on sociodemographic status, lifestyle, and disease history. Participants completed self-administered lifestyle and food frequency questionnaires (FFQ), which assessed nutrient intake over the past year of 166 food items. Anthropometrics and biochemical measurements were also described by the previous study [22]. We excluded 261 participants with missing data on at least one MetS component and 115 participants with missing data on at least one OBS component. We also excluded 79 participants with missing data for key covariates such as geographic area, age, and sex. Therefore, we used data for 6414 study participants for final analyses. Written informed consent was obtained from all participants at the KoGES and this research project was approved by the Institutional Review Board of Korea National Institute of Health.

2.2. Definition of Metabolic Syndrome and Related Disorders. MetS is characterized by the clustering of several components including abdominal obesity, hypertension, dyslipidemia, insulin resistance, and glucose intolerance that are important precursor of cardiovascular disease and type 2 diabetes. MetS was defined by the presence of three or more of the following five components according to the NCEP-ATP III criteria [23], except for the determination of central obesity. Waist circumference cut-off value was used based on the report by the Korean Society for the Study of Obesity [24]: (1) central obesity given as waist high circumference (≥90 cm for men and ≥85 cm for women), (2) high concentration for serum triglycerols (≥150 mg/dL), (3) low concentrations of serum HDL cholesterol (<40 mg/dL for men and <50 mg/dL for women), (4) hypertension (systolic/diastolic pressure ≥ 130/85 mmHg) or antihypertensive medication, and (5) high concentrations of fasting glucose (≥100 mg/dL) or antidiabetic medication.

Diabetes was diagnosed in subjects who had any one of the following: (1) fasting plasma glucose ≥ 126 mg/dL; (2) postprandial 2 h plasma glucose ≥ 200 mg/dL after a 75 g OGTT; and (3) HbA1c ≥ 6.5% [25]. Subjects who were using insulin or oral antidiabetic drugs at baseline were also defined as having diabetes.

2.3. OBS and OBS Weighting. The OBS was calculated by combining information from a total of 7 a priori selected pro- and antioxidant factors, including three prooxidant (smoking, alcohol consumption, and total iron intake) and four antioxidant exposures (β-carotene, vitamins C, retinol, and physical activity). The continuous variables reflecting prooxidant and antioxidant exposures divided into low, medium, and high categories based on each exposure's tertile values and points (0 to 2) were given according to tertile categorization. Prooxidants were scored in the opposed way to the antioxidants. A higher score represents a predominance of antioxidant exposures over prooxidant exposures. In our study, OBS is the sum of tertile (Q1 = 0; Q2 = 1; Q3 = 2) of intake of vitamin C, retinol and carotene, and physical activity (0–72.7 MET/day = 0; 72.8–92.4 MET/day = 1; 92.5

Table 1: Baseline characteristics of this study by OBS quantile[a].

Characteristics	Q1 (n = 2069)	Q2 (n = 1169)	Q3 (n = 2195)	Q4 (n = 910)	p trend[c]
Age (years)[a]	57.26 ± 9.00	56.62 ± 8.84	55.24 ± 8.60	54.30 ± 8.27	<0.001
Sex					<0.001
Male	1432 (69)	569 (49)	817 (37)	199 (22)	
Female	637 (31)	600 (51)	1378 (63)	711 (78)	
Region					<0.001
Rural (Ansung)	1194 (58)	618 (53)	989 (45)	419 (46)	
Urban (Ansan)	875 (42)	551 (47)	1206 (55)	491 (54)	
BMI	24.30 ± 3.12	24.58 ± 3.12	24.67 ± 2.92	24.65 ± 3.05	0.105
Education (years)					<0.001
Elementary school or less	261 (14)	300 (12)	98 (9)	88 (9)	
Middle school graduate	814 (44)	1122 (46)	475 (44)	420 (44)	
High school or higher	770 (42)	1036 (42)	503 (47)	440 (47)	
Monthly income[b]					<0.001
<1000	724 (40)	876 (36)	318 (30)	259 (27)	
1000–2000	422 (23)	550 (23)	238 (22)	200 (21)	
≥2000	682 (37)	450 (41)	516 (48)	486 (52)	
Total energy intake[d] (kcal/day)	1621.12 ± 471.95	1678.42 ± 519.85	1831.86 ± 589.55	2019.24 ± 848.68	<0.001

[a]Equal weight method; [b]US dollar in 2014; [c]p for linear trend was determined by the general linear model for continuous variables and by χ^2 test for categorical variables. [d]Total energy intake was calculated using food frequency questionnaires.

≥ MET/day = 2; MET, metabolic equivalent) with antioxidant components. OBS included smoking status (never = 2, former = 1, and current = 0) and alcohol consumption (nonregular drinker, 0–5 g/day = 0; regular drinker, 5 ≥ g/day = 2). Evaluations of individual OBS component according to quartile of OBS-equal weight (equal weighting of the selected components and a simple summation) were presented in Table 1.

Depending on contribution of OBS components on oxidative balance, we scored OBS with 2 additional weighting methods besides equal weighting method. For beta coefficient weighting, the coefficient estimates for each of the components obtained from the regression model were used to calculate weights for OBS-beta coefficient. Coefficients were multiplied by −1 so that components inversely associated with metabolic disease risk had positive weight and vice versa. Principal component analysis (PCA) was a weight method using variation reduction [26]. The number of PCs to retain was determined by using the diagram of eigenvalues and the interpretability of the PCs. The PC score for each pattern was constructed by summing up and observed OBS components weighted by the PC loading. For weighting of OBS, each model was adjusted for age, sex, geographic area, and BMI.

2.4. Genotyping. The KARE dataset consists of the individual SNP chip genotypes and the epidemiological/clinical phenotypes for studying the genetic components of Korean public health. DNA samples were isolated from the peripheral blood of all participants and were genotyped with Affymetrix Genome Wide Human SNP array 5.0 (Affymetrix Inc, Rockville, MD, USA). The obtained KARE dataset passed the quality control criteria and was reported in previous GWAS reports [27]. After sample and genotype quality controls, 344,396 SNPs for 6,414 individuals were available in the KARE data.

2.5. Pathway-Based Analysis. It has now been recognized that a majority of biological behaviors are manifested from a complex interaction of biological pathway. Pathway-based approaches using GWAS data are now used routinely to study complex disease like MetS [28, 29]. To analyse pathway involved in OBS and genome-wide interaction, we used the improved i-GSEA that estimates the pathway-level interactions between genetic variants and OBS.

In our study, 344,396 SNPs were mapped to genes with 100 kb boundaries and pathways with <20 genes or >200 genes were excluded from further analysis to reduce the multiple-testing issue and to avoid testing overly narrow or broad functional categories [30]. A false-discovery rate (FDR) was used for multiple-testing correction with <0.05 considered to be significant. Improved GSEA uses a comprehensive pathway/gene set database from SNP data with pathways integrated and curated from a variety of resources, including KEGG (Kyoto Encyclopedia of Genes and Genomes pathway database), Biocarta, and GO (gene ontology) database [31].

2.6. Statistical Analysis. OBS components except for physical activity were not normally distributed, so they were log-transformed when assigning OBS. Tests for linear trend were performed using a sum of scores with values from Q1 to Q4, consistent with the quartile grouping. Each OBS weighting method was divided into quartiles, with the lowest quartile (predominance of prooxidants) used as reference. Even though obesity is a main factor of oxidative stress, BMI is a strong risk factor for MetS; therefore, we remove it

from OBS components but controlled for it in the statistical models.

Logistic regression analyses were used to examine the relationship between OBS and incidence of MetS adjusting for age, geographic area, sex, and BMI. For comparing the effect of different weighting methods, receiver operating characteristics (ROC) curves and the respective areas under the curves (AUCs) were calculated.

For investigating relationship between OBS and inflammation, we examined the association of OBS with CRP (C-reactive protein) and WBC (white blood cell count). CRP was not normally distributed, and so it was log transformed. The results of the linear regression models were expressed as regression coefficients and their corresponding 95% confidence intervals adjusted for same potential confounding factors as the previous ones.

For elucidating biological process through interaction of gene and oxidative stress by pathway analysis, we used to test gene-environment interaction by performing a 1df test of H_0: $ß_{gobs} = 0$ (The context of the linear model: $\log[p/(1-p)] = ß_0 + ß_{age}\text{Age} + ß_{sex}\text{Sex} + ß_{area}\text{Area} + ß_{obs}\text{OBS} + ß_{bmi}\text{BMI} + ß_g G + ß_{gobs} G * \text{OBS}$). Due to the biological contributions to oxidative balance, we used OBS by beta coefficient weight. The interaction term was used to assess the significance of the interaction between genetic variants and OBS. The critical p values for accessing the significance of interaction were calculated by FDR q-value, at the 5% level. All statistical analyses were performed using R Statistical Software (version 2.14.0; R Foundation for Statistical Computing, Vienna, Austria).

3. Results

3.1. Baseline Characteristics. A total of 6414 participants (mean age, 56.07 years, SD, 8.29 years) were included in this study. The distribution of characteristics according to quartile of OBS-equal weight is shown in Table 2. Compared to those in the lowest OBS quartile, participants in the highest quartile were likely to be younger and more educated and had more female. Participants in the highest OBS quartile were also tended to have a higher income and reside in rural area and higher total energy intakes than those in the lowest quartile. There was no significant difference in BMI across OBS intervals.

3.2. OBS Components and Their Assessment with Metabolic Syndrome. As expected, intake of antioxidants including vitamin C, carotene, and retinol was higher among participants with higher OBS values (data not shown). Contrary to expectation, intakes of iron were higher in the upper OBS quartile group. Participants in the higher OBS quartiles were also more likely to never be smokers, nonregular drinkers, and higher physical activity (data not shown). Individual component level of OBS between non-MetS and MetS was provided in Table 3. In non-MetS patients, levels of dietary components were higher in the highest quartile of OBS. We found that higher consumption of alcohol in a day was observed in non-MetS patients although alcohol is a prooxidant component.

Table 2: Oxidative balance score assignment scheme.

OBS components	Score assignment scheme[a]
Iron	0 = high (3rd tertile), 1 = medium (2nd tertile), and 2 = low (1st tertile)
Vitamin C	0 = low (1st tertile), 1 = medium (2nd tertile), and 2 = high (3rd tertile)
Retinol	0 = low (1st tertile), 1 = medium (2nd tertile), and 2 = high (3rd tertile)
Carotene	0 = low (1st tertile), 1 = medium (2nd tertile), and 2 = high (3rd tertile)
Physical activity (Phy-MET)	0 = low (1st tertile), 1 = medium (2nd tertile), and 2 = high (3rd tertile)
Smoking	0 = current smoker, 1 = former smoker, and 2 = never smoker
Alcohol	0 = heavy drinker (≥50 g/day), 2 = nonheavy drinker (<50 g/day)

[a]Low, medium, and high categories corresponding to baseline tertile values among participants in the KARE cohort.

Table 3: Individual component level of OBS between non-MetS and MetS groups.

Characteristics	Non-MetS (n = 4838)	MetS (n = 1576)
Nutrients		
Iron, mg/day	9.74 ± 5.31	9.11 ± 4.54
Vitamin C, mg/day	103.04 ± 66.79	94.40 ± 59.82
Retinol, μg/day	62.47 ± 62.16	50.98 ± 53.46
Carotene, μg/day	2429.53 ± 2026.43	2412.37 ± 2030.09
Alcohol consumption, g/day	9.70 ± 22.68	9.26 ± 24.72
Nonregular drinker	4575	1470
Regular drinker[a]	248	101
Smoking status, n (%)		
Never	2944	1052
Former	977	238
Current	911	285
Physical activity, MET/day	82.46 ± 21.11	81.44 ± 21.36

[a]≥50 g/day of alcohol drinking; MET, metabolic equivalent.

We firstly confirmed that there is no association between each OBS component and MetS (data not shown). For categorical analyses, participants in the highest quartile of all three OBS by weighting methods were less likely to be at risk for MetS than those in the lowest quartile, with statistical significance (Table 4). We observed approximately 40% lower risk of MetS at the highest quantile of OBS compared to reference quantile (lowest quantile) among study participants by beta coefficient adjusted by area, sex, age, and BMI. For OBS-equal weight and OBS-PCA weight, there was around 28–32% reduction in risk of MetS. We used ROC curve for comparing each weighting method for MetS and found there was no difference of AUCs by different weighting

Table 4: Association of the OBS with metabolic syndrome by weighing method[a].

OBS	Number of cases (control)	OR (95% CI)	p	p trend
OBS-equal weight (AUC = 0.823)				
Quantile 1	547 (1522)	1		
Quantile 2	314 (855)	0.94 (0.78–1.15)	0.56	
Quantile 3	510 (1685)	0.81 (0.68–0.97)	0.02	<0.01
Quantile 4	186 (724)	0.65 (0.51–0.82)	<0.01	
OBS-equal weight[b] (AUC = 0.823)				
Quantile 1	353 (1351)	1		
Quantile 2	205 (774)	0.91 (0.72–1.14)	0.40	
Quantile 3	328 (1513)	0.79 (0.64–0.97)	0.02	<0.01
Quantile 4	118 (644)	0.60 (0.45–0.81)	<0.01	
OBS-beta coefficient (AUC = 0.824)				
Quantile 1	378 (1204)	1		
Quantile 2	397 (1161)	0.65 (0.52–0.81)	<0.01	
Quantile 3	431 (1209)	0.67 (0.49–0.90)	<0.01	<0.01
Quantile 4	355 (1212)	0.56 (0.76–0.41)	<0.01	
OBS-beta coefficient[b] (AUC = 0.829)				
Quantile 1	239 (1089)	1		
Quantile 2	272 (1047)	0.66 (0.50–0.87)	<0.01	
Quantile 3	376 (1050)	0.66 (0.47–0.91)	0.01	<0.01
Quantile 4	218 (1107)	0.56 (0.38–0.82)	<0.01	
OBS-PCA (AUC = 0.824)				
Quantile 1	375 (1203)	1 (reference)		
Quantile 2	389 (1174)	0.64 (0.51–0.79)	<0.01	
Quantile 3	419 (1189)	0.68 (0.50–0.92)	0.01	<0.01
Quantile 4	372 (1216)	0.55 (0.40–0.75)	<0.01	
OBS-PCA[b] (AUC = 0.828)				
Quantile 1	233 (1087)	1		
Quantile 2	251 (1068)	0.71 (0.55–0.92)	<0.01	
Quantile 3	292 (1037)	0.66 (0.46–0.96)	0.03	<0.01
Quantile 4	228 (1098)	0.62 (0.43–0.91)	0.01	

[a]Adjusting for age, sex, area, and BMI. [b]Excluded patients with type 2 diabetes; $n = 5363$.

methods: OBS-equal weight, beta coefficient weight, and PCA weight (AUC 0.823, 0.824, and 0.824, respectively). We also investigated association between OBS and the odds ratio of MetS without T2D patients. As a result, there is positive association between OBS and MetS regardless of T2D statues.

3.3. Association of the OBS and Metabolic Related Factors. Table 5 showed the association between OBS and metabolic related factors. Among components of MetS, ratio of hypertriglyceridemia and low HDL cholesterol had inverse correlation with OBS (p trend < 0.01). Persons in the highest quantile of OBS had the lowest level of MetS score, CRP, and WBC.

Oxidative stress and inflammation have been associated with MetS and oxidative stress can increase inflammation and vice versa. Confirming the role of OBS as oxidative stress indicator, we tested association of OBS with inflammatory markers. The CRP and WBC in blood serve as inflammatory markers although these markers have nonspecific features [32]. The regression beta coefficients indicate that OBS was negatively associated with CRP and WBC (Table 6). Compared to the reference group (using the lowest interval as reference), the highest group was negatively correlated with CRP, and all three groups were negatively correlated with WBC.

3.4. Pathway Interacted with OBS and Genotype for Metabolic Syndrome. With 352,228 SNPs having p values for interaction term in the logistic regression model, we first obtained the significance of the interaction between genetic variants and OBS at SNP level. Then, we tested pathway-based interaction between OBS and genetic variation with p values of SNPs for enriched biological processes in MetS.

To conduct the biological pathway analysis, we used all SNPs that were used in GWAS analysis. As shown in Table 7,

Table 5: Associations of the OBS with metabolic related disorders by OBS quantile.

Characteristics	Q1 (n = 2069)	Q2 (n = 1169)	Q3 (n = 2195)	Q4 (n = 910)	p trend
Metabolic syndrome, n (%)	547 (26)	314 (27)	510 (23)	186 (20)	<0.001
Metabolic components, n (%)					
Abdominal obesity	686 (30)	416 (36)	753 (34)	305 (34)	0.071
Hypertriglyceridemia	748 (36)	382 (33)	631 (29)	235 (26)	<0.001
Low HDL cholesterol	1087 (53)	667 (57)	1294 (59)	539 (59)	0.005
High blood pressure	486 (24)	287 (25)	432 (20)	161 (18)	0.267
High fasting glucose	465 (23)	244 (21)	392 (18)	131 (14)	0.163
MetS score	1.68 ± 1.30	1.71 ± 1.28	1.60 ± 1.25	1.51 ± 1.25	<0.001
CRP (mg/dL)	1.66 ± 3.19	1.49 ± 2.69	1.55 ± 3.93	1.35 ± 3.18	0.013
WBC ($10^3/\mu$L)	6.70 ± 2.04	6.35 ± 1.79	6.20 ± 1.82	5.97 ± 1.71	<0.001

CRP, C-reactive protein; WBC; white blood cell count; p trend was assessed by χ^2 test or general linear regression for linear trend.

Table 6: Association of the OBS with inflammatory markers[a].

OBS	Beta coefficient	95% CI	p	p trend	Beta coefficient	95% CI	p	p trend
	CRP (mg/dL)				WBC ($10^3/\mu$L)			
Quantile 1	0	(Reference)			0	(Reference)		
Quantile 2	−0.22	−0.30 to −0.14	<0.01		−0.77	−0.92 to −0.63	<0.01	
Quantile 3	−0.12	−0.23 to −0.01	0.04	<0.01	−0.82	−1.02 to −0.61	<0.01	<0.01
Quantile 4	−0.28	−0.40 to −0.17	<0.01		−0.98	−1.19 to −0.77	<0.01	

[a]Adjusting for age, sex, geographic area, and BMI.

we found that three canonical pathways (2 were from 190 KEGG pathways and 1 was from 260 Biocarta pathways) were significantly enriched with FDR < 0.05 for MetS, and other 2 pathways were possibly associated with MetS, with FDR < 0.10. The most significant pathway was VEGF signaling pathway (nominal $p < 0.001$, FDR = 0.020). Other significant pathways were glutathione metabolism (nominal $p < 0.001$, FDR = 0.022) and Rac-1 pathway (nominal $p < 0.001$, FDR = 0.045). These findings suggested that pathways of angiogenesis, oxidative stress, and inflammation can be involved in interaction with OBS on MetS risk.

4. Discussion

In this study, we examined the possibility of OBS as a predictor of MetS risk and found that higher OBS, which indicates predominance of antioxidant exposures, was associated with significant reduction of the risk of MetS. Considering different contribution of each component on risk of MetS, we used different weighting scheme for combination of pro- and antioxidant exposure into a single score. Dash et al. mentioned that combination of antioxidants and prooxidants into a single score may be more powerful measurement of oxidative stress than approaches that use a single antioxidant or prooxidant [33]. Several studies using OBS also concerned about using an equal weighting method for scoring of oxidative stress. We found that associations between OBS and the risk of MetS were not different depending on OBS weight methods.

CRP and WBC are inflammation markers which have been shown in multiple prospective epidemiological studies to predict the risk of cardiovascular disease and MetS [34]. We found that OBS was inversely associated with inflammatory markers of CRP and WBC, suggesting a role of OBS in the pathogenesis of MetS. High-sensitivity CRP, a marker of low-grade systemic inflammation, is reported as an independent risk factor of diabetes and cardiovascular disease [35]. WBC is also a routinely measured marker of systemic inflammation and is reported to be a risk factor of cardiovascular disease and MetS [36, 37]. Oxidative stress and inflammation are closely related pathophysiological processes, one of which can be easily induced by another. Kong et al. recently reported that OBS was inversely correlated with plasma concentrations of F2-IsoPs, an oxidative stress marker, and CRP levels in persons with colorectal adenoma [9]. We did not compare OBS with any oxidative stress markers that influenced directly oxidative cellular damages, but, we confirmed that OBS is closely associated with inflammation.

Pathway analysis on MetS focuses on the combined effects of multiple SNPs within a gene and multiple genes within a pathway that are grouped according to their shared biological function. Current GWAS-derived pathway analysis can provide insights into mechanism of disease and biological pathways considering interaction between genes and environment factors [38, 39]. We identified that oxidative balance was significantly associated with the risk of MetS in this study. Oxidative balance may interact with polygenic factors in complicated ways to influence MetS susceptibility. For precise biological mechanism of oxidative balance for the

Table 7: Pathway-based analysis for interaction between OBS and genetic variation for metabolic syndrome.

Resources	Biological process	Description	p value	FDR	Significant genes/selected genes/all genes
KEGG Hsa04370	VEGF signaling pathway	Genes involved in VEGF signaling pathway.	<0.001	0.020	25/54/70
KEGG Hsa00480	Glutathione metabolism	Genes involved in glutathione metabolism	<0.001	0.022	12/26/39
Biocarta	Rac-1 pathway	Rac-1 is a Rho family G protein that stimulates formation of actin-dependent structures	<0.001	0.045	14/20/22
Biocarta	Rho pathway	Rac-1 is a Rho family G protein that stimulates formation of actin-dependent structures such as filopodia and lamellipodia	0.001	0.062	14/25/31
Biocarta	TNFR1 pathway	Tumor necrosis factor alpha binds to its receptor TNFR1 and induces caspase-dependent apoptosis	0.005	0.085	13/23/29

risk of MetS, we considered the interaction between endogenous factor and OBS which suggested the comprehensive biological pathways which might modify the risk of MetS. Of the 15,576 genes mapped, 3 pathways had enrichment scores better than FDR < 0.05 (Table 7): VEGF pathway, glutathione metabolism, and Rac-1 pathway which are involved in oxidative stress, angiogenesis, or inflammation [2, 40, 41].

VEGF (vascular endothelial growth factor) and its receptor, VEGFR, have been shown to play major roles not only in physiological but also in most pathological angiogenesis. Angiogenesis requires initiation by proangiogenic factors, such as VEGF, and mediated the Rho GTPases Rac-1. In addition angiogenesis via VEGF involves the main mechanism of oxidative stress [42]. VEGF also plays a pivotal role in diabetes that mediates the hyperglycemia-induced pathological effect by oxidative stress [43], which activates VEGF and IGF-1 signaling pathways via protein kinase C (PKC) and interrelated each other. VEGF is secreted by human fat cells and other tissues are stimulated by hypoxia, as well as several hormones and growth factors like insulin, IGF-1, estrogen leptin, and so on [44].

Glutathione (GSH)/glutathione disulfide is the major redox couple in animal cells and effectively scavenges free radicals and other reactive oxidative species directly and indirectly through enzymatic reactions. GHS has critical role in regulating lipid, glucose, and amino acid utilization [45]. The reduction in tissue levels of glutathione, a cellular antioxidant, increased oxidative stress markers and impaired glucose homeostasis. Increased numbers of lipid peroxidation markers have been observed in the liver of animal models of diabetes and obesity, but GSH reductase activates antioxidant defense mechanism and decreases lipid peroxidation markers [46].

Rac-1, small GTP binding protein, plays many important biological functions in cells adhesion, migration, and inflammation. Rac-1 is a mediator of VEGF signaling pathway that involves permeability and cell migration. Rac-1 is associated with adiponectin and has a direct connection with hyperglycemia and ß-cell apoptosis [47]. In addition, Rac-1 and NADPH have been reported to be a key regulator of oxidative stress through its coregulatory effects on nitric oxide synthase and NADPH oxidase [48]. In addition, Rac-1/NADPH oxidase-derived oxidative stress is involved in the pathogenesis of MetS [48] and participates in the production of cardiac hypertrophy [49]. Besides, three pathways related to OBS in our study were also involved in inflammation [2, 41], supported by our result that OBS was inversely associated with CRP and WBC. OBS may interact with gene and modify the risk of MetS via several biological pathways.

Several studies using OBS mentioned their limitations for lacking of endogenous factors that modify oxidative stress [7, 9, 33, 50]. One of the limitations of our study is that we did not consider oxidative stress induced by endogenous factors such as mitochondrial function and antioxidant enzymes or insulin signaling on MetS. However, some papers found that OBS was associated with oxidative stress biomarkers (F2-isoprostane, fluorescent oxidation products, and so on) and was predictor for incident, sporadic colorectal adenoma [9, 33]. None of the adjusted associations between hypertension and oxidative stress markers (including mitochondrial DNA copy number) were statistically significant except OBS [6]. Labadie et al. reported that *SOD2*, *CAT*, and *GSTP1* did not modify OBS even though OBS was associated risk of disease [51]. Impaired insulin signaling could be central to the development of the MetS and can promote cardiovascular diseases through abnormal lipid metabolism. Even though we did not check insulin signaling with OBS for MetS, we checked HOMA level without T2D patients and we found that HOMA level was significantly decreased by OBS levels (beta = −0.87, $p < 0.01$, data not shown). We also considered the biological process with genetic factor and oxidative stress level of OBS on MetS. Another limitation of this study is that OBS components are based on self-report data to assess dietary pro- and antioxidant exposure. FFQ is the

most practical and common assessment in cohort studies. Although a 24 h diet recall survey has been conducted in this study [22], recall bias and error still remained.

5. Conclusion

In summary, we identified that individuals with high OBS may have lower risk of MetS. In addition, we showed interactions between genetic polymorphism and OBS through several signaling pathways. Such information would provide scientific knowledge of comprehensive biological contribution by complex exposures to pro- and antioxidants. Further research is needed to understand that modification of oxidative balance could be preventive strategy for the development of MetS.

Competing Interests

The authors declare that they have no competing interests.

Acknowledgments

This work was supported by the Bio-Synergy Research Project of the Ministry of Science, ICT and Future Planning through the National Research Foundation (2013M3A9C4078158).

References

[1] B. Poljsak, D. Šuput, and I. Milisav, "Achieving the balance between ROS and antioxidants: when to use the synthetic antioxidants," *Oxidative Medicine and Cellular Longevity*, vol. 2013, Article ID 956792, 11 pages, 2013.

[2] S. Reuter, S. C. Gupta, M. M. Chaturvedi, and B. B. Aggarwal, "Oxidative stress, inflammation, and cancer: how are they linked?" *Free Radical Biology and Medicine*, vol. 49, no. 11, pp. 1603–1616, 2010.

[3] D. Fusco, G. Colloca, M. R. Lo Monaco, and M. Cesari, "Effects of antioxidant supplementation on the aging process," *Clinical interventions in aging*, vol. 2, no. 3, pp. 377–387, 2007.

[4] M. Gao, Z. Zhao, P. Lv et al., "Quantitative combination of natural anti-oxidants prevents metabolic syndrome by reducing oxidative stress," *Redox Biology*, vol. 6, pp. 206–217, 2015.

[5] S. Lakkur, M. Goodman, R. M. Bostick et al., "Oxidative balance score and risk for incident prostate cancer in a prospective U.S. cohort study," *Annals of Epidemiology*, vol. 24, no. 6, pp. 475–478, 2014.

[6] F. B. Annor, M. Goodman, I. S. Okosun et al., "Oxidative stress, oxidative balance score, and hypertension among a racially diverse population," *Journal of the American Society of Hypertension*, vol. 9, no. 8, pp. 592–599, 2015.

[7] S. Lakkur, S. Judd, R. M. Bostick et al., "Oxidative stress, inflammation, and markers of cardiovascular health," *Atherosclerosis*, vol. 243, no. 1, pp. 38–43, 2015.

[8] T. O. Ilori, Y. Sun Ro, S. Y. Kong et al., "Oxidative balance score and chronic kidney disease," *American Journal of Nephrology*, vol. 42, no. 4, pp. 320–327, 2015.

[9] S. Y. J. Kong, R. M. Bostick, W. D. Flanders et al., "Oxidative balance score, colorectal adenoma, and markers of oxidative stress and inflammation," *Cancer Epidemiology Biomarkers and Prevention*, vol. 23, no. 3, pp. 545–554, 2014.

[10] J. Kaur, "A comprehensive review on metabolic syndrome," *Cardiology Research and Practice*, vol. 2014, Article ID 943162, 21 pages, 2014.

[11] K. Esposito, P. Chiodini, A. Colao, A. Lenzi, and D. Giugliano, "Metabolic syndrome and risk of cancer: a systematic review and meta-analysis," *Diabetes Care*, vol. 35, no. 11, pp. 2402–2411, 2012.

[12] E. M. Yubero-Serrano, J. Delgado-Lista, P. Peña-Orihuela et al., "Oxidative stress is associated with the number of components of metabolic syndrome: LIPGENE study," *Experimental and Molecular Medicine*, vol. 45, no. 6, article e28, 2013.

[13] F. Armutcu, M. Ataymen, H. Atmaca, and A. Gurel, "Oxidative stress markers, C-reactive protein and heat shock protein 70 levels in subjects with metabolic syndrome," *Clinical Chemistry and Laboratory Medicine*, vol. 46, no. 6, pp. 785–790, 2008.

[14] J. C. Fernández-García, F. Cardona, and F. J. Tinahones, "Inflammation, oxidative stress and metabolic syndrome: dietary modulation," *Current Vascular Pharmacology*, vol. 11, no. 6, pp. 906–919, 2013.

[15] T. Fall and E. Ingelsson, "Genome-wide association studies of obesity and metabolic syndrome," *Molecular and Cellular Endocrinology*, vol. 382, no. 1, pp. 740–757, 2014.

[16] M. L. Slattery, A. Lundgreen, B. Welbourn, R. K. Wolff, and C. Corcoran, "Oxidative balance and colon and rectal cancer: interaction of lifestyle factors and genes," *Mutation Research—Fundamental and Molecular Mechanisms of Mutagenesis*, vol. 734, no. 1-2, pp. 30–40, 2012.

[17] M. L. Slattery, E. M. John, G. Torres-Mejia et al., "Angiogenesis genes, dietary oxidative balance and breast cancer risk and progression: the breast cancer health disparities study," *International Journal of Cancer*, vol. 134, no. 3, pp. 629–644, 2014.

[18] J. W. Stephens, S. C. Bain, and S. E. Humphries, "Gene-environment interaction and oxidative stress in cardiovascular disease," *Atherosclerosis*, vol. 200, no. 2, pp. 229–238, 2008.

[19] M. G. Andreassi, "Metabolic syndrome, diabetes and atherosclerosis: influence of gene-environment interaction," *Mutation Research/Fundamental and Molecular Mechanisms of Mutagenesis*, vol. 667, no. 1-2, pp. 35–43, 2009.

[20] D. Thomas, "Methods for investigating gene-environment interactions in candidate pathway and genome-wide association studies," *Annual Review of Public Health*, vol. 31, pp. 21–36, 2010.

[21] D. J. Hunter, "Gene-environment interactions in human diseases," *Nature Reviews Genetics*, vol. 6, no. 4, pp. 287–298, 2005.

[22] N. H. Cho, K. M. Kim, and S. H. Choi, "High blood pressure and its association with incident diabetes over 10 years in the Korean Genome and Epidemiology Study (KoGES)," *Diabetes Care*, vol. 38, no. 7, pp. 1333–1338, 2015.

[23] Y. Ahn, S.-J. Park, H.-K. Kwack, M. K. Kim, K.-P. Ko, and S. S. Kim, "Rice-eating pattern and the risk of metabolic syndrome especially waist circumference in Korean Genome and Epidemiology Study (KoGES)," *BMC Public Health*, vol. 13, article 61, 2013.

[24] J. C. Bae, N. H. Cho, S. Suh et al., "Cardiovascular disease incidence, mortality and case fatality related to diabetes and metabolic syndrome: a community-based prospective study (Ansung-Ansan cohort 2001–12)," *Journal of Diabetes*, vol. 7, no. 6, pp. 791–799, 2015.

[25] American Diabetes Association, "2. Classification and diagnosis of diabetes," *Diabetes Care*, vol. 39, supplement 1, pp. S13–S22, 2016.

[26] A. D. A. C. Smith, P. M. Emmett, P. K. Newby, and K. Northstone, "Dietary patterns obtained through principal components analysis: the effect of input variable quantification," *British Journal of Nutrition*, vol. 109, no. 10, pp. 1881–1891, 2013.

[27] Y. S. Cho, M. J. Go, Y. J. Kim et al., "A large-scale genome-wide association study of Asian populations uncovers genetic factors influencing eight quantitative traits," *Nature Genetics*, vol. 41, no. 5, pp. 527–534, 2009.

[28] A. Torkamani, E. J. Topol, and N. J. Schork, "Pathway analysis of seven common diseases assessed by genome-wide association," *Genomics*, vol. 92, no. 5, pp. 265–272, 2008.

[29] K. Wang, M. Li, and H. Hakonarson, "Analysing biological pathways in genome-wide association studies," *Nature Reviews Genetics*, vol. 11, no. 12, pp. 843–854, 2010.

[30] K. Wang, M. Li, and M. Bucan, "Pathway-based approaches for analysis of genomewide association studies," *The American Journal of Human Genetics*, vol. 81, no. 6, pp. 1278–1283, 2007.

[31] K. Zhang, S. Chang, L. Guo, and J. Wang, "I-GSEA4GWAS v2: a web server for functional analysis of SNPs in trait-associated pathways identified from genome-wide association study," *Protein and Cell*, vol. 6, no. 3, pp. 221–224, 2015.

[32] K. Kotani and N. Sakane, "White blood cells, neutrophils, and reactive oxygen metabolites among asymptomatic subjects," *International Journal of Preventive Medicine*, vol. 3, no. 6, pp. 428–431, 2012.

[33] C. Dash, R. M. Bostick, M. Goodman et al., "Oxidative balance scores and risk of incident colorectal cancer in a US prospective cohort study," *American Journal of Epidemiology*, vol. 181, no. 8, pp. 584–594, 2015.

[34] T. A. Pearson, G. A. Mensah, R. W. Alexander et al., "Markers of inflammation and cardiovascular disease: application to clinical and public health practice: a statement for healthcare professionals from the centers for disease control and prevention and the American Heart Association," *Circulation*, vol. 107, no. 3, pp. 499–511, 2003.

[35] S. K. Singh, M. V. Suresh, B. Voleti, and A. Agrawal, "The connection between C-reactive protein and atherosclerosis," *Annals of Medicine*, vol. 40, no. 2, pp. 110–120, 2008.

[36] C. D. Lee, A. R. Folsom, F. J. Nieto, L. E. Chambless, E. Shahar, and D. A. Wolfe, "White blood cell count and incidence of coronary heart disease and ischemic stroke and mortality from cardiovascular disease in African-American and White men and women: Atherosclerosis Risk in Communities Study," *American Journal of Epidemiology*, vol. 154, no. 8, pp. 758–764, 2001.

[37] C. Pei, J.-B. Chang, C.-H. Hsieh et al., "Using white blood cell counts to predict metabolic syndrome in the elderly: a combined cross-sectional and longitudinal study," *European Journal of Internal Medicine*, vol. 26, no. 5, pp. 324–329, 2015.

[38] L. L. Marchand and L. R. Wilkens, "Design considerations for genomic association studies: importance of gene-environment interactions," *Cancer Epidemiology Biomarkers and Prevention*, vol. 17, no. 2, pp. 263–267, 2008.

[39] D. C. Thomas, "The need for a systematic approach to complex pathways in molecular epidemiology," *Cancer Epidemiology Biomarkers and Prevention*, vol. 14, no. 3, pp. 557–559, 2005.

[40] R. Hwaiz, Z. Hasan, M. Rahman et al., "Rac1 signaling regulates sepsis-induced pathologic inflammation in the lung via attenuation of Mac-1 expression and CXC chemokine formation," *Journal of Surgical Research*, vol. 183, no. 2, pp. 798–807, 2013.

[41] M. Mittal, M. R. Siddiqui, K. Tran, S. P. Reddy, and A. B. Malik, "Reactive oxygen species in inflammation and tissue injury," *Antioxidants and Redox Signaling*, vol. 20, no. 7, pp. 1126–1167, 2014.

[42] Y.-W. Kim and T. V. Byzova, "Oxidative stress in angiogenesis and vascular disease," *Blood*, vol. 123, no. 5, pp. 625–631, 2014.

[43] R. A. Kowluru and M. Mishra, "Oxidative stress, mitochondrial damage and diabetic retinopathy," *Biochimica et Biophysica Acta - Molecular Basis of Disease*, vol. 1852, no. 11, pp. 2474–2483, 2015.

[44] S. Cowey and R. W. Hardy, "The metabolic syndrome: a high-risk state for cancer?" *American Journal of Pathology*, vol. 169, no. 5, pp. 1505–1522, 2006.

[45] G. Wu, Y.-Z. Fang, S. Yang, J. R. Lupton, and N. D. Turner, "Glutathione metabolism and its implications for health," *Journal of Nutrition*, vol. 134, no. 3, pp. 489–492, 2004.

[46] B. K. Tiwari, K. B. Pandey, A. B. Abidi, and S. I. Rizvi, "Markers of oxidative stress during diabetes mellitus," *Journal of Biomarkers*, vol. 2013, Article ID 378790, 8 pages, 2013.

[47] W.-D. Li, H. Jiao, K. Wang et al., "Pathway-based genome-wide association studies reveal that the Rac1 pathway is associated with plasma adiponectin levels," *Scientific Reports*, vol. 5, Article ID 13422, 2015.

[48] M. T. Elnakish, H. H. Hassanain, P. M. Janssen, M. G. Angelos, and M. Khan, "Emerging role of oxidative stress in metabolic syndrome and cardiovascular diseases: important role of Rac/NADPH oxidase," *Journal of Pathology*, vol. 231, no. 3, pp. 290–300, 2013.

[49] M. Satoh, H. Ogita, K. Takeshita, Y. Mukai, D. J. Kwiatkowski, and J. K. Liao, "Requirement of Rac1 in the development of cardiac hypertrophy," *Proceedings of the National Academy of Sciences of the United States of America*, vol. 103, no. 19, pp. 7432–7437, 2006.

[50] S. Y. Kong, M. Goodman, S. Judd, R. M. Bostick, W. D. Flanders, and W. McClellan, "Oxidative balance score as predictor of all-cause, cancer, and noncancer mortality in a biracial US cohort," *Annals of Epidemiology*, vol. 25, no. 4, pp. 256–262, 2015.

[51] J. Labadie, M. Goodman, B. Thyagarajan et al., "Associations of oxidative balance-related exposures with incident, sporadic colorectal adenoma according to antioxidant enzyme genotypes," *Annals of Epidemiology*, vol. 23, no. 4, pp. 223–226, 2013.

Hindawi Publishing Corporation
Oxidative Medicine and Cellular Longevity
Volume 2016, Article ID 2423547, 10 pages
http://dx.doi.org/10.1155/2016/2423547

Review Article

Potential Role of Protein Disulfide Isomerase in Metabolic Syndrome-Derived Platelet Hyperactivity

Renato Simões Gaspar,[1] Andrés Trostchansky,[2,3] and Antonio Marcus de Andrade Paes[1,3]

[1]*Laboratory of Experimental Physiology, Department of Physiological Sciences, Federal University of Maranhão, São Luís, MA, Brazil*
[2]*Departamento de Bioquímica and Center for Free Radical and Biomedical Research, Facultad de Medicina, Universidad de la República, Montevideo, Uruguay*
[3]*Health Sciences Graduate Program, Biological and Health Sciences Center, Federal University of Maranhão, São Luís, MA, Brazil*

Correspondence should be addressed to Antonio Marcus de Andrade Paes; marcuspaes@ufma.br

Received 12 August 2016; Revised 17 October 2016; Accepted 1 November 2016

Academic Editor: Nageswara Madamanchi

Metabolic Syndrome (MetS) has become a worldwide epidemic, alongside with a high socioeconomic cost, and its diagnostic criteria must include at least three out of the five features: visceral obesity, hypertension, dyslipidemia, insulin resistance, and high fasting glucose levels. MetS shows an increased oxidative stress associated with platelet hyperactivation, an essential component for thrombus formation and ischemic events in MetS patients. Platelet aggregation is governed by the peroxide tone and the activity of Protein Disulfide Isomerase (PDI) at the cell membrane. PDI redox active sites present active cysteine residues that can be susceptible to changes in plasma oxidative state, as observed in MetS. However, there is a lack of knowledge about the relationship between PDI and platelet hyperactivation under MetS and its metabolic features, in spite of PDI being a mediator of important pathways implicated in MetS-induced platelet hyperactivation, such as insulin resistance and nitric oxide dysfunction. Thus, the aim of this review is to analyze data available in the literature as an attempt to support a possible role for PDI in MetS-induced platelet hyperactivation.

1. Introduction

Definition of Metabolic Syndrome (MetS) has been a matter of intense scientific output over the last decades, reaching a consensus by The National Cholesterol Education Program–Adult Treatment Panel (NCEP ATP III) to include five major features: visceral obesity, hypertension, dyslipidemia, insulin resistance, and high fasting glucose levels. Diagnostic criteria for MetS must include at least three out of these five features [1]. MetS has become a worldwide epidemic, alongside with a high socioeconomic cost whose prevalence widely ranges from 8% to 43% in men and 7% to 56% in women [2–4]. Importantly, the presence of MetS is associated with a substantial 5-fold increased risk of developing diabetes mellitus (DM) and a 2-fold increase in the development of cardiovascular disease, concurring for higher likelihood to suffer ischemic events [2–5]. In fact, MetS is an independent risk factor for cardiovascular disease (CVD), leading patients to exhibit a prothrombotic and proinflammatory status [6, 7]. As a long-term outcome, MetS individuals tend to develop atherosclerotic plaque as a chronic inflammatory process characterized by increased levels of inflammatory markers, such as tumor necrosis factor α, interleukin-6, leptin, angiotensin II, and plasminogen activator factor 1, all of them capital prothrombotic factors [6, 7].

Besides increased inflammatory markers, the prothrombotic state in MetS is mainly caused by endothelial dysfunction and platelet hyperactivity. Both lipotoxicity and insulin resistance contribute to increased oxidative stress (OxS) in the endothelium, leading to enhanced production of reactive oxygen species (ROS) by various isoforms of NADPH oxidase (Nox) and reduced nitric oxide (NO) production and bioavailability, consequent to lower expression and/or uncoupling of endothelial nitric oxide synthase (eNOS) as well as increased reactivity with superoxide ($O_2^{\bullet -}$) [8]. Platelets are key players involved in pathologic thrombosis through

increased adhesion to the compromised endothelium, being also affected by the increased OxS present in MetS [9, 10]. It has been shown that MetS subjects have increased mean platelet volume, an independent predictor of vascular events [11]. Moreover, there is an increase of proaggregatory and prothrombotic mediators such as thromboxane A_2(TxA_2) and adhesion molecules such as P-selectin, while inhibitory components, like NO, are decreased [12]. Overall, there is an increase in prothrombotic factors with a concomitant decrease in inhibitory components in both endothelium and platelets that concur for increased CVD in MetS.

The Protein Disulfide Isomerase (PDI) is a family of thiol isomerases originally found in the endoplasmic reticulum (ER) that were later discovered in the cytosol and surface of endothelial cells and platelets, among others [13, 14]. The most abundant and physiologically relevant member is PDIA1, the product of the *P4HB* gene, with a molecular weight of 57,000 Da and five subunits: four thioredoxin-like domains (a-b-b′-a′), one C-terminal extension domain, besides one x-linker sequence between b′ and a′ [15, 16]. PDIA1 is also an important regulator of thrombus formation, rapidly binding to β_3 integrins on the endothelium upon injury [17]. In platelets, membrane PDI members, such as PDIA1, ERP5, and ERP57, are known for their paramount importance in platelet aggregation through the isomerization of a disulfide bond in the $\alpha_{2b}\beta_3$ integrin, which is the final convergent pathway in virtually all mechanisms of platelet aggregation [18]. In addition, platelet surface PDI participates in platelet adhesion through a close interaction with collagen receptor $\alpha_2\beta_1$ [19], GP1bα [20], vitronectin [21], and thrombospondin 1 [22]. Despite the already established importance of PDI proteins, precise mechanisms through which surface thiol isomerases interact with integrins and other platelet membrane receptors are still unclear. Since MetS involves many risk factors associated to changes in the coagulation pathway, the aim of this review is to analyze the potential role of platelet surface PDIA1, henceforth referred as PDI, as a central player in platelet hyperactivation under MetS.

2. Metabolic Syndrome and Vascular Oxidative Stress

ROS, specially $O_2^{\bullet-}$ and hydrogen peroxide (H_2O_2), are ubiquitous oxidants of moderate reactivity and brief half-life found in virtually all biological systems as byproducts of oxygen metabolism [23]. At low levels, ROS are key players in many biochemical processes, such as signaling cascades, gene transcription, cellular growth and migration, and apoptosis [24]. In particular at the vascular system, ROS participate in controlling vasodilation and platelet adherence/aggregation [23]. However, when ROS generation is excessive and not compartmentalized, exceeding endogenous antioxidant capacity, cells and tissues progress to OxS, which is considered an early event in the pathophysiology of most chronic noncommunicable diseases associated to MetS [25, 26].

The vascular OxS observed in MetS leads to a change in plasma redox state, inciting a prooxidant environment due to the imbalance of two central thiol/disulfide couples, glutathione/glutathione disulfide (GSH/GSSG), and cysteine/cystine (Cys/CySS) [25, 27]. The reduced partners (GSH or Cys) help in maintaining the thiol/disulfide redox state in proteins, as well as the redox state of ascorbate and vitamin E in their reduced healthy forms by their participation in peroxides removal. Under prooxidant conditions, GSH levels decline in both intracellular and extracellular environment of vascular cells in parallel with an increase in GSSG. Thus, measurement of reduced and oxidized products, as well as their ratios, can provide a useful indicator of OxS in human plasma [25]. Several thiol-containing proteins at the surface of vascular cells, such as thioredoxin and its relatives from PDI family, in response to variable concentrations of ROS, alter the redox state of critical thiols that leads to ROS-driven cellular activation [28]. Noteworthy, recent reports have corroborated the impact of MetS on plasma redox state, with particular emphasis on the assessment of redox status as a tool to predict different outcomes in prediabetic patients [29, 30].

The phagocytic and nonphagocytic isoforms of Noxes are the primary source of ROS and have been consistently implicated in different vascular pathologies [31, 32]. Nox complexes are composed of multiple subunits comprising catalytic (Nox 1–5) and regulatory ($p22^{phox}$, $p40^{phox}$, $p47^{phox}$, $p67^{phox}$, Noxo 1, Noxa 1, and the small GTPases Rac 1 and Rac 2) components, whose expression may vary according to the cell type [33]. Nox4 is associated to cell differentiation of vascular smooth muscle cells [34], whereas Nox1 supports cellular proliferation and migration [35]. Endothelial cells express four Nox isoforms (Nox1, Nox2, Nox4, and Nox5), from which Nox4 is the most highly expressed, and promote H_2O_2-derived endothelium preservative actions [36, 37]. On the other hand, expression levels of the other isoforms have been directly implicated in endothelial dysfunction [38].

In platelets, Nox2 was identified by the localization of membrane $p22^{phox}$, cytosolic $p47^{phox}$ subunits, and more recently the catalytic $gp91^{phox}$ subunit [39, 40]. Similarly, Nox1 is also expressed in human platelets, although in a lesser extent when compared to Nox2 [41]. The same study failed to localize Nox4 and Nox5 in platelets, even though further studies are needed to address this matter. Since platelets express Nox1 and Nox2, Delaney and colleagues [42] compared the differential roles of these enzymes in platelet activation and thrombosis. They showed that Nox2, but not Nox1, is required for thrombus formation, whereas none of the enzymes altered tail bleeding time in mice, suggesting further studies should focus on whether Nox-dependent ROS generation may become a potential antithrombotic target without significant bleeding complications [42].

In addition to Nox enzymes, there are different nonenzymatic and enzymatic pathways involved in the formation of ROS in vascular milieu, among them, spontaneous dysmutation of oxygen, leakage of the mitochondrial electron transport chain, myeloperoxidase, xanthine oxidase, cyclooxygenases, and uncoupled NOS [43]. Virtually all these mechanisms may concur for MetS-associated cellular damage, which leads to increased formation of advanced glycation

end products (AGE) and its receptors, hexosamine pathway overactivity, increased polyol pathway flux, activation of protein kinase C isoforms [44, 45], lipotoxicity [46], and increased inflammatory profile [47]. Therefore, endothelial cells and platelets from MetS patients suffer from this marked increase in ROS generation, playing a pivotal role in the macro- and microvascular complications of this syndrome.

3. Metabolic Syndrome and Platelet Hyperactivity

The damage caused by OxS has been shown to increase platelet aggregation in MetS subjects and decrease aspirin response in DM [6, 10, 48]. These can be explained by several mechanisms: increased platelet secretion of TxA_2 and prostaglandins (PG), decreased expression of NOS in both endothelium and platelets in addition to a decreased production of prostacyclin (PGI_2) at the endothelium; decreased platelet response to NO and platelet insulin resistance. Among these, the development of insulin resistance and the impairment of NO homeostasis are arguably the most substantial pathways involved in platelet hyperactivation in MetS.

3.1. Thromboxane and F2-Isoprostanes Overproduction in Platelets. TxA_2 is one of the byproducts of arachidonic acid (AA) oxidation by prostaglandin endoperoxide H_2synthase-1 (PGHS-1), also known as cyclooxygenase-1 (COX-1), in platelets [49]. TxA_2 is synthesized by platelets and acts as an agonist in platelet aggregation and activation, through the ligation of its own G protein-coupled receptor, leading to increased $\alpha_{2b}\beta_3$ expression, the latter being blocked by the COX-inhibitor aspirin [50]. Besides TxA_2, F2-isoprostanes are also derived from AA oxidation, stimulating platelet aggregation and complementing TxA_2 actions. Specifically, 8-iso-PGF2α is secreted by platelets upon stimulus, enhancing platelet activation and adhesive reactions to other agonists at low concentrations, through interaction with thromboxane receptor [51, 52]. Noteworthy, urinary secretion of 8-iso-PGF2α is also considered a clinical marker of platelet activity [52], which has been found to be increased in obese women [53].

Increased platelet ROS formation in MetS overactivates platelet Nox2 partly through oxidized low-density lipoprotein (oxLDL) ligation of platelet CD36 [54], causing an increase in cytosolic peroxide tone, that is, increased peroxynitrite generation, that subsequently stimulates COX-1 activity [49, 55]. This setting enhances TxA_2 and 8-iso-PGF2α levels through lipid peroxidation and redox-catalyzed conversion of AA into F2-isoprostanes [52]. Interestingly, it seems platelet Nox2 is an important regulator of 8-iso-PGF2α, since chemical or hereditary inhibition of Nox2 strongly decreases 8-iso-PGF2α generation in platelets [39]. Since COX-1 activity is based in the continuous generation of a lipid-derived radical, besides the reductant environment of the platelet, TxA_2 pathway is continuously interrupted and requires a permanent reactivation by peroxides [49]. Therefore, OxS can exacerbate platelet aggregation in MetS by changing the intracellular peroxide and peroxynitrite levels, culminating in TxA_2 and F2-isoprostanes overproduction, a mechanism at least partially regulated by Nox2.

3.2. Dysfunctional NO Effects in Platelets. NO is a potent vasodilator and antiplatelet mediator whose bioavailability is inversely correlated with cardiovascular risk [56–59]. Under normal conditions, NO derived from endothelial and platelet NOS diffuses toward circulating platelets in order to activate guanylate cyclase (GC), thus augmenting cyclic guanosine monophosphate (cGMP) levels. Increased levels of cGMP as well as cyclic adenosine monophosphate (cAMP) induce the phosphorylation of vasodilator-stimulated phosphoprotein (VASP) that will inactivate integrin $\alpha_{2b}\beta_3$ [60–62]. NO also decreases intracellular Ca^{2+} levels [63], inhibits thromboxane receptors in platelets [64], and diminishes platelet recruitment in thrombus formation [65]. Furthermore, in vascular smooth muscle cells, NO is a potent vasodilator that reduces intracellular Ca^{2+} levels by the abovementioned mechanisms [66].

However, in the context of increased OxS induced by MetS or aging, intraplatelet ROS overproduction decreases NO bioavailability by forming reactive nitrogen species (RNS), such as peroxynitrite, leading to platelet hyperactivation [61, 67]. Of note, peroxynitrite induces platelet aggregation with increased intracellular Ca^{2+} concentration [68], while it also oxidizes several proteins that blunt NOS and reduce platelet antioxidant capacity [58, 69]. Platelet NOS was found to be downregulated in MetS patients, which could partially explain the decreased NO production in these subjects when compared to healthy ones [70]. Besides compromised NO bioavailability, platelets from patients with unstable coronary syndrome showed impaired antiplatelet response to the NO donor sodium nitroprusside, suggesting a platelet NO resistance that could be associated to increased OxS [71]. Thus, OxS causes not only a decrease in platelet NO bioavailability, but also a dysfunctional response to its action.

3.3. Dysfunctional Insulin Effects in Platelets. Since the discovery of insulin receptors in human platelets, insulin signaling has been considered an important regulator of its function. Hajek and colleagues were the first to demonstrate that platelets possess insulin receptors, with a density of roughly 500 receptors/cell, comparable to other insulin-sensitive cell types [72]. Physiologically, insulin binds to its membrane receptor, provoking the autophosphorylation of its β-chain and activating the classical insulin's signaling pathway [73]. In fact, it has been shown that insulin inhibits platelet aggregation in healthy nonobese subjects [74, 75], by a mechanism involving inhibition of tissue factor (TF) and modulation of plasminogen activator inhibitor-1 (PAI-1) concentrations [69]. Moreover, other groups reported that insulin decreases intraplatelet Ca^{2+} content [76] and reduces platelets' response to agonists possibly due to the activation of eNOS [77] and sensitization of platelets to the inhibitory effects of NO [12, 78].

Similar to NO dysfunctional effects in MetS, it has been shown that obese DM subjects blunted insulin's antiplatelet

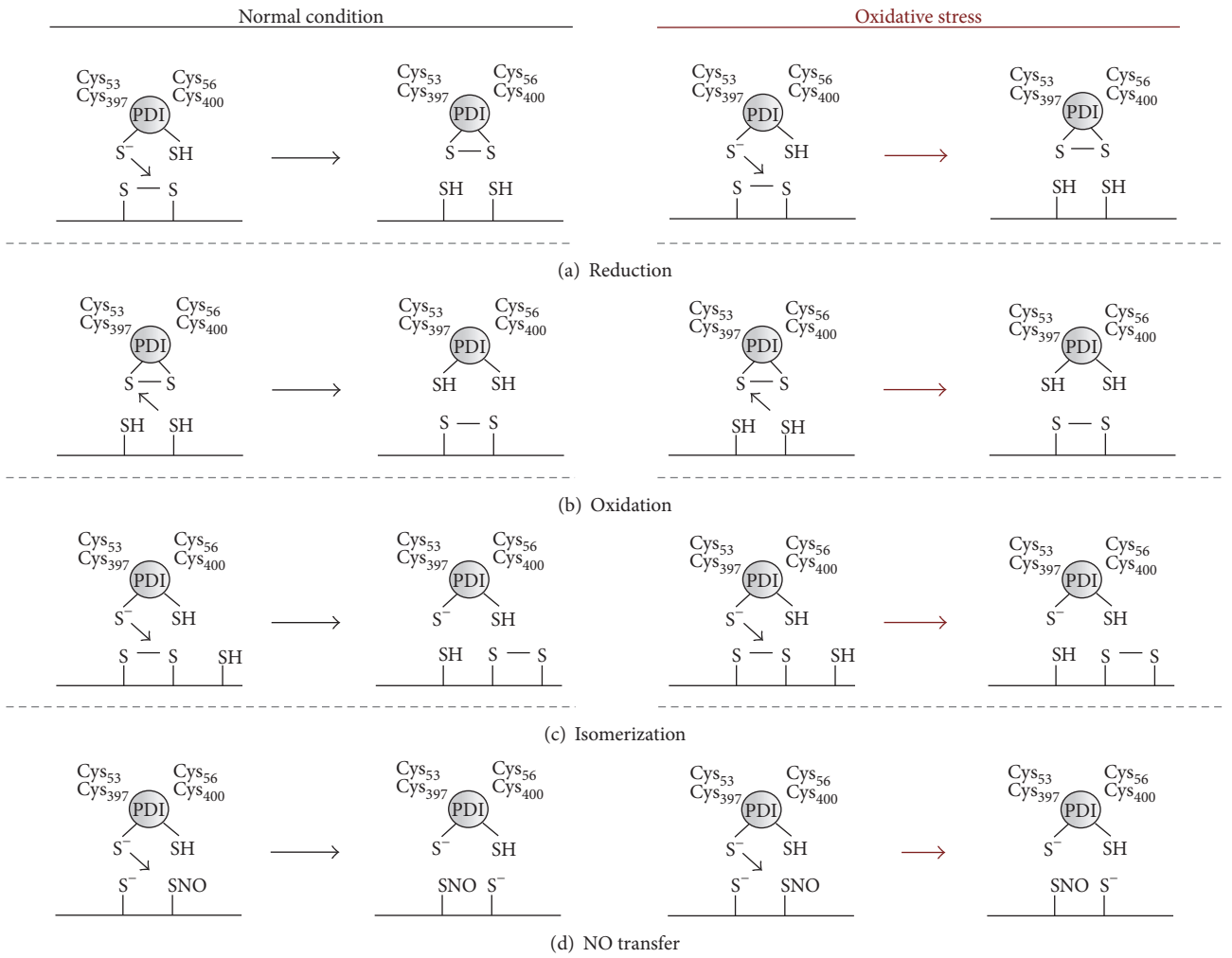

Figure 1: Reactions catalyzed by PDI and possible unbalance in oxidative stress. In (a), PDI catalyzes reduction of a disulfide bond to a dithiol through an attack from its thiolate anion located in Cys_{53} or Cys_{397}, whereas in (b) shows PDI oxidizing a dithiol into a disulfide bond. In (c), PDI isomerizes a disulfide bond in the same molecule. These reactions are expected to be increased in OxS, since the reduction of disulfide bonds has been shown to promote platelet aggregation and isomerization is an essential step towards $\alpha_{2b}\beta_3$ activation [18]. In (d), PDI reacts with NO to promote transnitrosation, shifting NO from one molecule to another or within the same molecule. It should be noted that PDI might also catalyze denitrosation, releasing NO from S-nitrosothiols. This reaction is expected to be decreased in oxidative stress mainly due to the decreased NO bioavailability.

effects, confirming that human platelets can undergo insulin resistance. Insulin resistance is defined by the lack of insulin's actions in platelets, which downregulates IRS-1/Akt pathway, culminating in elevated intracellular Ca^{2+} content and proaggregatory mediators. In fact, platelets from diabetic patients exhibit faster and higher aggregation when compared to healthy ones [69, 79]. Moreover, insulin resistance augments intraplatelet synthesis of PAI-1 and secretion of thromboxane metabolites, thus creating a proaggregatory environment [69]. Finally, there is increased thrombin and fibrin generation, with a prothrombotic fibrin clot phenotype in diabetic patients [80]. Thus, platelet insulin resistance is one of the main contributors to OxS-derived platelet hyperactivation in MetS, even though there is no pathophysiological model to explain how platelets become insulin resistant.

4. Protein Disulfide Isomerase and Platelet Hyperactivation in MetS

PDI is an ubiquitous chaperone, structurally divided in five subunits: four thioredoxin-like domains (a-b-b′-a′) and one C-terminal extension domain, besides one x-linker sequence between b′ and a′ [15, 16]. Among these, its catalytic redox motif CGHC is present in both a and a′ domains in a constant balance between disulfide and dithiol forms. These CGHC motives confer PDI its ability to catalyze oxidation, reduction, and isomerization reactions (Figure 1), through redox exchanges apparently guided by a trial and error process [16]. Even though containing a C-terminal KDEL ER-retention sequence, PDI is also found in cytosol and surface membrane of numerous cell types, including platelets

[14]. Interestingly, besides surface membrane, platelet PDI was localized in the sarco-/endoplasmic reticulum, being mobilized to the surface during platelet activation through a mechanism requiring actin polymerization [81]. Important to this review, we refer specifically to platelet surface PDI.

In platelets, PDI is known for its paramount importance in platelet aggregation through the isomerization of a disulfide bond in the $\alpha_{2b}\beta_3$ integrin [18]. Such integrin is considered the most important component and final convergent pathway in virtually all mechanisms of platelet aggregation [18]. In fact, anti-PDI antibody inhibits platelet aggregation [82], whereas the addition of reduced PDI prior to agonists enhances maximum aggregation [83]. Of note, it has been recently showed that the C-terminal CGHC motif of PDI is essential for its function in thrombus formation and platelet aggregation [83]. Moreover, PDI is also implicated in the function of other integrins, such as the collagen receptor $\alpha_2\beta_1$ [19] and the von Willebrand factor receptor glycoprotein 1bα [20], even though the precise mechanism of such interactions is unclear. Overall, PDI is considered a prothrombotic enzyme, directly implicated in platelet activation, aggregation, and adhesion.

Strikingly, PDI seems to be related to platelet insulin resistance and consequent hyperactivity in OxS induced by MetS. Contrasting with insulin's TF inhibition, PDI has been described as an essential component of TF activation. A proposed working model states that reduced PDI, secreted by activated platelets, reacts with low procoagulant activity TF to yield a TF with high procoagulant activity through the formation of a disulfide bond between Cys_{186} and Cys_{209} residues on TF molecule. Additionally, PDI may promote fibrin generation [84]. Overall, this suggests that while insulin inhibits TF activation, PDI works on the opposite side by augmenting TF procoagulant activity and increasing fibrin generation upon injury. Nonetheless, insulin resistance and PDI seem to exert similar effects on platelet activation. Even though no study has ever demonstrated whether PDI can desensitize platelet's insulin receptors, the likewise effects of insulin resistance and PDI on platelet function could lead to a possible connection between these two factors.

A plausible hypothesis is that PDI's procoagulant reactions could be increased in insulin resistance and OxS in detriment of decreased insulin activity or even that insulin resistance could be, at least in part, accounted for increased PDI activity. This is supported by the well-characterized in vitro reaction between PDI and insulin, where the first reduces a disulfide bond in the latter, causing the precipitation of insulin's β-chain [85]. In vivo, it has been reported that DM patients release more platelet-derived microparticles (pMPs) [86]. Importantly, pMPs contain catalytically active PDI, and DM subjects have increased levels of PDI-containing pMPs [87]. In fact, plasma samples from DM patients present roughly 50% more pMPs than healthy subjects, also exhibiting 60% more PDI and 70% more PDI activity [87]. Noteworthy, these microparticles were able to catalyze insulin disulfide reduction, abrogating insulin's activity, as shown by loss of Akt phosphorylation in 3T3-L1 cells [87]. Therefore, it is reasonable to suggest that the increased PDI secretion from DM platelets reduces insulin's bioavailability, contributing to the lack of insulin's action found in MetS platelets (Figure 2). Nonetheless, it should be stressed that further studies are needed to address whether PDI is an important cue in MetS-induced platelet hyperactivity, specifically if secreted platelet PDI is able to desensitize insulin receptor in various cell types.

PDI is also involved in platelet NO homeostasis [88], providing evidence for a paradoxical effect of PDI in platelet activation. Previous studies have shown that PDI acts as an NO carrier through vascular cells by transnitrosation reactions, exchanging the nitrosonium ions between cysteines (Figure 1(d)) [89, 90]. Likewise, it was also shown that platelet PDI denitrosates S-nitrosothiols (RSNOs), thus releasing NO and increasing its bioavailability [91]. Moreover, RSNOs seem to be denitrosated by the same CGHC active site that gives PDI its proaggregatory properties [83, 91]. These findings were further supported by Bell et al. [92] that showed PDI is implicated in a wide range of NO-related signals and not only with RSNOs, as previously thought. However, NO can also attack PDI in an S-nitrosylation reaction, which transfers NO to critical cysteines in CGHC active sites. Such reaction inhibits PDI isomerization and chaperone activities by roughly 50%, which could in turn compromise the aforementioned mechanisms of platelet aggregation through $\alpha_{2b}\beta_3$ [93]. Despite acting as a NO donor, PDI paradoxically inhibits NO effects in vascular smooth cells by a thiol-disulfide exchange between PDI's CGHC active site and the α or β domains of soluble GC [94, 95]. Therefore, platelet PDI improves NO bioavailability, acts as an NO carrier, while it can also be inhibited by NO itself, whereas in vascular smooth cells PDI abrogates NO effects.

Nevertheless, it is important to notice that the above-mentioned studies took place under physiological conditions and the interaction between PDI and NO was not tested under increased OxS, nor was it tested in MetS subjects. One could hypothesize that increased ROS production, causing cellular damage and increased OxS, coupled with alterations in plasma GSH/GSSG and Cys/CySS could interfere with PDI's denitrosation activity or even revert its effect. Additionally, decreased NO bioavailability due to peroxynitrite formation leads to lower extents of PDI reacting with available NO and/or less NO inhibiting PDI isomerase activity, which would shift the enzyme's activity to proaggregatory pathways (Figure 2). These hypotheses are based on the well-established decrease of NO bioavailability in MetS (detailed in Section 3.2) and should be addressed in future studies, since dysfunctional NO effect on platelets is an important cue to better understand platelet hyperactivity. Nonetheless, studies are needed to investigate whether there is a link between PDI and decreased NO bioavailability or diminished platelet NO response, given that this protein is of capital importance to platelet function.

Last but not least, it has been suggested that PDI act as a modulator of distinct members of Nox enzymes in the vascular system [96]. There is a close association between PDI and Nox1 [96–98], phagocytic Nox2 [99, 100], and Nox4 [97, 101], which has been demonstrated through biochemical and molecular approaches of gene silencing and overexpression. Specifically to Nox2, PDI regulates its function possibly

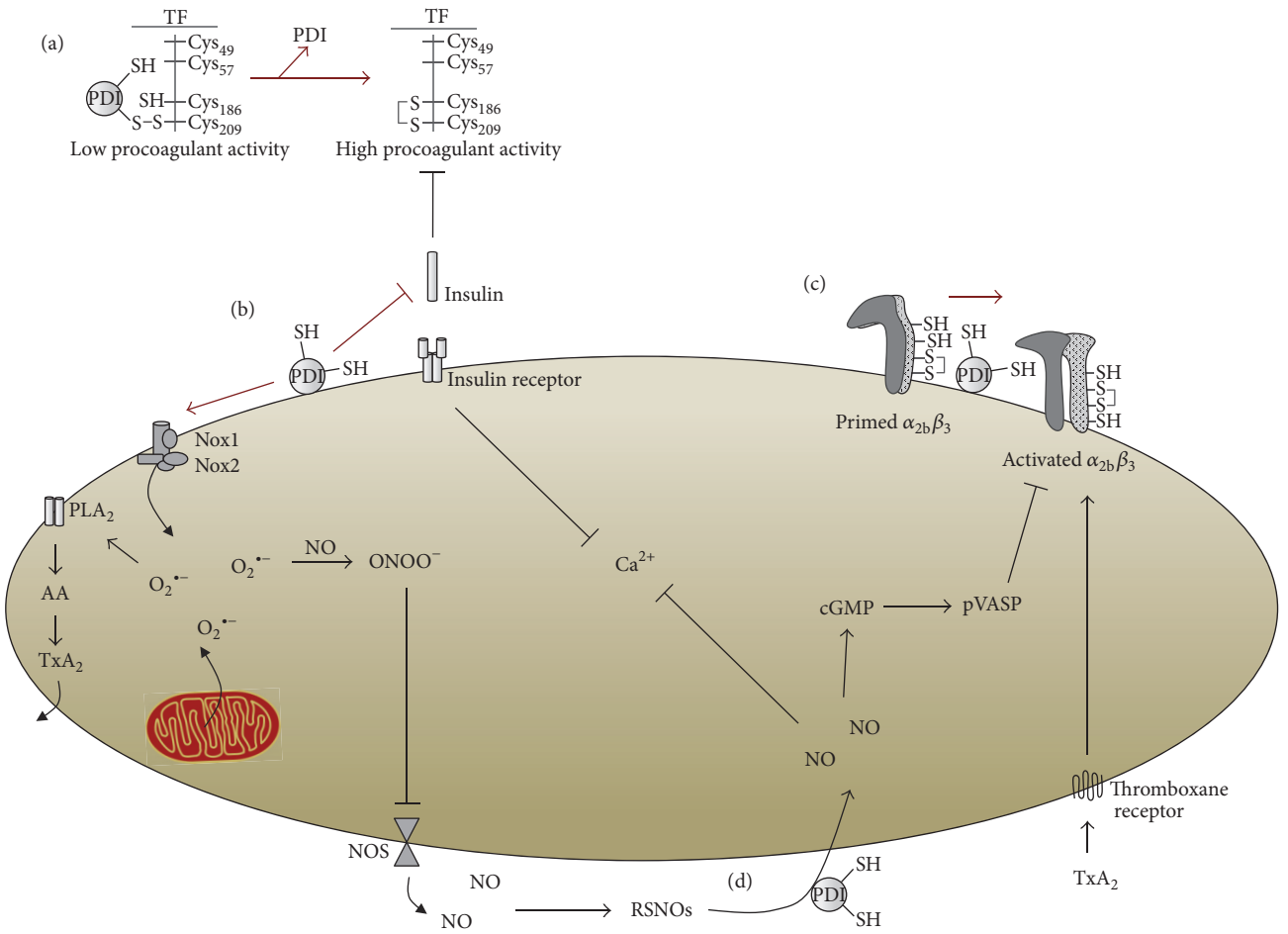

FIGURE 2: PDI participates in mechanisms of platelet hyperactivation induced by metabolic syndrome. In (a), PDI promotes the procoagulant activity of tissue factor (TF) through the formation of a disulfide bond between TF Cys_{186} and Cys_{209}. In (b), PDI inhibits insulin's action by reducing a disulfide bond that precipitates insulin's β-chain, preventing insulin's inhibitory activity upon TF and insulin's intracellular signaling in platelets. Also, PDI regulates Nox enzymes, promoting stronger generation of $O_2^{\bullet-}$ that can either react with NO, forming peroxynitrite that will inhibit nitric oxide synthase (NOS) or induce thromboxane (e.g., A_2) generation through phospholipase A_2 (PLA_2) and subsequent COX-derived arachidonic acid (AA) platelet metabolism. (c) PDI promotes the isomerization of a disulfide bond in $\alpha_{2b}\beta_3$ integrin. Finally, in (d), PDI has a paradoxical effect in platelet aggregation, acting as a nitric oxide (NO) carrier and releaser through transnitrosation and denitrosation reactions of S-nitrosothiols (RSNOs). Arrows in red indicate overactivated mechanisms.

through mechanisms involving thiol groups on its various subunits and therefore contribute to ROS generation [96]. Early studies have found increased protein expression and activity of Nox2 subunits $p22^{phox}$ and $gp91^{phox}$ in pMPs from septic patients [102], which were later demonstrated also to present higher levels of PDI, as well [103]. Even though there is no study addressing such interaction in platelets from MetS patients, it is plausible to infer that PDI might also regulate Nox2 activity in these cells, further contributing for OxS-driven NOS uncoupling, thromboxane generation as well as insulin resistance.

5. Conclusions

MetS increases cardiovascular risk and mortality, being considered a worldwide epidemic. Among the cardiovascular outcomes implicated in MetS, platelet hyperactivation plays a pivotal role in morbidity and mortality. At the same time, PDI is an important regulator of platelet function. However, to the best of our knowledge, no study has investigated the likely contribution of PDI in MetS-induced platelet hyperactivity, nor has it ever been proposed. Therefore, we propose that PDI could be a potential culprit of MetS-induced platelet hyperactivity, possibly through a deficient PDI denitrosation activity, decreased PDI S-nitrosylation and/or less PDI needed for transnitrosation reactions, an increase in TF activation, and insulin resistance caused by increased quantity and/or activity of secreted platelet PDI. Novel original studies are needed to corroborate or reject this hypothesis.

Competing Interests

The authors declare no actual or potential conflict of interests.

Acknowledgments

The authors thank the Fundação de Amparo à Pesquisa e ao Desenvolvimento Científico e Tecnológico do Maranhão, FAPEMA (APP 0395/12, ESTAGIO 0814/13, APCINTER 02698/14) and Conselho Nacional de Desenvolvimento Científico e Tecnológico, CNPq (485251/2012-4). Andrés Trostchansky was supported by CSIC grupos I+D 2014 (536) and FAPEMA (PVI-05558/15).

References

[1] K. G. Alberti, R. H. Eckel, S. M. Grundy et al., "Harmonizing the metabolic syndrome: a joint interim statement of the International Diabetes Federation Task Force on Epidemiology and Prevention; National Heart, Lung, and Blood Institute; American Heart Association; World Heart Federation; International Atherosclerosis Society; and International Association for the Study of Obesity," *Circulation*, vol. 120, pp. 1640–1645, 2009.

[2] J. Kaur, "A Comprehensive Review on Metabolic Syndrome," *Cardiology Research and Practice*, vol. 2014, Article ID 943162, 21 pages, 2014.

[3] E. S. Ford, W. H. Giles, and W. H. Dietz, "Prevalence of the metabolic syndrome among US adults: findings from the third National Health and Nutrition Examination Survey," *The Journal of the American Medical Association*, vol. 287, no. 3, pp. 356–359, 2002.

[4] A. Towfighi and B. Ovbiagele, "Metabolic syndrome and stroke," *Current Diabetes Reports*, vol. 8, no. 1, pp. 37–41, 2008.

[5] E. Kassi, P. Pervanidou, G. Kaltsas, and G. Chrousos, "Metabolic syndrome: definitions and controversies," *BMC Medicine*, vol. 9, article 48, 2011.

[6] M.-J. van Rooy, W. Duim, R. Ehlers, A. V. Buys, and E. Pretorius, "Platelet hyperactivity and fibrin clot structure in transient ischemic attack individuals in the presence of metabolic syndrome: a microscopy and thromboelastography® study," *Cardiovascular Diabetology*, vol. 14, article 86, 2015.

[7] M.-J. Van Rooy and E. Pretorius, "Metabolic syndrome, platelet activation and the development of transient ischemic attack or thromboembolic stroke," *Thrombosis Research*, vol. 135, no. 3, pp. 434–442, 2015.

[8] M. Mathew, E. Tay, and K. Cusi, "Elevated plasma free fatty acids increase cardiovascular risk by inducing plasma biomarkers of endothelial activation, myeloperoxidase and PAI-1 in healthy subjects," *Cardiovascular Diabetology*, vol. 9, article 9, 2010.

[9] L. K. Jennings, "Mechanisms of platelet activation: need for new strategies to protect against platelet-mediated atherothrombosis," *Thrombosis and Haemostasis*, vol. 102, no. 2, pp. 248–257, 2009.

[10] F. Santilli, D. Lapenna, S. La Barba, and G. Davì, "Oxidative stress-related mechanisms affecting response to aspirin in diabetes mellitus," *Free Radical Biology and Medicine*, vol. 80, pp. 101–110, 2015.

[11] L. Vizioli, S. Muscari, and A. Muscari, "The relationship of mean platelet volume with the risk and prognosis of cardiovascular diseases," *International Journal of Clinical Practice*, vol. 63, no. 10, pp. 1509–1515, 2009.

[12] F. Santilli, N. Vazzana, R. Liani, M. T. Guagnano, and G. Davì, "Platelet activation in obesity and metabolic syndrome," *Obesity Reviews*, vol. 13, no. 1, pp. 27–42, 2012.

[13] S.-W. Wan, C.-F. Lin, Y.-T. Lu, H.-Y. Lei, R. Anderson, and Y.-S. Lin, "Endothelial cell surface expression of protein disulfide isomerase activates β1 and β3 integrins and facilitates dengue virus infection," *Journal of Cellular Biochemistry*, vol. 113, no. 5, pp. 1681–1691, 2012.

[14] K. Chen, Y. Lin, and T. C. Detwiler, "Protein disulfide isomerase activity is released by activated platelets," *Blood*, vol. 79, no. 9, pp. 2226–2228, 1992.

[15] C. Wang, W. Li, J. Ren et al., "Structural insights into the redox-regulated dynamic conformations of human protein disulfide isomerase," *Antioxidants & Redox Signaling*, vol. 19, no. 1, pp. 36–45, 2013.

[16] M. Schwaller, B. Wilkinson, and H. F. Gilbert, "Reduction-reoxidation cycles contribute to catalysis of disulfide isomerization by protein-disulfide isomerase," *The Journal of Biological Chemistry*, vol. 278, no. 9, pp. 7154–7159, 2003.

[17] J. Cho, D. R. Kennedy, L. Lin et al., "Protein disulfide isomerase capture during thrombus formation in vivo depends on the presence of β3 integrins," *Blood*, vol. 120, no. 3, pp. 647–655, 2012.

[18] D. W. Essex, "Redox control of platelet function," *Antioxidants & Redox Signaling*, vol. 11, no. 5, pp. 1191–1225, 2009.

[19] J. Lahav, E. M. Wijnen, O. Hess et al., "Enzymatically catalyzed disulfide exchange is required for platelet adhesion to collagen via integrin $\alpha_2\beta_1$," *Blood*, vol. 102, no. 6, pp. 2085–2092, 2003.

[20] J. K. Burgess, K. A. Hotchkiss, C. Suter et al., "Physical proximity and functional association of glycoprotein 1bα and protein-disulfide isomerase on the platelet plasma membrane," *The Journal of Biological Chemistry*, vol. 275, no. 13, pp. 9758–9766, 2000.

[21] D. W. Essex, A. Miller, M. Swiatkowska, and R. D. Feinman, "Protein disulfide isomerase catalyzes the formation of disulfide-linked complexes of vitronectin with thrombin-antithrombin," *Biochemistry*, vol. 38, no. 32, pp. 10398–10405, 1999.

[22] K. A. Hotchkiss, C. N. Chesterman, and P. J. Hogg, "Catalysis of disulfide isomerization in thrombospondin 1 by protein disulfide isomerase," *Biochemistry*, vol. 35, no. 30, pp. 9761–9767, 1996.

[23] V. Darley-Usmar and B. Halliwell, "Blood radicals: reactive nitrogen species, reactive oxygen species, transition metal ions, and the vascular system," *Pharmaceutical Research*, vol. 13, no. 5, pp. 649–662, 1996.

[24] K. K. Griendling, "NADPH oxidases: new regulators of old functions," *Antioxidants and Redox Signaling*, vol. 8, no. 9-10, pp. 1443–1445, 2006.

[25] D. P. Jones, "Redefining oxidative stress," *Antioxidants and Redox Signaling*, vol. 8, no. 9-10, pp. 1865–1879, 2006.

[26] C. K. Roberts and K. K. Sindhu, "Oxidative stress and metabolic syndrome," *Life Sciences*, vol. 84, no. 21-22, pp. 705–712, 2009.

[27] D. P. Jones and Y.-M. Go, "Redox compartmentalization and cellular stress," *Diabetes, Obesity and Metabolism*, vol. 12, supplement 2, pp. 116–125, 2010.

[28] Y.-M. Go and D. P. Jones, "Cysteine/cystine redox signaling in cardiovascular disease," *Free Radical Biology and Medicine*, vol. 50, no. 4, pp. 495–509, 2011.

[29] Y. Spanidis, A. Mpesios, D. Stagos et al., "Assessment of the redox status in patients with metabolic syndrome and type 2 diabetes reveals great variations," *Experimental and Therapeutic Medicine*, vol. 11, no. 3, pp. 895–903, 2016.

[30] L. J. da Fonseca, V. Nunes-Souza, S. Guedes Gda, G. Schettino-Silva, M. A. Mota-Gomes, and L. A. Rabelo, "Oxidative status imbalance in patients with metabolic syndrome: role of the myeloperoxidase/hydrogen peroxide axis," *Oxidative Medicine and Cellular Longevity*, vol. 2014, Article ID 898501, 14 pages, 2014.

[31] B. Lassègue and K. K. Griendling, "NADPH oxidases: functions and pathologies in the vasculature," *Arteriosclerosis, Thrombosis, and Vascular Biology*, vol. 30, no. 4, pp. 653–661, 2010.

[32] B. Lassègue, A. San Martín, and K. K. Griendling, "Biochemistry, physiology, and pathophysiology of NADPH oxidases in the cardiovascular system," *Circulation Research*, vol. 110, no. 10, pp. 1364–1390, 2012.

[33] J. D. Lambeth, T. Kawahara, and B. Diebold, "Regulation of Nox and Duox enzymatic activity and expression," *Free Radical Biology and Medicine*, vol. 43, no. 3, pp. 319–331, 2007.

[34] R. E. Clempus, D. Sorescu, A. E. Dikalova et al., "Nox4 is required for maintenance of the differentiated vascular smooth muscle cell phenotype," *Arteriosclerosis, Thrombosis, and Vascular Biology*, vol. 27, no. 1, pp. 42–48, 2007.

[35] M. Y. Lee, A. San Martin, P. K. Mehta et al., "Mechanisms of vascular smooth muscle NADPH oxidase 1 (Nox1) contribution to injury-induced neointimal formation," *Arteriosclerosis, Thrombosis, and Vascular Biology*, vol. 29, no. 4, pp. 480–487, 2009.

[36] K. D. Martyn, L. M. Frederick, K. Von Loehneysen, M. C. Dinauer, and U. G. Knaus, "Functional analysis of Nox4 reveals unique characteristics compared to other NADPH oxidases," *Cellular Signalling*, vol. 18, no. 1, pp. 69–82, 2006.

[37] J. D. Van Buul, M. Fernandez-Borja, E. C. Anthony, and P. L. Hordijk, "Expression and localization of NOX2 and NOX4 in primary human endothelial cells," *Antioxidants and Redox Signaling*, vol. 7, no. 3-4, pp. 308–317, 2005.

[38] G. R. Drummond and C. G. Sobey, "Endothelial NADPH oxidases: which NOX to target in vascular disease?" *Trends in Endocrinology and Metabolism*, vol. 25, no. 9, pp. 452–463, 2014.

[39] P. Pignatelli, R. Carnevale, S. Di Santo et al., "Inherited Human gp91phox deficiency is associated with impaired isoprostane formation and platelet dysfunction," *Arteriosclerosis, Thrombosis, and Vascular Biology*, vol. 31, no. 2, pp. 423–434, 2011.

[40] T. Seno, N. Inoue, D. Gao et al., "Involvement of NADH/NADPH oxidase in human platelet ROS production," *Thrombosis Research*, vol. 103, no. 5, pp. 399–409, 2001.

[41] D. Vara, M. Campanella, and G. Pula, "The novel NOX inhibitor 2-acetylphenothiazine impairs collagen-dependent thrombus formation in a GPVI-dependent manner," *British Journal of Pharmacology*, vol. 168, no. 1, pp. 212–224, 2013.

[42] M. K. Delaney, K. Kim, B. Estevez et al., "Differential roles of the NADPH-oxidase 1 and 2 in platelet activation and thrombosis," *Arteriosclerosis, Thrombosis, and Vascular Biology*, vol. 36, no. 5, pp. 846–854, 2016.

[43] C. A. Papaharalambus and K. K. Griendling, "Basic mechanisms of oxidative stress and reactive oxygen species in cardiovascular injury," *Trends in Cardiovascular Medicine*, vol. 17, no. 2, pp. 48–54, 2007.

[44] M. Kitada, Z. Zhang, A. Mima, and G. L. King, "Molecular mechanisms of diabetic vascular complications," *Journal of Diabetes Investigation*, vol. 1, no. 3, pp. 77–89, 2010.

[45] M. Brownlee, "Biochemistry and molecular cell biology of diabetic complications," *Nature*, vol. 414, no. 6865, pp. 813–820, 2001.

[46] R. P. Robertson, J. Harmon, P. O. T. Tran, and V. Poitout, "β-Cell glucose toxicity, lipotoxicity, and chronic oxidative stress in type 2 diabetes," *Diabetes*, vol. 53, supplement 1, pp. S119–S124, 2004.

[47] D. C. L. Masquio, A. De Piano, R. M. S. Campos et al., "The role of multicomponent therapy in the metabolic syndrome, inflammation and cardiovascular risk in obese adolescents," *British Journal of Nutrition*, vol. 113, no. 12, pp. 1920–1930, 2015.

[48] G. Anfossi, I. Russo, and M. Trovati, "Resistance to aspirin and thienopyridines in diabetes mellitus and metabolic syndrome," *Current Vascular Pharmacology*, vol. 6, no. 4, pp. 313–328, 2008.

[49] S. Schildknecht, B. van der Loo, K. Weber, K. Tiefenthaler, A. Daiber, and M. M. Bachschmid, "Endogenous peroxynitrite modulates PGHS-1-dependent thromboxane A2 formation and aggregation in human platelets," *Free Radical Biology and Medicine*, vol. 45, no. 4, pp. 512–520, 2008.

[50] C. Patrono, "The Multifaceted clinical readouts of platelet inhibition by low-dose aspirin," *Journal of the American College of Cardiology*, vol. 66, no. 1, pp. 74–85, 2015.

[51] L. P. Audoly, B. Rocca, J. E. Fabre et al., "Cardiovascular responses to the isoprostanes iPF(2α)-III and iPE(2)-III are mediated via the thromboxane A(2) receptor in vivo," *Circulation*, vol. 101, no. 24, pp. 2833–2840, 2000.

[52] C. Patrono, A. Falco, and G. Davì, "Isoprostane formation and inhibition in atherothrombosis," *Current Opinion in Pharmacology*, vol. 5, no. 2, pp. 198–203, 2005.

[53] G. Davì, M. T. Guagnano, G. Ciabattoni et al., "Platelet activation in obese women: role of inflammation and oxidant stress," *Journal of the American Medical Association*, vol. 288, no. 16, pp. 2008–2014, 2002.

[54] S. Magwenzi, C. Woodward, K. S. Wraith et al., "Oxidized LDL activates blood platelets through CD36/NOX2-mediated inhibition of the cGMP/protein kinase G signaling cascade," *Blood*, vol. 125, no. 17, pp. 2693–2703, 2015.

[55] A. Trostchansky, V. B. O'Donnell, D. C. Goodwin et al., "Interactions between nitric oxide and peroxynitrite during prostaglandin endoperoxide H synthase-1 catalysis: a free radical mechanism of inactivation," *Free Radical Biology and Medicine*, vol. 42, no. 7, pp. 1029–1038, 2007.

[56] N. P. Andrews, M. Husain, N. Dakak, and A. A. Quyyumi, "Platelet inhibitory effect of nitric oxide in the human coronary circulation: impact of endothelial dysfunction," *Journal of the American College of Cardiology*, vol. 37, no. 2, pp. 510–516, 2001.

[57] J. C. de Graaf, J. D. Banga, S. Moncada, R. M. J. Palmer, P. G. de Groot, and J. J. Sixma, "Nitric oxide functions as an inhibitor of platelet adhesion under flow conditions," *Circulation*, vol. 85, no. 6, pp. 2284–2290, 1992.

[58] U. Hink, H. Li, H. Mollnau et al., "Mechanisms underlying endothelial dysfunction in diabetes mellitus," *Circulation research*, vol. 88, no. 2, pp. E14–E22, 2001.

[59] A. Lerman and A. M. Zeiher, "Endothelial function: cardiac events," *Circulation*, vol. 111, no. 3, pp. 363–368, 2005.

[60] I. Russo, G. Doronzo, L. Mattiello, A. De Salve, M. Trovati, and G. Anfossi, "The activity of constitutive nitric oxide synthase is increased by the pathway cAMP/cAMP-activated protein kinase in human platelets. New insights into the antiaggregating effects of cAMP-elevating agents," *Thrombosis Research*, vol. 114, no. 4, pp. 265–273, 2004.

[61] E. Fuentes and I. Palomo, "Role of oxidative stress on platelet hyperreactivity during aging," *Life Sciences*, vol. 148, pp. 17–23, 2016.

[62] H. W. Kwon, J. H. Shin, H. J. Cho, M. H. Rhee, and H. J. Park, "Total saponin from Korean Red Ginseng inhibits binding of adhesive proteins to glycoprotein IIb/IIIa via phosphorylation of VASP (Ser(157)) and dephosphorylation of PI3K and Akt," *Journal of Ginseng Research*, vol. 40, pp. 76–85, 2016.

[63] D. Banerjee, S. Mazumder, and A. Kumar Sinha, "Involvement of nitric oxide on calcium mobilization and arachidonic acid pathway activation during platelet aggregation with different aggregating agonists," *International Journal of Biomedical Science*, vol. 12, pp. 25–35, 2016.

[64] G.-R. Wang, Y. Zhu, P. V. Halushka, T. M. Lincoln, and M. E. Mendelsohn, "Mechanism of platelet inhibition by nitric oxide: In vivo phosphorylation of thromboxane receptor by cyclic GMP-dependent protein kinase," *Proceedings of the National Academy of Sciences of the United States of America*, vol. 95, no. 9, pp. 4888–4893, 1998.

[65] J. E. Freedman, J. Loscalzo, M. R. Barnard, C. Alpert, J. F. Keaney Jr., and A. D. Michelson, "Nitric oxide released from activated platelets inhibits platelet recruitment," *The Journal of Clinical Investigation*, vol. 100, no. 2, pp. 350–356, 1997.

[66] L. A. Blatter and W. G. Wier, "Nitric oxide decreases $[Ca^{2+}]_i$ in vascular smooth muscle by inhibition of the calcium current," *Cell Calcium*, vol. 15, no. 2, pp. 122–131, 1994.

[67] P. F. Monteiro, R. P. Morganti, M. A. Delbin et al., "Platelet hyperaggregability in high-fat fed rats: a role for intraplatelet reactive-oxygen species production," *Cardiovascular Diabetology*, vol. 11, article 5, 2012.

[68] A. S. Brown, M. A. Moro, J. M. Masse, E. M. Cramer, M. Radomski, and V. Darley-Usmar, "Nitric oxide-dependent and independent effects on human platelets treated with peroxynitrite," *Cardiovascular Research*, vol. 40, no. 2, pp. 380–388, 1998.

[69] F. Paneni, J. A. Beckman, M. A. Creager, and F. Cosentino, "Diabetes and vascular disease: pathophysiology, clinical consequences, and medical therapy: part I," *European Heart Journal*, vol. 34, no. 31, pp. 2436–2443, 2013.

[70] T. E. Suslova, A. V. Sitozhevskii, O. N. Ogurkova et al., "Platelet hemostasis in patients with metabolic syndrome and type 2 diabetes mellitus: cGMP- and NO-dependent mechanisms in the insulin-mediated platelet aggregation," *Frontiers in Physiology*, vol. 6, article 501, 2015.

[71] R. A. Anderson, G. R. Ellis, Y. Y. Chirkov et al., "Determinants of platelet responsiveness to nitric oxide in patients with chronic heart failure," *European Journal of Heart Failure*, vol. 6, no. 1, pp. 47–54, 2004.

[72] A. S. Hajek, J. H. Joist, R. K. Baker, L. Jarett, and W. H. Daughaday, "Demonstration and partial characterization of insulin receptors in human platelets," *The Journal of Clinical Investigation*, vol. 63, no. 5, pp. 1060–1065, 1979.

[73] C. Falcon, G. Pfliegler, H. Deckmyn, and J. Vermylen, "The platelet insulin receptor: detection, partial characterization, and search for a function," *Biochemical and Biophysical Research Communications*, vol. 157, no. 3, pp. 1190–1196, 1988.

[74] M. Trovati, E. M. Mularoni, S. Burzacca et al., "Impaired insulin-induced platelet antiaggregating effect in obesity and in obese NIDDM patients," *Diabetes*, vol. 44, no. 11, pp. 1318–1322, 1995.

[75] M. Udvardy, G. Pfliegler, and K. Rak, "Platelet insulin receptor determination in non-insulin dependent diabetes mellitus," *Experientia*, vol. 41, no. 3, pp. 422–423, 1985.

[76] R. M. Touyz and E. L. Schiffrin, "Blunted inhibition by insulin of agonist-stimulated calcium, ph and aggregatory responses in platelets from hypertensive patients," *Journal of Hypertension*, vol. 12, no. 11, pp. 1255–1263, 1994.

[77] M. Trovati, G. Anfossi, F. Cavalot, P. Massucco, E. Mularoni, and G. Emanuelli, "Insulin directly reduces platelet sensitivity to aggregating agents. Studies in vitro and in vivo," *Diabetes*, vol. 37, no. 6, pp. 780–786, 1988.

[78] M. Trovati, G. Anfossi, P. Massucco et al., "Insulin stimulates nitric oxide synthesis in human platelets and, through nitric oxide, increases platelet concentrations of both guanosine- 3',5'-cyclic monophosphate and adenosine-3',5'-cyclic monophosphate," *Diabetes*, vol. 46, no. 5, pp. 742–749, 1997.

[79] A. I. Vinik, T. Erbas, T. Sun Park, R. Nolan, and G. L. Pittenger, "Platelet dysfunction in type 2 diabetes," *Diabetes Care*, vol. 24, no. 8, pp. 1476–1485, 2001.

[80] M. Konieczynska, K. Fil, M. Bazanek, and A. Undas, "Prolonged duration of type 2 diabetes is associated with increased thrombin generation, prothrombotic fibrin clot phenotype and impaired fibrinolysis," *Thrombosis and Haemostasis*, vol. 111, no. 4, pp. 685–693, 2014.

[81] M. Crescente, F. G. Pluthero, L. Li et al., "Intracellular trafficking, localization, and mobilization of platelet-borne thiol isomerases," *Arteriosclerosis, Thrombosis, and Vascular Biology*, vol. 36, no. 6, pp. 1164–1173, 2016.

[82] D. W. Essex, K. Chen, and M. Swiatkowska, "Localization of protein disulfide isomerase to the external surface of the platelet plasma membrane," *Blood*, vol. 86, no. 6, pp. 2168–2173, 1995.

[83] J. Zhou, Y. Wu, L. Wang et al., "The C-terminal CGHC motif of protein disulfide isomerase supports thrombosis," *The Journal of Clinical Investigation*, vol. 125, no. 12, pp. 4391–4406, 2015.

[84] C. Reinhardt, M.-L. Von Brühl, D. Manukyan et al., "Protein disulfide isomerase acts as an injury response signal that enhances fibrin generation via tissue factor activation," *Journal of Clinical Investigation*, vol. 118, no. 3, pp. 1110–1122, 2008.

[85] A. Holmgren, "Thioredoxin catalyzes the reduction of insulin disulfides by dithiothreitol and dihydrolipoamide," *The Journal of Biological Chemistry*, vol. 254, no. 19, pp. 9627–9632, 1979.

[86] G. Tsimerman, A. Roguin, A. Bachar, E. Melamed, B. Brenner, and A. Aharon, "Involvement of microparticles in diabetic vascular complications," *Thrombosis and Haemostasis*, vol. 106, no. 2, pp. 310–321, 2011.

[87] A. Raturi, S. Miersch, J. W. Hudson, and B. Mutus, "Platelet microparticle-associated protein disulfide isomerase promotes platelet aggregation and inactivates insulin," *Biochimica et Biophysica Acta (BBA)—Biomembranes*, vol. 1778, no. 12, pp. 2790–2796, 2008.

[88] J. Chiu, F. Passam, D. Butera, and P. J. Hogg, "Protein disulfide isomerase in thrombosis," *Seminars in Thrombosis and Hemostasis*, vol. 41, no. 7, pp. 765–773, 2015.

[89] N. Ramachandran, P. Root, X.-M. Jiang, P. J. Hogg, and B. Mutus, "Mechanism of transfer of NO from extracellular S-nitrosothiols into the cytosol by cell-surface protein disulfide isomerase," *Proceedings of the National Academy of Sciences of the United States of America*, vol. 98, no. 17, pp. 9539–9544, 2001.

[90] A. Zai, M. A. Rudd, A. W. Scribner, and J. Loscalzo, "Cell-surface protein disulfide isomerase catalyzes transnitrosation and regulates intracellular transfer of nitric oxide," *Journal of Clinical Investigation*, vol. 103, no. 3, pp. 393–399, 1999.

[91] P. Root, I. Sliskovic, and B. Mutus, "Platelet cell-surface protein disulphide-isomerase mediated S-nitrosoglutathione consumption," *Biochemical Journal*, vol. 382, no. 2, pp. 575–580, 2004.

[92] S. E. Bell, C. M. Shah, and M. P. Gordge, "Protein disulfide-isomerase mediates delivery of nitric oxide redox derivatives into platelets," *Biochemical Journal*, vol. 403, no. 2, pp. 283–288, 2007.

[93] T. Uehara, T. Nakamura, D. Yao et al., "S-Nitrosylated protein-disulphide isomerase links protein misfolding to neurodegeneration," *Nature*, vol. 441, no. 7092, pp. 513–517, 2006.

[94] E. J. Heckler, V. Kholodovych, M. Jain, T. Liu, H. Li, and A. Beuve, "Mapping soluble guanylyl cyclase and protein disulfide isomerase regions of interaction," *PLoS ONE*, vol. 10, no. 11, Article ID e0143523, 2015.

[95] E. J. Heckler, P.-A. Crassous, P. Baskaran, and A. Beuve, "Protein disulfide-isomerase interacts with soluble guanylyl cyclase via a redox-based mechanism and modulates its activity," *Biochemical Journal*, vol. 452, no. 1, pp. 161–169, 2013.

[96] F. R. M. Laurindo, D. C. Fernandes, A. M. Amanso, L. R. Lopes, and C. X. C. Santos, "Novel role of protein disulfide isomerase in the regulation of NADPH oxidase activity: pathophysiological implications in vascular diseases," *Antioxidants and Redox Signaling*, vol. 10, no. 6, pp. 1101–1113, 2008.

[97] D. C. Fernandes, A. H. O. Manoel, J. Wosniak Jr., and F. R. Laurindo, "Protein disulfide isomerase overexpression in vascular smooth muscle cells induces spontaneous preemptive NADPH oxidase activation and Nox1 mRNA expression: effects of nitrosothiol exposure," *Archives of Biochemistry and Biophysics*, vol. 484, no. 2, pp. 197–204, 2009.

[98] L. A. Pescatore, D. Bonatto, F. L. Forti, A. Sadok, H. Kovacic, and F. R. M. Laurindo, "Protein disulfide isomerase is required for platelet-derived growth factor-induced vascular smooth muscle cell migration, Nox1 NADPH oxidase expression, and RhoGTPase activation," *The Journal of Biological Chemistry*, vol. 287, no. 35, pp. 29290–29300, 2012.

[99] A. M. A. de Paes, S. Veríssimo-Filho, L. L. Guimarães et al., "Protein disulfide isomerase redoxdependent association with $p47^{phox}$: evidence for an organizer role in leukocyte NADPH oxidase activation," *Journal of Leukocyte Biology*, vol. 90, no. 4, pp. 799–810, 2011.

[100] C. X. C. Santos, B. S. Stolf, P. V. A. Takemoto et al., "Protein disulfide isomerase (PDI) associates with NADPH oxidase and is required for phagocytosis of *Leishmania chagasi* promastigotes by macrophages," *Journal of Leukocyte Biology*, vol. 86, no. 4, pp. 989–998, 2009.

[101] M. Janiszewski, L. R. Lopes, A. O. Carmo et al., "Regulation of NAD(P)H oxidase by associated protein disulfide isomerase in vascular smooth muscle cells," *Journal of Biological Chemistry*, vol. 280, no. 49, pp. 40813–40819, 2005.

[102] M. Janiszewski, A. O. Do Carmo, M. A. Pedro, E. Silva, E. Knobel, and F. R. M. Laurindo, "Platelet-derived exosomes of septic individuals possess proapoptotic NAD(P)H oxidase activity: a novel vascular redox pathway," *Critical Care Medicine*, vol. 32, no. 3, pp. 818–825, 2004.

[103] M. H. Gambim, A. de Oliveira do Carmo, L. Marti, S. Veríssimo-Filho, L. R. Lopes, and M. Janiszewski, "Platelet-derived exosomes induce endothelial cell apoptosis through peroxynitrite generation: experimental evidence for a novel mechanism of septic vascular dysfunction," *Critical Care*, vol. 11 article R107, 2007.

Hindawi Publishing Corporation
Oxidative Medicine and Cellular Longevity
Volume 2016, Article ID 1089364, 7 pages
http://dx.doi.org/10.1155/2016/1089364

Research Article

Resolving Contributions of Oxygen-Consuming and ROS-Generating Enzymes at the Synapse

Engy A. Abdel-Rahman, Ali M. Mahmoud, Abdullah Aaliya, Yasmine Radwan, Basma Yasseen, Abdelrahman Al-Okda, Ahmed Atwa, Eslam Elhanafy, Moaaz Habashy, and Sameh S. Ali

Center for Aging and Associated Diseases, Helmy Institute of Medical Sciences, Zewail City of Science and Technology, Giza, Egypt

Correspondence should be addressed to Sameh S. Ali; sameh.ali@zewailcity.edu.eg

Received 23 June 2016; Revised 10 October 2016; Accepted 6 November 2016

Academic Editor: Andrés Trostchansky

Disruption of cellular redox homeostasis is implicated in a wide variety of pathologic conditions and aging. A fundamental factor that dictates such balance is the ratio between mitochondria-mediated complete oxygen reduction into water and incomplete reduction into superoxide radical by mitochondria and NADPH oxidase (NOX) enzymatic activity. Here we determined mitochondrial as well as NOX-dependent rates of oxygen consumption in parallel with H_2O_2 generation in freshly isolated synaptosomes using high resolution respirometry combined with fluorescence or electrochemical sensory. Our results indicate that although synaptic mitochondria exhibit substantially higher respiratory activities (8–82-fold greater than NOX oxygen consumption depending on mitochondrial respiratory state), NADPH-dependent oxygen consumption is associated with greater H_2O_2 production (6-7-fold higher NOX-H_2O_2). We also show that, in terms of the consumed oxygen, while synaptic mitochondria "leaked" 0.71% ± 0.12 H_2O_2 during NAD^+-linked resting, 0.21% ± 0.04 during NAD^+-linked active respiration, and 0.07% ± 0.02 during FAD^+-linked active respiration, NOX converted 38% ± 13 of O_2 into H_2O_2. Our results indicate that NOX rather than mitochondria is the major source of synaptic H_2O_2. The present approach may assist in the identification of redox-modulating synaptic factors that underlie a variety of physiological and pathological processes in neurons.

1. Introduction

Substantial evidence indicates that the synapse is a center stage for brain physiology and pathology [1]. Synaptic activity is now known to produce ROS that are essential regulators of multitudes of normal physiological processes in neurons including cognition and memory. The high levels of ROS generation in synapses, alongside their high-energy demands, make them more vulnerable to stressful insults encountered in aging, neurodegenerative, neuropsychological, and neurodevelopmental disorders [2]. The relative importance of specific enzymatic sources of ROS in synapses is not fully understood. Mitochondria are one source of cellular ROS. A portion of oxygen consumed by mitochondria escapes the aerobic ATP production pathway and forms oxygen radicals primarily in the form of superoxide anions ($O_2^{\bullet-}$) that are instantaneously dismutated to hydrogen peroxide (H_2O_2) by mitochondrial superoxide dismutase (SOD) [3–5]. Since the brain is highly metabolically active organ that exhibits robust oxygen consumption [6], mitochondria respiratory activity was often considered the prime source of brain ROS. However, recent data indicate that NADPH oxidases (NOX), the enzyme family known to generate ROS as their only and primary function, are widely expressed in the CNS where they considerably contribute to ROS generation [7, 8]. While NOX2 is found principally in phagocytes, recent reports showed that NOX2 and homologs (NOX1, NOX3–5, Duox1, and 2) are expressed in a miscellaneous array of tissues and cell types. NOX2 and NOX4 have been characterized in the neurons of adult mouse nervous system, potentially contributing to wide range of physiologic functions and to several neurological disorders [9]. Although it is likely that the initial product of all NOX enzymes is $O_2^{\bullet-}$, which spontaneously dismutates to H_2O_2 *via* superoxide dismutase (SOD), it is now clear that H_2O_2 is predominantly produced by several NOX isoforms, particularly NOX4, Duox1, and

Doux2. This apparent H_2O_2 generation may be attributed to the rapid dismutation of $O_2^{\bullet-}$. However, recent reports showed that for, NOX4, H_2O_2 generation is mediated by the third extracellular loop of the enzyme (reviewed in [10]).

Synaptic localization of mitochondria [11, 12] and some NOX isoforms have been documented [8, 13]. Synaptosomes (isolated nerve terminals), which have been extensively used for studying brain synaptic physiology, were found to contain mitochondria with distinct biophysical properties from those of neuronal body mitochondria [11, 12]. NOX2 and NOX4 are also expressed in synaptosomal plasma membrane [8, 13] and we previously reported that synaptosomes exhibit NADPH-dependent oxygen consumption [13]. Given the critical role of NOX and mitochondria in cellular ROS production and the presence of some NOX isoforms and distinctive mitochondria in synaptosomes, it is of paramount importance to characterize the interplay between their respiratory functions and ROS generation in synapses. Our previous study using spin-trapping electron paramagnetic resonance spectroscopy showed that NOX rather than mitochondria was the main contributor of synaptic superoxide generation [8]. However, the relationship between mitochondria and/or NOX-dependent O_2 consumption and resulting ROS generation is still ambiguous, despite the long-held idea that augmented energy expenditure will result in higher ROS generation [14]. Much vagueness exists over the relationship between the rate of oxygen consumption and the production of reactive oxygen species (ROS) such as hydrogen peroxide by mitochondria and NOX in synapses. Here, we use combined high resolution respirometry and fluorometry to simultaneously monitor oxygen consumption and H_2O_2 production by synaptosomal mitochondria and NOX. We will describe for the first time how the well-established Amplex Red assay or an electrochemical sensor can be used to quantify H_2O_2 production by NOX combined with the simultaneous measurement of NOX-dependent oxygen consumption by high resolution respirometry.

2. Materials and Methods

2.1. Animals. C57BL6/C males (6 weeks old) were purchased from Misr University for Science and Technology (Cairo, Egypt) and were housed for at least one month in Zewail City animal facility until sacrificed. All animals were maintained in pathogen-free, individually ventilated cages in 12 h light/12 h dark cycles at 24°C and 50% relative humidity, with free access to water and standard laboratory rodent chow. Animals were decapitated following quick cervical dislocation which is an approved and considered humane method of small animal euthanasia by the American Veterinary Medical Association (AVMA) (https://www.avma.org/KB/Policies/Documents/euthanasia.pdf). All experiments were conducted in adherence to the NIH Institutional Animal Care and Use Committee guidelines https://grants.nih.gov/grants/olaw/GuideBook.pdf.

2.2. Isolation of Synaptosomes. Isolation of synaptosomes was performed as previously described [13]. Briefly, brains were quickly removed; forebrains were dissected and homogenized using a Dounce homogenizer in ice-cold isolation buffer (0.32 M sucrose, 1 mM EDTA, 10 mM Tris-HCl buffer, pH 7.4, 10 mM glucose). The homogenate was then centrifuged at 3,100 ×g for 3 min at 4°C. The supernatant was removed and the pellet was resuspended in half the volume of isolation buffer, then homogenized again, and recentrifuged. The supernatant was collected and mixed with percoll to a final concentration of 15% by volume. The mixture was then layered onto a step gradient of 23% and 40% percoll. Centrifugation was then performed at 16,000 rpm for 5 min at 4°C. The band at the interface of the two layers was collected and rinsed in isolation buffer, followed by centrifugation and resuspension in synaptosomal buffer (120 mM NaCl, 4.7 mM Kcl, 2.2 mM $CaCl_2$, 1.2 mM $MgCl_2$, 25 mM HEPES, 1.2 mM $MgSO_4$, 1.2 mm KH_2PO_4, and 10 mM glucose).

2.3. Determination of NOX Activity in Synaptosomes by Oroboros® High Resolution O2k Oxygraph. NOX activity in synaptosomal preparations was determined by measuring, in the same sample, NADPH-induced oxygen consumption and the associated rate of hydrogen peroxide formation simultaneously using Amplex Red fluorescence/or H_2O_2 electrochemical HPO-ISO-2 mm sensor (WPI, Sarasota, USA) which is compatible with the O2k-NO Amp-Module (Oroboros®).

2.4. Measurements of NADPH Oxidase Respiratory Rates. NADPH oxidase respiratory assessments (and hydrogen peroxide determinations) were carried out at 37°C using the high resolution respirometry system Oxygraph-2K (Oroboros Instruments, Innsbruck, Austria) in 2 mL chambers. Before starting the experiment, calibration at air saturation was performed by allowing the respiration medium, MIR05, to equilibrate with air in the oxygraph chambers and be stirred at 540 to 560 rpm for 30 to 40 min, until a stable signal was detected. Synaptosomal protein (0.2 mg) was added to the respiration medium in the chamber. Activation of NOX was evoked by the addition of 200 μM NADPH (3 doses). The rates of oxygen consumption were calculated as the negative time derivative of oxygen concentration. The rate of NOX-dependent hydrogen peroxide formation was detected in parallel to oxygen consumption in the same sample by using two different approaches. In the fluorometric method, horseradish peroxidase (1 U per mL) and Amplex Ultra-Red fluorescent dye (10 μM) were utilized. The excitation wavelength was 525 nm and fluorescence detection was at 587 nm. For determination of NOX-dependent hydrogen peroxide production by amperometric detection in parallel with oxygen consumption, the fluorescent dye was substituted by inserting an HPO-ISO-2 WPI electrode in the O2k chamber. Signals were calibrated using known amounts of hydrogen peroxide that were exogenously added by the end of each run. At the peak of oxygen-consuming, HPO-producing NADPH activity, specific NOX inhibitor VAS-2870 (10 μM) or ebselen (10 μM) was added to confirm that the activity recorded was mediated by NOX. Data acquisition and analysis were performed with the DatLab® software, version 4.3 (Oroboros Instruments). This enables continuous

monitoring and recording of the oxygen concentration in the chambers as well as of the derived oxygen flux over time, normalized for the amount of homogenized tissue acquired at rates of 0.5–1 Hz.

2.5. Measurements of Synaptic Mitochondrial Oxygen Consumption and Hydrogen Peroxide Production. After blocking NOX activity, synaptosomes were permeabilized by the addition of saponin (25 μg/mL). State 4 respiration was triggered by adding the following substrates: 10 mM pyruvate + 10 mM malate + 10 mM glutamate. State 3 respiration was then induced by adding ADP (1 mM) for measuring OXPHOS I followed by 10 mM succinate to assess OXPHOS I+II. Parallel assessment of oxygen consumption and hydrogen peroxide formation by synaptosomal mitochondria was performed as described above. In a control experiment, we confirmed that outer mitochondrial membrane integrity was not affected by the saponification process as exogenously added cytochrome c (10 μM) did not impact mitochondrial OCR (data not shown).

3. Results

3.1. NADPH Oxidases Are Minor Oxygen Consumers but Major Hydrogen Peroxide Producers in Synaptosomes. We have previously reported the detection of oxygen consumption by synaptosomal NOX using Oxygraphy [8, 13]. Here, we utilized high resolution respirometry (Oroboros O2k-Station) to follow NADPH-induced oxygen consumption in isolated C57BL6/C male synaptosomes. Additionally, we simultaneously used the O2k-Fluorometer or the HPO sensor, for the first time, to monitor the rate of hydrogen peroxide production in the same sample. In the fluorometric assay the highly sensitive AR/HRP system has been used for assessment of H_2O_2 production by recording changes in resorufin fluorescence [15]. Since HRP has been shown to catalyze the oxidation of NADPH with subsequent generation of H_2O_2 [16], we compared NOX-dependent oxygen consumption and hydrogen peroxide production obtained by using the AR/HRP system and the HPO sensor. In Figures 1(a)–1(f), we show representative traces of NADPH-induced, VAS-2870-inhibitable (a, c, e), or ebselen-inhibitable (b, d, f) synaptosomal oxygen consumption (a, b) and parallel hydrogen peroxide production obtained using AR/HRP fluorometric assay (c and d), or Oroboros-compatible amperometric HPO sensor (e, f). Using the AR/HRP assay, we could continuously monitor H_2O_2 generated during NOX activation. We calibrated our H_2O_2 fluorescence signal using high resolution measurements of oxygen production due to selective decomposition of H_2O_2 by exogenous catalase (not shown). This allowed us to quantify the O_2 proportions that are converted to H_2O_2 in real time. Previous studies showed that NADPH can generate H_2O_2 nonenzymatically through its interaction with HRP [17]. In this regard, we found that, in the absence of added synaptosomes, the addition of NADPH alone in our AR/HRP assay resulted in enhanced fluorescence. However, under our experimental conditions, this increase in background fluorescence was far less than the resorufin fluorescence detected in the presence of synaptosomes. Our results are in tune with another study utilizing the AR/HRP system for microsomal enzymes activity, which showed that increased resorufin fluorescence resulting from the interaction between HRP and NADPH was less than 2–5% of the fluorescence monitored in the presence microsomal enzymes [17].

After subtraction of background fluorescence, there were no significant differences in oxygen consumption by synaptosomal NOX between fluorometric ($n = 5$) and electrochemical ($n = 5$) experiments. As shown in Figure 1(g), the hydrogen peroxide production by synaptosomal NOX did not significantly differ between the two experimental approaches. Using O2k combined with the AR/HRP fluorescence module, the addition of 200 μM NADPH (3 doses) to synaptosomal proteins (0.2 mg) in our study resulted in absolute rates of oxygen consumption and H_2O_2 production of 0.0055 ± 0.0011 μM/s and 0.0018 ± 0.0005 μM/s H_2O_2. Similar rates of H_2O_2 production were obtained when the AR/HRP system was replaced by HPO electrode 0.0023 ± 0.0005 μM/s H_2O_2, confirming that there was minor or no interference from components of the reaction mix.

Both VAS-2870 and ebselen significantly inhibited NADPH-induced oxygen consumption by about 50–75% ($N = 5$–8, $p < 0.05$). However, while VAS-2870 reduced H_2O_2 production proportionately by ~60% ($N = 8$, $p < 0.05$), we observed a strong elimination of hydrogen peroxide by ebselen, which is in tune with reports showing that the later possesses glutathione peroxidase activity (reviewed in [18]).

3.2. Relative to NOX, Mitochondria Are Major Oxygen Consumers but Minor Hydrogen Peroxide Producers in Synaptosomes. To investigate the relative importance of NOX and mitochondria in energy expenditure and H_2O_2 production at the synapse, we employed isolated nerve terminals (synaptosomes) that contain both pre- and postsynaptic vesicles. Synaptosomal preparations are populated with NOX isoforms and mitochondria of characteristic biophysical properties. Experiments typically involved parallel measurements of oxygen consumption and hydrogen peroxide production using high resolution respirometry combined with the HRP/Amplex Red fluorescence assay. This approach allows one to follow both NOX and mitochondrial activities in synaptosomes and estimate resultant hydrogen peroxide production in the same sample. When NADPH was added to synaptosomes, oxygen consumption and hydrogen peroxide production due to NOX activity were triggered as described above. This activity was abolishable by the specific NOX inhibitor VAS-2870 (10 μM) or ebselen (10 μM). Subsequent addition of pyruvate, malate, and glutamate to synaptosomes elicited oxygen consumption due to NAD^+-linked resting mitochondrial metabolic activity (Figure 2(a)) while also "leaking" hydrogen peroxide in parallel (Figure 2(b)). In a separate experiment, we confirmed the involvement of synaptosomal mitochondria in the substrate-triggered oxygen consumption (Figure 2(c)). As can be seen in Figure 2(c), both NAD^+- and FAD^+-linked respiratory activities were completely inhibitable by oligomycin (complex V), rotenone

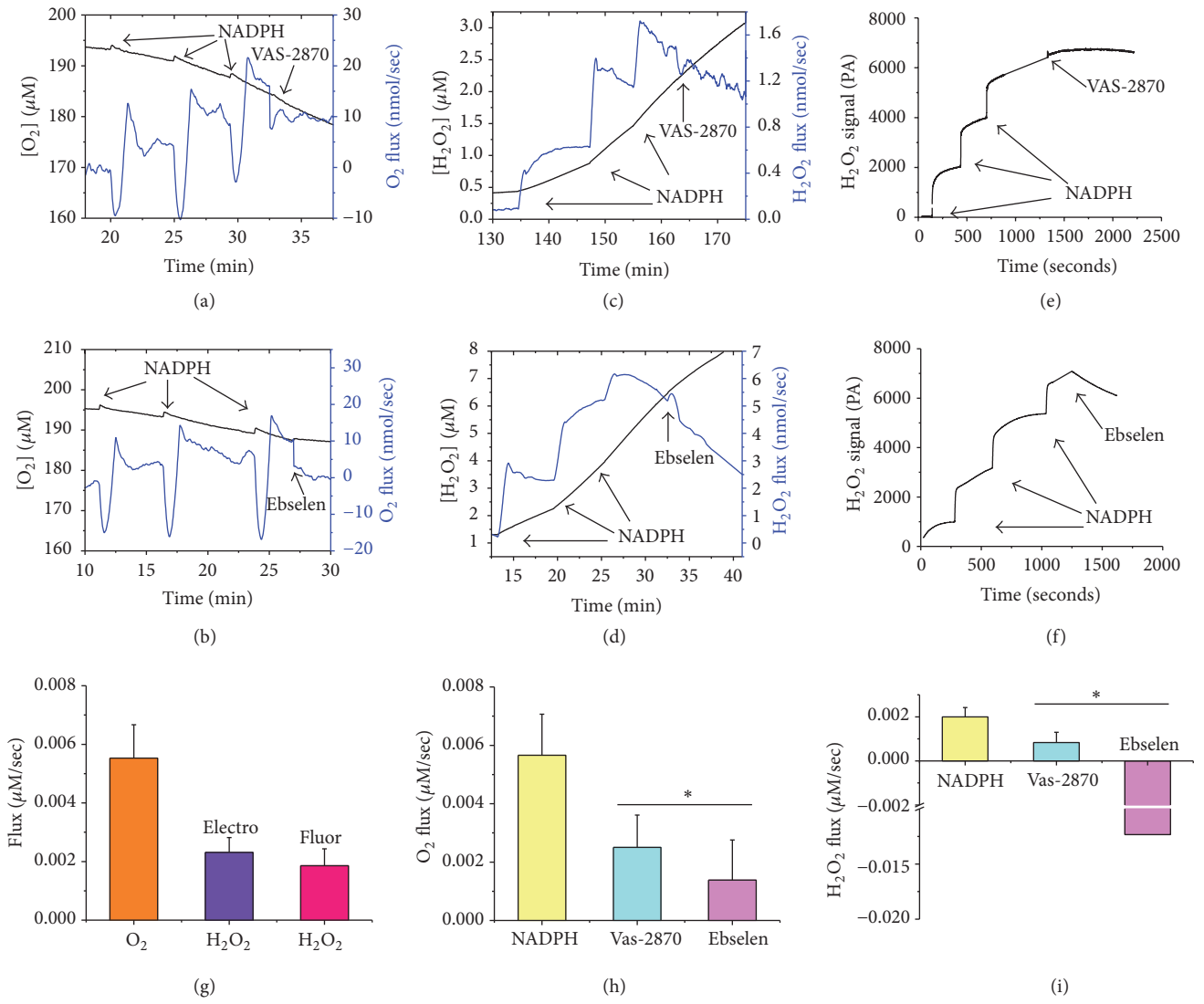

FIGURE 1: NADPH oxidases are actively consuming O_2 and producing H_2O_2 in freshly isolated synaptosomes. Successive injections of 200 μM deoxygenated NADPH batches on synaptosomes triggered reproducible oxygen consumption (a, b) and H_2O_2 production as detected simultaneously by HRP/Amplex Red fluorescence (c, d) or using electrochemical sensor (e, f). The effects of inclusion of the NOX inhibitors Vas-2870 (10 μM) (a, c, e) or ebselen (10 μM) (b, d, f) are shown. (g) Quantifications of the overall O_2 and H_2O_2 fluxes induced by the three added doses of NADPH. The two methods of H_2O_2 detection yielded similar results. Both of the added NOX inhibitors, VAS-2870 (10 μM) and Ebselen (10 μM), caused significant inhibition of NADPH-triggered oxygen flux (h) and H_2O_2 flux (i). Values are given as mean ± SEM, paired Student t-test was used for paired groups to determine statistical significance in comparison with NADPH-induced activity, $^*p < 0.05$, and $n = 5$–8.

(complex I), and Antimycin A (complex III) which demonstrate the presence of viable mitochondria within the prepared synaptosomes. Quantifications of the results in Figures 2(a) and 2(b) over $n = 7$ independent synaptosomal preparations are given in Figures 2(d) and 2(e). It can be readily seen that NOX-mediated hydrogen peroxide production was 38.85% ± 13 of NOX-dependent oxygen consumption detected in the same samples (Figure 2(f)). In contrast, synaptosomal mitochondrial oxygen consumptions during state 4, state 3 (OXPHOS I), and state 3 (OXPHOS I+II) were only associated with 0.71% ± 0.12, 0.20% ± 0.04, and 0.075% ± 0.020, H_2O_2 production, respectively (Figure 2(f)). Additionally, Figure 2(d) shows that the rates of oxygen consumption during state 4 (*Leak I*), state 3 (OXPHOS I), and state 3 (OXPHOS I+II) in synaptosomal mitochondria are significantly higher than NOX-dependent oxygen consumption rate in synaptosomes (0.041 ± 0.007 μM/s, 0.117 ± 0.050 μM/s, 0.408 ± 0.120 μM/s, 0.005 ± 0.002 μM/s, resp., for mitochondria, and NOX, $n = 7$). However, Figure 2(e) shows that NOX-dependent H_2O_2 production rate in synaptosomes is higher than H_2O_2 generated during state 4 (*Leak I*), state 3 (OXPHOS I), and state 3 (OXPHOS I+II) by synaptosomal mitochondria (0.0020 ± 0.0007 μM/s; 0.00030 ± 0.00005 μM/s; 0.00025 ± 0.00005 μM/s; 0.00030 ± 0.00008 μM/s, resp., for NOX and mitochondria $n = 7$, $p < 0.05$).

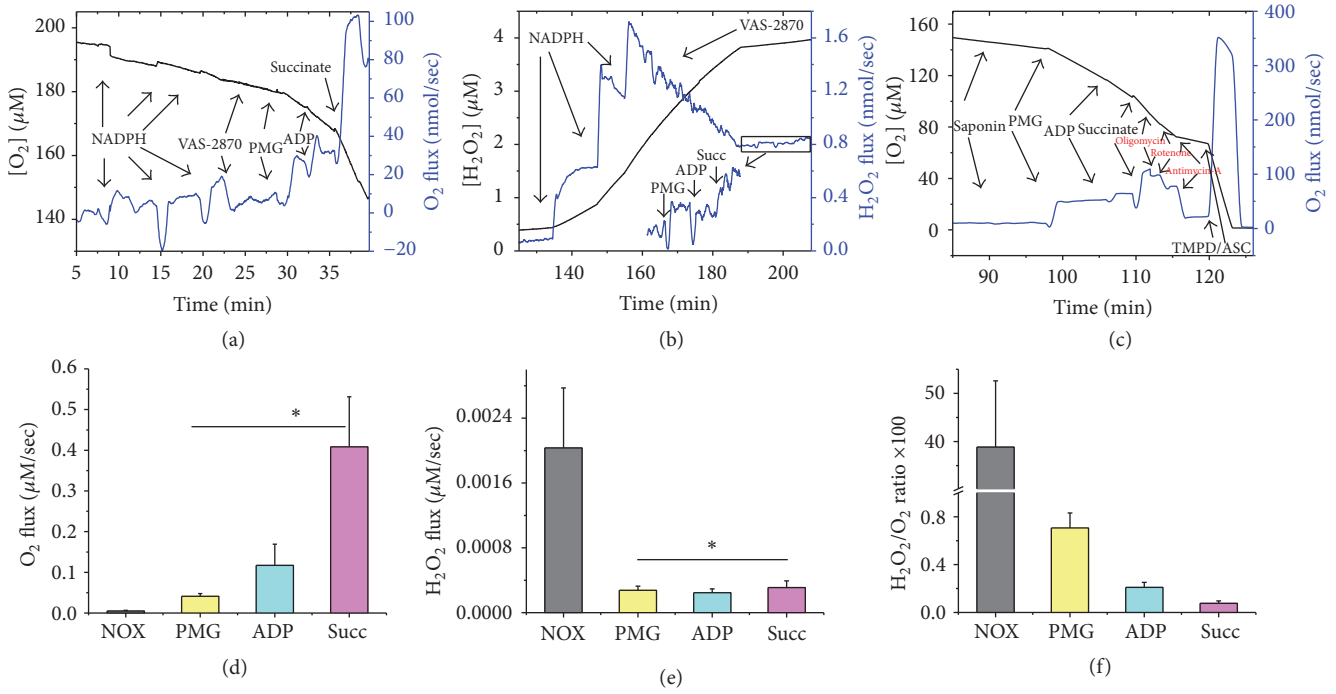

Figure 2: Comparing NADPH oxidase and mitochondrial activities in isolated synaptosomes using high resolution respirometry and fluorescence spectroscopy. (a, b) Representative traces of NADPH oxidase and synaptosomal mitochondria activity assessed by simultaneous measurement of rates of oxygen consumption (a) and H_2O_2 production (b) using high resolution respirometry combined with HRP/Amplex Red, in the same sample under identical conditions except that NOX substrate is substituted by mitochondria ones. Activities were monitored as described in Figure 1's legend. Mitochondrial resting (state 4) respiration was triggered by the addition of 10 mM pyruvate + 10 mM malate + 10 mM glutamate. Active phosphorylating (state 3) respiration was induced by adding 1 mM ADP (OXPHOS I) followed by 10 mM succinate for (OXPHOS I+II). (c) Representative traces depicting ETC substrate-specific O_2 utilization by mitochondria in saponin-permeabilized synaptosomes during substrate-uncoupler inhibitor-titration. (d, e) Quantifications of the sum of the absolute values of O_2 (d) and H_2O_2 (e) fluxes following NOX and mitochondria activations. (f) Percept ratios of the H_2O_2-produced to the O_2-consumed. Values are given as mean ± SEM, paired Student t-test was used to determine statistical significance in comparison with NADPH-induced collective activity, and $n = 7$. $^*p < 0.05$.

4. Discussion

Probing the relation between oxygen consumption and ROS production makes it possible to understand how specific ROS sources might shape cellular physiology and pathology [19, 20]. The use of the highly stable Clark-type oxygen electrode in the Oroboros O2k Station with its superb picomole sensitivity in addition to the fluorescence module designed to follow H_2O_2 in the same sample has enabled the interrogation of each mitochondrial respiratory state while quantifying ROS leakage simultaneously [15]. We now demonstrate that this approach can also be used successfully for parallel monitoring of NOX-dependent oxygen consumption as well as H_2O_2 production in synaptosomes. Our findings reveal for the first time a negative correlation between synaptic energy utilization and ROS production and provide evidence that synaptosomal NOX consumes significantly less oxygen while producing remarkably more synaptic H_2O_2. However, synaptosomal mitochondria were more effectively utilizing oxygen while producing smaller ROS amounts.

We have previously reported a synaptic localization of NOX2 and NOX4 isoforms as well as NOX-dependent oxygen consumption in synaptosomes [13]. In the present study, we describe the use of a highly sensitive assay using AR/HRP and an electrochemical approach to quantify H_2O_2 production by NOX in synaptosomes combined with the simultaneous measurement of NOX-dependent oxygen consumption by high resolution respirometry. In mammalian cells, H_2O_2 was found to play a fundamental role in the redox regulation of several physiological and pathological processes. Although it is likely that H_2O_2 arises as a major by-product of mitochondrial respiratory activity with complex I being the main source of mitochondrial ROS [21], it has been increasingly recognized that NADPH oxidase is a key source of cellular ROS. Among the ROS generated, H_2O_2 is produced by NOX activity [22]. Despite the fact that the rate of ROS generation is not governed by the oxygen availability in its physiological range, ROS are produced as a consequence of oxygen consumption. It is therefore of fundamental importance to resolve how much of the total oxygen consumed by NOX and mitochondria are directed toward ROS formation. In this context, we used the high resolution O2k sensor combined with AR/HRP system to follow the relative contributions of mitochondria and NOX to the process of hydrogen peroxide generation in synaptosomes.

Our study revealed that NOX considerably contributes to the levels of hydrogen peroxide in synaptosomes. However, the higher level of NOX-dependent H_2O_2 was associated with a lower oxygen consumption rate. We also found that 38.85% of oxygen consumed by synaptic NOX is converted to H_2O_2. The initial product of all NOX enzymes is $O_2^{\bullet-}$, which spontaneously dismutates to H_2O_2, (reviewed in: [10]). H_2O_2 is predominantly detected for several NOX isoforms, particularly NOX4, Duox1, and Doux2. This apparent direct H_2O_2 generation may be attributed to the rapid dismutation of $O_2^{\bullet-}$. The ~0.4 stoichiometry of H_2O_2 formation relative to NOX-dependent oxygen consumption obtained in our study is in accordance with the previously suggested superoxide dismutase-like mechanism involving two oxygen binding/reduction steps for every H_2O_2 generated in NOX4 active site [23]. This is inconsistent with a proposed mechanism involving single oxygen molecule binding, followed with reduction by heme center in two sequential electron transfer steps, to produce superoxide intermediate [24]. Therefore, while either mechanism could participate in the generation of small amounts of superoxide [24], our results are in agreement with a mechanism involving two oxygen binding/reduction steps. However, since it is not possible to dismiss that the detected H_2O_2 is resulting from the dismutation of $O_2^{\bullet-}$ by synaptosomal SOD, both NOX2 and NOX4 might be contributing to the generation of NADPH-induced H_2O_2 signals. We attempted to disentangle NOX isoforms contributions using the established NOX inhibitors VAS-2870 (preassembled NOX2 and NOX4 inhibitor) and ebselen (proposed as a potent NOX2 inhibitor), recently reviewed in [25]. Interestingly, 10 μM VAS-2870 inhibited ~50% of NADPH-induced activity whether it is recorded as oxygen consumption or as H_2O_2 production (Figures 1(h) and 1(i)). Meanwhile, 10 μM ebselen quenched ~75% of NADPH-induced oxygen consumption while completely reversing H_2O_2 signal (Figures 1(h) and 1(i)). This is consistent with previous reports that selenium-containing ebselen is able to consume hydrogen peroxide in a catalytic cycle that utilizes thiol-containing compounds, such as glutathione, as a substrate (reviewed in [18]). Although not sufficient to quantify individual contributions, these results indicate that both NOX2 and NOX4 are important contributors to the observed NADPH-induced activities in synaptosomes.

Finally, we evaluated in the same synaptosomal sample the proportion of the mitochondrially utilized oxygen that converts into hydrogen peroxide during complex I-mediated resting respiration and complex I and complex I+II-mediated active respiration. Mitochondria residing at synapses play crucial role in synaptic function and failure. Synaptic mitochondria have biophysical properties that are distinct from that of their siblings in the soma [11, 12]. Our results revealed that only 0.71% of oxygen consumed by synaptic mitochondria during complex I resting respiration was converted to H_2O_2, which is not markedly different from that previously reported for isolated rat brain mitochondria. That is, previous report showed that 0.79% percent of the total oxygen consumption by isolated rat brain mitochondria produced hydrogen peroxide during complex I resting respiration [26]. The underlying mechanism of the observed low rates of hydrogen peroxide production by mitochondria compared to NOX may involve a respiratory protection conferred by slips (intrinsic decoupling) in mitochondrial redox proton pumps. In fact, consensus from several studies demonstrating that intrinsic decoupling between the flow of electrons and proton translocation prevents excessive electronegativity of redox carriers in complexes I and III, which lowers free $[O_2]$ and retards the generation of $O_2^{\bullet-}$. In addition, respiratory protection conveyed by "mild" uncoupling that is caused by H^+ leakage across the mitochondrial membrane could contribute to the observed lower rates of mitochondrial hydrogen peroxide production in synaptosomes. In line with this reasoning, it has been shown that a minor reduction in $\Delta\Psi$, due to mild uncoupling, would, in fact, prevent $O_2^{\bullet-}$ formation. Therefore intrinsic decoupling and mild uncoupling were suggested to have a natural antioxidant effect, contributing to lower rates of mitochondrial hydrogen peroxide production [reviewed in [27]]. No previous study has investigated the relationship between the rate of oxygen consumption and the production of reactive oxygen species (ROS) such as hydrogen peroxide by synaptosomal mitochondria and NOX. Therefore, we believe that this is the first report that addressed in detail the interplay between synaptic ROS generation by NADPH oxidases and mitochondria and their respiratory functions.

5. Conclusion

We employed high resolution respirometry equipped with a fluorescence detection module to simultaneously monitor oxygen consumption and H_2O_2 production by NADPH oxidase and mitochondria in synaptosomes. Using this assay, we showed that NOX consumes less oxygen and produces more ROS, contributing considerably to synaptic H_2O_2 generation. However, mitochondria at synapses were utilizing oxygen more efficiently while producing smaller ROS amounts. Our results may eventually assist in understanding the synaptic mechanisms by which specific ROS sources are implicated in neuronal physiological as well as pathological processes.

Disclosure

Engy A. Abdel-Rahman is on leave from the Pharmacology Department, School of Medicine, Assiut University, Assiut, Egypt. Sameh S. Ali is on leave from the Department of Anesthesiology, The University of California, San Diego.

Competing Interests

No competing interests are declared for any of the contributing authors and received funding did not lead to any conflict of interests regarding the publication of this manuscript.

Acknowledgments

The authors thank Mr. Mahmoud Aboulsauod and Mr. Abdelrahman Khalifa for logistical and technical help during this study. This work was supported by a National Research

Grant no. 6364 by the Science and Technology Development Fund, Egypt, awarded to SSA.

References

[1] C. Lüscher and J. T. Isaac, "The synapse: center stage for many brain diseases," *Journal of Physiology*, vol. 587, no. 4, pp. 727–729, 2009.

[2] M. P. Mattson and D. Liu, "Energetics and oxidative stress in synaptic plasticity and neurodegenerative disorders," *Neuro-Molecular Medicine*, vol. 2, no. 2, pp. 215–231, 2002.

[3] S. Dröse and U. Brandt, "Molecular mechanisms of superoxide production by the mitochondrial respiratory chain," *Advances in Experimental Medicine and Biology*, vol. 748, pp. 145–169, 2012.

[4] A. J. Kowaltowski, N. C. de Souza-Pinto, R. F. Castilho, and A. E. Vercesi, "Mitochondria and reactive oxygen species," *Free Radical Biology and Medicine*, vol. 47, no. 4, pp. 333–343, 2009.

[5] E. B. Tahara, F. D. T. Navarete, and A. J. Kowaltowski, "Tissue-, substrate-, and site-specific characteristics of mitochondrial reactive oxygen species generation," *Free Radical Biology and Medicine*, vol. 46, no. 9, pp. 1283–1297, 2009.

[6] C. A. Massaad and E. Klann, "Reactive oxygen species in the regulation of synaptic plasticity and memory," *Antioxidants and Redox Signaling*, vol. 14, no. 10, pp. 2013–2054, 2011.

[7] Q.-G. Zhang, M. D. Laird, D. Han et al., "Critical role of nadph oxidase in neuronal oxidative damage and microglia activation following traumatic brain injury," *PLoS ONE*, vol. 7, no. 4, Article ID e34504, 2012.

[8] S. S. Ali, J. W. Young, C. K. Wallace et al., "Initial evidence linking synaptic superoxide production with poor short-term memory in aged mice," *Brain Research*, vol. 1368, pp. 65–70, 2011.

[9] D. W. Infanger, R. V. Sharma, and R. L. Davisson, "NADPH oxidases of the brain: distribution, regulation, and function," *Antioxidants and Redox Signaling*, vol. 8, no. 9-10, pp. 1583–1596, 2006.

[10] Z. Nayernia, V. Jaquet, and K.-H. Krause, "New insights on NOX enzymes in the central nervous system," *Antioxidants and Redox Signaling*, vol. 20, no. 17, pp. 2815–2837, 2014.

[11] M. O. Breckwoldt, A. A. Armoundas, M. A. Aon et al., "Mitochondrial redox and pH signaling occurs in axonal and synaptic organelle clusters," *Scientific Reports*, vol. 6, article 2023251, 2016.

[12] M. R. Brown, P. G. Sullivan, and J. W. Geddes, "Synaptic mitochondria are more susceptible to Ca^{2+} overload than non-synaptic mitochondria," *The Journal of Biological Chemistry*, vol. 281, no. 17, pp. 11658–11668, 2006.

[13] M. M. Behrens, S. S. Ali, D. N. Dao et al., "Ketamine-induced loss of phenotype of fast-spiking interneurons is mediated by NADPH-oxidase," *Science*, vol. 318, no. 5856, pp. 1645–1647, 2007.

[14] Y. Li, Y. Xia, J. Li et al., "Prognostic nomograms for pre- and postoperative predictions of long-term survival for patients who underwent liver resection for huge hepatocellular carcinoma," *Journal of the American College of Surgeons*, vol. 221, no. 5, pp. 962–974.e4, 2015.

[15] G. Krumschnabel, M. Fontana-Ayoub, Z. Sumbalova et al., "Simultaneous high-resolution measurement of mitochondrial respiration and hydrogen peroxide production," *Methods in Molecular Biology*, vol. 1264, pp. 245–261, 2015.

[16] J. L. Michot, A. Virion, D. Deme, S. De Prailaune, and J. Pommier, "NADPH oxidation catalyzed by the peroxidase/H_2O_2 system. Guaiacol-mediated and scopoletin-mediated oxidation of NADPH to $NADP^+$," *European Journal of Biochemistry*, vol. 148, no. 3, pp. 441–445, 1985.

[17] V. Mishin, J. P. Gray, D. E. Heck, D. L. Laskin, and J. D. Laskin, "Application of the Amplex red/horseradish peroxidase assay to measure hydrogen peroxide generation by recombinant microsomal enzymes," *Free Radical Biology and Medicine*, vol. 48, no. 11, pp. 1485–1491, 2010.

[18] M. J. Parnham and H. Sies, "The early research and development of ebselen," *Biochemical Pharmacology*, vol. 86, no. 9, pp. 1248–1253, 2013.

[19] G. S. Shadel and T. L. Horvath, "Mitochondrial ROS signaling in organismal homeostasis," *Cell*, vol. 163, no. 3, pp. 560–569, 2015.

[20] E. Abdel-Rahman, A. M. Mahmoud, A. M. Khalifa, and S. S. Ali, "Physiological and pathophysiological ROS as probed by EPR spectroscopy: the underutilized research window on muscle aging," *The Journal of Physiology*, vol. 594, no. 16, pp. 4591–4613, 2016.

[21] D. F. Stowe and A. K. S. Camara, "Mitochondrial reactive oxygen species production in excitable cells: modulators of mitochondrial and cell function," *Antioxidants and Redox Signaling*, vol. 11, no. 6, pp. 1373–1414, 2009.

[22] G. Groeger, C. Quiney, and T. G. Cotter, "Hydrogen peroxide as a cell-survival signaling molecule," *Antioxidants and Redox Signaling*, vol. 11, no. 11, pp. 2655–2671, 2009.

[23] I. Takac, K. Schröder, L. Zhang et al., "The E-loop is involved in hydrogen peroxide formation by the NADPH oxidase Nox4," *The Journal of Biological Chemistry*, vol. 286, no. 15, pp. 13304–13313, 2011.

[24] Y. Nisimoto, B. A. Diebold, D. Constentino-Gomes, and J. D. Lambeth, "Nox4: a hydrogen peroxide-generating oxygen sensor," *Biochemistry*, vol. 53, no. 31, pp. 5111–5120, 2014.

[25] E. Cifuentes-Pagano, D. N. Meijles, and P. J. Pagano, "The quest for selective nox inhibitors and therapeutics: challenges, triumphs and pitfalls," *Antioxidants and Redox Signaling*, vol. 20, no. 17, pp. 2741–2754, 2014.

[26] A. A. Starkov, "The role of mitochondria in reactive oxygen species metabolism and signaling," *Annals of the New York Academy of Sciences*, vol. 1147, pp. 37–52, 2008.

[27] S. Papa and V. P. Skulachev, "Reactive oxygen species, mitochondria, apoptosis and aging," *Molecular and Cellular Biochemistry*, vol. 174, no. 1-2, pp. 305–319, 1997.

Hindawi Publishing Corporation
Oxidative Medicine and Cellular Longevity
Volume 2016, Article ID 2386068, 17 pages
http://dx.doi.org/10.1155/2016/2386068

Research Article

Thioredoxin-Interacting Protein Mediates NLRP3 Inflammasome Activation Involved in the Susceptibility to Ischemic Acute Kidney Injury in Diabetes

Ye Da Xiao, Ya Yi Huang, Hua Xin Wang, Yang Wu, Yan Leng, Min Liu, Qian Sun, and Zhong-Yuan Xia

Department of Anesthesiology, Renmin Hospital of Wuhan University, 99 Zi Yang Road, Wuhan, Hubei 430060, China

Correspondence should be addressed to Zhong-Yuan Xia; xiazhongyuan2005@aliyun.com

Received 27 April 2016; Revised 10 August 2016; Accepted 19 September 2016

Academic Editor: Eric E. Kelley

Kidney in diabetic state is more sensitive to ischemic acute kidney injury (AKI). However, the underlying mechanisms remain unclear. Herein, we examined the impact of diabetes mellitus on thioredoxin-interacting protein (TXNIP) expression and whether mediated NLRP3 activation was associated with renal ischemia/reperfusion- (I/R-) induced AKI. In an *in vivo* model, streptozotocin-induced diabetic rats showed higher susceptibility to I/R injury with increased TXNIP expression, which was significantly attenuated by resveratrol (RES) treatment (10 mg/kg intraperitoneal daily injection for 7 consecutive days prior to I/R induction). RES treatment significantly inhibited TXNIP binding to NLRP3 in diabetic rats subjected to renal I/R injury. Furthermore, RES treatment significantly reduced cleaved caspase-1 expression and production of IL-1β and IL-18. In an *in vitro* study using cultured human kidney proximal tubular cell (HK-2 cells) in high glucose condition (HG, 30 mM) subjected to hypoxia/reoxygenation (H/R), HG combined H/R (HH/R) stimulated TXNIP expression which was accompanied by increased NLRP3 expression, ROS generation, caspase-1 activity and IL-1β levels, and aggravated HK-2 cells apoptosis. All these changes were significantly attenuated by TXNIP RNAi and RES treatment. In conclusion, our results demonstrate that TXNIP-mediated NLRP3 activation through oxidative stress is a key signaling mechanism in the susceptibility to AKI in diabetic models.

1. Introduction

It is estimated that 1-2% of new hospital admissions and 2–7% of cases acquired during hospital stays are due to acute kidney injury (AKI) [1]. The major risk factors for AKI include diabetes mellitus (DM), hypertension, and congestive heart failure [2]. In developed countries, DM is the primary cause of chronic kidney disease (CKD) and diabetic nephropathy (DN) is an important complication of diabetic patients [3]. Furthermore, studies have shown that hyperglycemia induces oxidative stress in kidney cells [4, 5]. The major causes of AKI include ischemia, hypoxia, or nephrotoxicity [6]. Diabetic patients are also at a risk of requiring hospitalization and undergoing AKI [7], but the underlying mechanisms remain unknown. Studies in rat models of type-1 diabetes indicated that diabetic rats had increased susceptibility to AKI compared to nondiabetic rats [8, 9]. Another research study suggested that inflammation was involved in the mechanism [10], while Gao et al. further demonstrated that TNF-α mediated the increased susceptibility to ischemic AKI in diabetes [11].

The Nod-like receptor protein 3 (NLRP3) inflammasome, a key mediator of the innate immune system in response to a host of initiating factors, is activated in response to various diseases [12–14]. The NLRP3 inflammasome is composed of apoptosis-associated speck-like adaptor protein containing a CARD (caspase recruitment domain) (ASC), oligomers of the receptor (NLRP3), and pro-caspase-1. Upon activation, NLRP3 is ligated with ASC, which in turn combines pro-caspase-1, causing its transformation to cleaved caspase-1 that regulates the maturation of proinflammatory cytokines IL-1β and IL-18 [15, 16]. Recent studies have demonstrated that NLRP3 contributes to renal ischemia/reperfusion (I/R) injury *via* a direct effect on renal tubular epithelium [17, 18].

However the signaling pathways that lead to the activation of NLRP3 inflammasome due to kidney I/R injury have not been fully elucidated. Many activators of the NLRP3 inflammasome have been identified, including K^+ channels, lysosomal membrane, and ROS [19]. A previous study determined that ROS activity played an important role in AKI with models of I/R [6]. Meanwhile, the production of ROS and the generation of oxidative stress are important elements for the pathophysiology of DM [20]. Hyperglycemia induced generation of ROS in renal tubular epithelial cells in *in vitro* studies [21, 22]. However, the mechanisms by which ROS activates the inflammasome are unclear. Recently, the significant work by Zhou et al. revealed that thioredoxin-interacting protein (TXNIP) is an upstream partner to NLRP3 and that the association between these two proteins was necessary for downstream inflammasome activation [23].

TXNIP, the endogenous inhibitor and regulator of TRX, is a major cellular antioxidant and antiapoptotic protein [24]. Overexpression of TXNIP inhibits the activity of TRX and thus can modulate the cellular redox state and stimulate oxidative stress [25, 26]. In addition, experimental evidence has indicated that hyperglycemia can induce TXNIP expression in renal tubular epithelial cells [21, 22], and diabetes can potentially enhance TXNIP expression and reduce TRX activity [27]. However, there is no direct evidence to support a causative role of TXNIP in hyperglycemia or high blood glucose which exasperates renal I/R injury.

Resveratrol (trans-3,4,5-trihydroxystilbene, RES), a natural polyphenolic mixture concentrated in grape skin and red wine [28], is reported to have beneficial effects on renal diseases. Resveratrol is reported to be a strong scavenger of ROS [29]. RES treatment can ameliorate hyperglycemia-mediated renal dysfunction or DN [30]. Several studies have demonstrated that RES exerts protective effects against I/R injury in the kidneys [31], as well as the liver and brain ischemia injury by reducing oxidative stress and downregulating TXNIP expression [32, 33].

The present study was designed to investigate the role of TXNIP during ischemia AKI in diabetic models and examine a key role of TXNIP in bridging redox signals with activation of NLRP3 inflammasome in AKI injury.

2. Materials and Methods

2.1. Antibodies and Reagents. The following antibodies were used in this study: TXNIP (ab86983, Abcam, UK), NLRP3 (NBP-12446, Novus Biologicals, USA), and caspase-1 and cleaved caspase-1 (Santa-514, Santa Cruz, CA). VDUP-1 (TXNIP) siRNA Plasmid (sc-44943) and control siRNA Plasmid were from Santa Cruz Biotechnology.

2.2. Cell Culture and Transfection. HK-2 cells (ATCC, American Type Culture Collection, Manassas, VA) were cultured in MEM medium (#31985, Gibco, Grand Island, USA) supplemented with 10% fetal bovine serum (FBS, #10099-141, Gibco, Grand Island, USA) and 1% Penicillin-Streptomycin solution in 95% air and 5% CO_2 atmosphere. For siRNA transfections of HK-2 cells (VDUP-1 siRNA or scrambled siRNA as a nonspecific control), cells were seeded (2×10^5 per well) in 6-well plates and transfected using with Lipofectamine 2000 reagent (#11668-019, Invitrogen, USA) according to the manufacturer's instructions. The cells were used for further experiments 48 hours after transfection. After this time period, the cells were randomly divided into eight groups: NG group (stimulated with NG (5.6 mM)); HG group (30 mM); NG + mannitol (24.4 mM) group (M) as an osmotic control; NH/R (hypoxia 4 hours and reoxygenation 2 hours) group; HH/R group; HH/R treated with scrambled siRNA group; HH/R treated with TXNIP siRNA group; and HH/R treated with RES (50 μM) during the 72 hours of high glucose (HG) incubation [34].

2.3. Cell In Vitro Simulated Ischemia/Reperfusion Model (Hypoxia and Reoxygenation, H/R). For hypoxic treatment, after 72 h HG stimulation in the absence or presence of RES (50 μM) [22, 34], HK-2 cells were incubated in glucose-free Krebs-Ringer bicarbonate buffer for 4 hours in a hypoxic chamber equilibrated with 5% CO_2, 1% O_2, and 94% N_2. After hypoxic incubation, the cells were returned to full culture medium for 2-hour reoxygenation. Control cells were incubated in normal cell culture incubator with 21% oxygen [35].

2.4. Rat Models of Diabetes. Male Sprague-Dawley rats weighing 250–300 g were used (purchased from Beijing HFK Bioscience Co. Ltd., Beijing, China). All procedures involved in animals were approved by the Ethics Committee of Renmin Hospital of Wuhan University. For streptozotocin-(STZ-) induced diabetes, rats were injected with 65 mg/kg body-weight STZ (Sigma-Aldrich, St. Louis, MO, USA). Two weeks after the STZ injection, the animals were considered to have type-1 diabetes if the plasma glucose level was >300 mg/dL and other diabetic features such as polyuria, polydipsia, and hyperphagia were observed [36]. STZ-induced rats were maintained for another 2 weeks before renal I/R. To examine the effect of RES, 10 mg/kg RES (Sigma-Aldrich, St. Louis, MO, USA) was intraperitoneally injected daily for 7 consecutive days before renal I/R [37]. The diabetic and normal rats were randomly divided into six groups of 4–6 rats each: ND sham group (NS); ND I/R group (NI/R); DM sham group (DS); DM + RES sham group (DS-RES); DM I/R group (DI/R); and DM + RES I/R group (DI/R-RES). All animals were maintained in the animal center of Wuhan University within an environment-controlled room (ambient temperature of 25 ± 1°C and a light/dark period of 12 h) with free access to normal chow and water. All the animal experiments were double-blind. The data statistics were unblinded.

2.5. Renal Ischemia-Reperfusion. Renal I/R was induced in rats as previously described [38]. Briefly, rats were anesthetized with 60 mg/kg (intraperitoneally) pentobarbital sodium and kept on homeothermic pad to maintain body temperature at 37°C. Kidneys were exposed by abdominal midline incisions, and the renal pedicles were clamped for 25 min to induce ischemia. After ischemia, the clamps were released for 48 h reperfusion. Sham control animals were subjected to identical operation without renal pedicle clamping.

Surgical wounds were sutured and rats were given 1 mL of warm saline intraperitoneally and kept in a warm incubator until they regained consciousness. At 48 h after reperfusion, animals were sacrificed and plasma and tissue samples were collected and stored at −80°C until analysis.

2.6. Renal Function, Histology, and Apoptosis. BUN and serum creatinine were determined using commercial kits (Jiancheng Biotech, Nanjing, China) to indicate renal function. Renal histology was examined by H&E staining. Histopathological changes were evaluated by the percentage of tubular injury as indicated by tubular epithelial swelling, loss of brush border, vacuolar degeneration, necrotic tubules, cast formation, and desquamation. The degree of kidney damage was estimated using five randomly selected fields for each rat assessed using quantitative analysis with the following criteria: 0, no abnormalities; 1, slight abnormalities (<25%); 2, moderate abnormalities (25 to 50%); 3, severe abnormalities (50 to 75%); and 4, more severe abnormalities (>75%). Histological sections were evaluated by two examiners blinded to the source of the samples. Renal apoptosis was examined by TUNEL assay using the *in situ* Apoptosis Detection kit from Roche Applied Science. TUNEL-positive cells were identified through the nucleus, which was stained either tan or brown. Five fields were randomly selected and the apoptosis index was calculated as the ratio of apoptotic-to-total cells.

2.7. Measurement of Inflammatory Cytokines and Caspase-1 Activity. IL-1β and IL-18 levels in kidney were assessed using a rat ELISA kit (Elabscience Biotechnology Co., Ltd., Wuhan, China) according to the manufacturer's instructions. Caspase-1 activity in HK-2 cells was determined using an enzyme activity assay kit (Beyotime Biotechnology, Shanghai, China), according to the manufacturer's instructions.

2.8. Measurement of Oxidative Stress. The intracellular formation of ROS was detected using the fluorescence probe 2′,7′-dichlorodihydrofluorescein diacetate (DCHF-DA, Jiancheng Biotech, Nanjing, China). Cells were incubated with 1 mmol/L DCHF-DA for 30 min at 37°C and washed in PBS 3 times, and the fluorescence intensity was measured using a fluorometer with excitation at 485 nm and emission at 525 nm. The malondialdehyde (MDA) levels, superoxide dismutase (SOD), and superoxide anion radical scavenging capacity were detected using commercially available kits (Jiancheng Biotech, Nanjing, China), according to the manufacturer's instructions. The detection of superoxide anion radical scavenging capacity was *via* a spectrophotometer test. Briefly, kidney samples were harvested into PBS buffer and homogenized under high-speed cryogenic centrifugation and the supernatant was extracted. The extract and corresponding reagent were mixed in a constant temperature water bath at 37°C for 40 minutes, before the color reagent was added and allowed to incubate for 10 min. Distilled water was used to calibrate the spectrophotometer and the absorbance value of each sample at wavelength 550 nm with an optical diameter of 1 cm was obtained.

2.9. Immunofluorescence Staining. HK-2 cells were seeded on cover slips and were later subjected to fixation with 4% paraformaldehyde for 15 min and permeabilization in 0.5% Triton X-100 (Beyotime, Shanghai, China: ST795) for 20 min at room temperature. Then the cells were blocked with normal goat serum (Boster, Wuhan, China: AR1009) for 30 min at room temperature and incubated with primary antibody against TXNIP (1 : 50) and NLRP3 (1 : 50) overnight at 4°C. After incubation with secondary antibody (Boster, Wuhan, China: BA1032) for 1 hour at 20–37°C, the cover slips were washed with PBS and stained with DAPI (Beyotime, Shanghai, China: C1002). Under 400 (200)x magnification, images were taken by fluorescence microscope (Olympus, Japan).

2.10. Immunohistochemical Staining. The IHC staining for TXNIP expression in renal tissues was performed on formalin-fixed, paraffin-embedded samples; 4 μM sections were deparaffinized in graded xylene-alcohol solutions. Subsequently, the samples were subjected to antigen retrieval and then incubated in 3% H_2O_2 15 min and washed by PBS. The sections were incubated overnight (15 hours) at 4°C with a primary antibody anti-TXNIP (1 : 50) and then incubated with horseradish peroxidase-conjugated anti-IgG secondary antibody for 20–30 min. The reaction was visualized with a solution of diaminobenzidine (DAB) and counterstained with hematoxylin.

2.11. Western Blot Analysis. The expressions of TXNIP, NLRP3, caspase-1, and cleaved caspase-1 were examined using Western blot. Protein content was determined with BCA protein assay and protein samples were separated by electrophoresis on SDS-PAGE and transferred to a polyvinylidene difluoride membrane. The membranes were blocked with 5% milk and incubated overnight with the appropriate primary antibodies (anti-TXNIP, anti-NLRP3, and anti-caspase-1 antibody), respectively, followed by incubation with the corresponding secondary antibodies. The blots were visualized with ECL-plus reagent. GAPDH was used as the internal loading control.

2.12. Cell Viability and Lactate Dehydrogenase (LDH) Activity. Cell viability was determined by using a cell counting kit-8 (CCK-8) assay, according to the manufacturer's instructions. HK-2 cells (1×10^5 cells/well) were plated into 96-well plates and pretreated with various conditions (NG, HG, NH/R, HH/R, HH/R-siRNA, HH/R-scrambled siRNA, and HH/R-RES) as described, following which, 10 μL CCK-8 (Beyotime: C0037, China) was added and cells were incubated for 4 hours, and the absorbance was measured at 450 nm with an ELISA assay plate reader. LDH content was measured by LDH Cytotoxicity Assay Kit (Jiancheng Biotech, Nanjing, China).

2.13. Apoptosis Assay. After reoxygenation, cells were trypsinized, washed twice with PBS, and resuspended in binding buffer. The percentage of apoptosis was evaluated by using an Annexin V-APC/7-AAD detection kit (Nanjing KeyGen

Table 1: General characteristics of the experimental animals before ischemia/reperfusion modeling.

	NS ($n = 6$)	NI/R ($n = 7$)	DS ($n = 7$)	DI/R ($n = 7$)	DI/R-RES ($n = 8$)
Blood glucose (mM)	8.15 ± 0.58	7.44 ± 0.6	27.17 ± 1.1*	25.24 ± 1.5*	18.9 ± 0.86$^{\star\#}$
Body weight (g)	359.67 ± 9.55	366.43 ± 9.81	217.43 ± 9.92*	204.86 ± 12.33*	224 ± 9.89*

The data in the table are means ± SE ($n = 6$–8), $^{\star}P < 0.05$ versus NS group, and $^{\#}P < 0.05$ versus DS group.
NS and DS: nondiabetic and STZ-induced diabetic rats were subjected to sham operation. NI/R and DI/R: nondiabetic and STZ-induced diabetic rats were subjected to 25 min ischemia followed by 48 h reperfusion. DI/R-RES: STZ-induced diabetic rats that underwent I/R were treated with RES (10 mg/kg, ip daily) for 7 consecutive days before renal ischemia-reperfusion.

Biotech, Nanjing, China) according to the manufacturer's instructions. Cells were stained with Annexin V-APC and 7-AAD for 15 min in the dark. Samples were assayed by flow cytometry with the FACScan system (BD Biosciences). Apoptotic cells were defined as the cells situated in the right two quadrants of each plot and the percentages were determined by flow cytometry.

2.14. Statistical Analysis. The data are reported as means ± SE. Statistical significance was assessed by one-way or two-way ANOVA followed by Tukey's test for multiple comparisons (GraphPad Prism 5.0). Two-way ANOVA was used for testing differences among the multiple experimental groups between the types of injury (sham versus I/R) across the groups of rats (diabetes versus nondiabetes, for the animal experiments). $P < 0.05$ was considered to be statistically significant.

3. Results

3.1. General Characteristics of the Experimental Animals before I/R Modeling. As shown in Table 1, STZ-induced diabetic rats had obvious diabetic symptoms of hyperglycemia, polydipsia, polyphagia, and weight loss. The plasma glucose of the diabetic rats increased but their body weight decreased compared to nondiabetic rats. RES treatment had no significant effect on body weight compared to DS group, but plasma glucose was significantly elevated in the RES group compared to NS group but lower than DS group (Table 1).

3.2. STZ-Induced Diabetic Rats Exhibit Aggravated Ischemia AKI-Induced Kidney Dysfunction. As shown in Figure 1, we initially compared sensitivity of I/R injury to STZ-induced diabetic rat (DM) and nondiabetic rat without STZ (ND). For functional analysis, renal histology revealed significantly more tissue damage in DI/R group. I/R48 induced severe tubular dilation and interstitial edema, tubular epithelial swelling, loss of brush border, vacuolar degeneration, necrotic tubules, cast formation, and desquamation in DM rats, while, in ND rats, there were fewer injured tubules and the injury in each tubule was less severe as compared to DI/R rats (Figure 1(a)). Quantitatively, tubular damage was significantly higher at I/R48 in DI/R group than NI/R group (by 1.5-fold) (Figure 1(c)). Moreover, apoptotic cells assays by TUNEL were rare in kidney tissues of both NS and DS groups, and after I/R48, the percentage of apoptotic cells was significantly higher in DI/R group than NI/R group (by 1.5-fold) (Figures 1(b) and 1(d)). Compared to NS and DS groups, I/R48 resulted in marked increase with BUN (Figure 1(e)) and serum creatinine (Figure 1(f)) in both NI/R and DI/R groups, but the BUN and serum creatinine were significantly higher in DI/R group than NI/R group.

3.3. STZ-Induced Diabetic Rats Exhibit Increased Oxidative Stress in Kidney after Ischemia AKI. As shown in Figure 2, we determined superoxide anion radical scavenging capacity which indicated the general scavenging ability of kidney tissue on superoxide anion free radicals in each group and found that I/R48 resulted in reducing superoxide anion radical scavenging capacity (Figure 2(a)) in both NI/R and DI/R groups, but the superoxide anion radical scavenging capacity was significantly lower by 68.4% in DI/R group than NI/R group. In addition, antioxidant enzymes SOD content, which is a natural superoxide free radical scavenging factor, was significantly decreased in both DI/R and NI/R groups as compared to each sham group. Furthermore, SOD was markedly lower by 50% in DI/R group than NI/R group (Figure 2(b)). In contrast, MDA activity was used as a biomarker to measure the level of oxidative stress and showed a significant increase of MDA production in both DI/R and NI/R groups as compared to each sham group, but MDA was markedly higher in DI/R group than NI/R group (by 1.76-fold) (Figure 2(c)).

3.4. Effects of RES on Renal Function and Oxidative Stress in the STZ-Induced Diabetic Kidneys. As shown in Figure 3, histology score (Figures 3(a) and 3(c)), apoptosis (Figures 3(b) and 3(d)), and BUN (Figure 3(e)) levels were significantly increased in the sham group of diabetic rats (DS). Meanwhile, the indicators of oxidative stress including the activities of SOD (Figure 3(g)) and MDA (Figure 3(h)) were slightly but not significantly increased in the kidney tissues of DS rats as compared with NS rats ($P > 0.05$). RES administration markedly ameliorated apoptosis (Figures 3(b) and 3(d)) and BUN (Figure 3(e)) levels. There was no remarkable attenuation on the histology score (Figure 3(c)) and serum creatinine (Figure 3(f)) levels after RES treatment in the STZ-induced DM rats. Furthermore, treatment with the RES significantly increased the SOD levels (Figure 3(g)) and decreased the MDA levels (Figure 3(h)) in the diabetic rats. Additionally, the plasma glucose of the diabetic rats increased but their body weight decreased as compared to nondiabetic rats. RES treatment had no significant effects on body weight

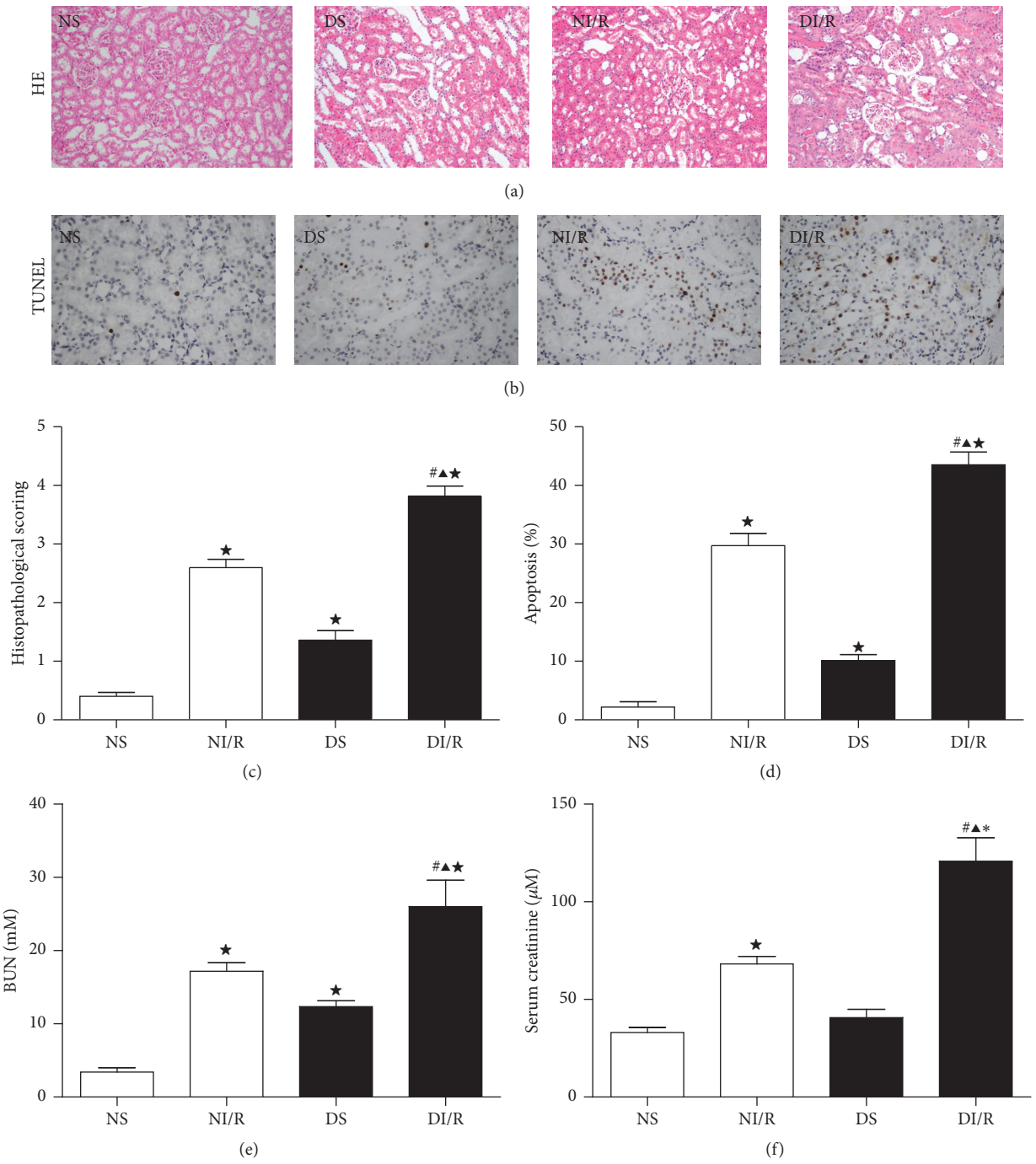

FIGURE 1: Induction of diabetes in male SD rats with STZ. The rats were subjected to sham operation or renal ischemia/reperfusion injury (I/R48). Renal tissues for hematoxylin and eosin staining and semiquantification of tubular damage (a, c). TUNEL assay apoptosis% (b, d). Blood samples were collected to measure BUN (e) and serum creatinine (f). The data in (c, d, e, f) are means ± SE ($n = 6$). $^{\star}P < 0.05$ versus NS group; $^{\#}P < 0.05$ versus DS group; $^{\blacktriangle}P < 0.05$ versus NI/R group. NS and DS: nondiabetic and STZ-induced diabetic rats were subjected to sham operation. NI/R and DI/R: nondiabetic and STZ-induced diabetic rats were subjected to 25 min ischemia followed by 48 h reperfusion. DI/R-RES: STZ-induced diabetic rats that underwent I/R were treated with RES (10 mg/kg, ip daily) for 7 consecutive days before renal ischemia-reperfusion.

but significantly attenuated plasma glucose as compared to DS group, though the blood glucose in RES group was still significantly higher than DS group (Figures 3(i) and 3(j)). Of note, RES had no significant effects on blood glucose, body weight, BUN, serum creatinine, SOD, and MDA in the normal rats (data not shown).

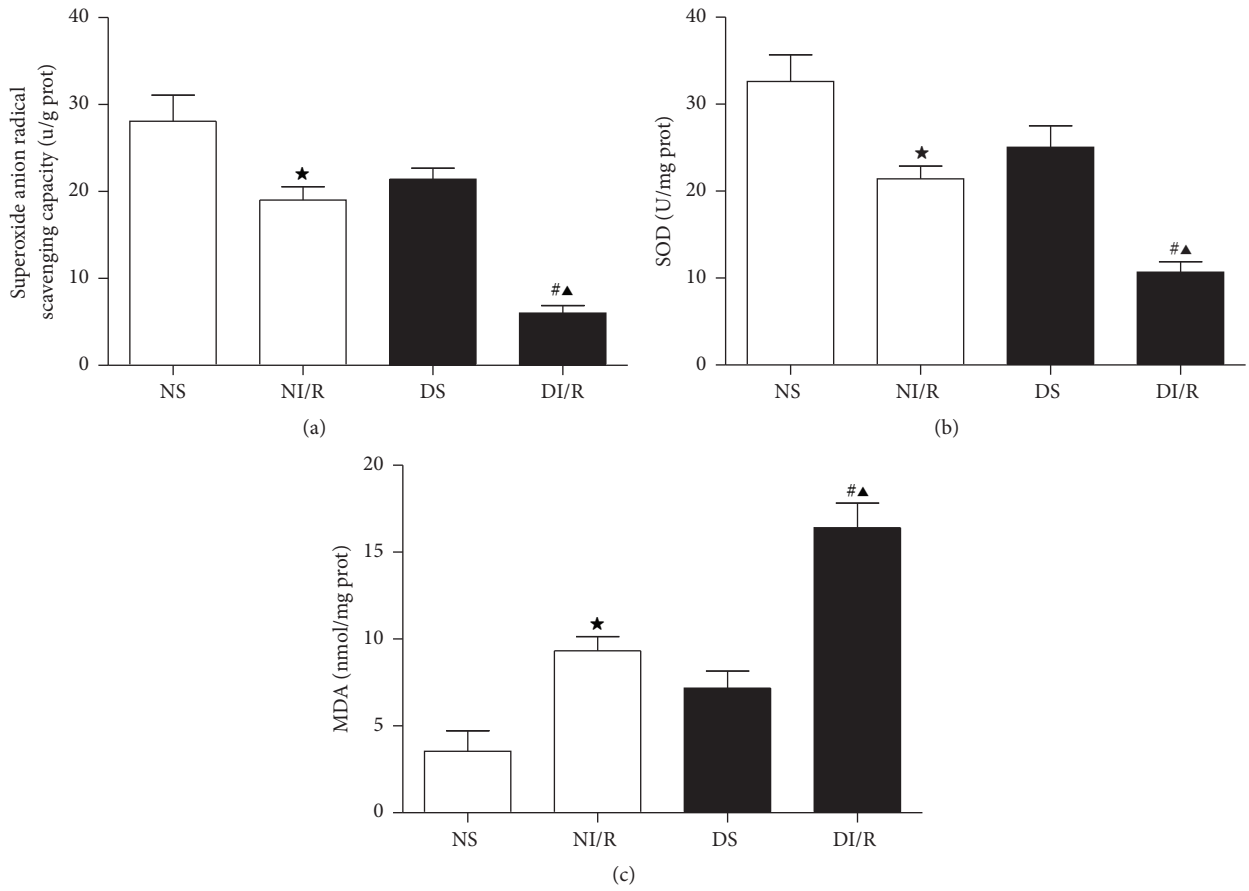

Figure 2: STZ-induced diabetes enhances oxidative stress in rats subjected to ischemia AKI. Kidney tissues were collected to measure superoxide anion radical scavenging capacity (a), kidney superoxide dismutase (SOD) contents (b), and malondialdehyde (MDA) activity (c). The data in (a, b, c) are means ± SE ($n = 6$). $^{\star}P < 0.05$ versus NS group; $^{\#}P < 0.05$ versus DS group; $^{\blacktriangle}P < 0.05$ versus NI/R group. NS and DS: nondiabetic and STZ-induced diabetic rats were subjected to sham operation. NI/R and DI/R: nondiabetic and STZ-induced diabetic rats were subjected to 25 min ischemia followed by 48 h reperfusion. DI/R-RES: STZ-induced diabetic rats that underwent I/R were treated with RES (10 mg/kg, ip daily) for 7 consecutive days before renal ischemia-reperfusion.

3.5. RES Treatment of STZ-Induced Diabetic Rats Attenuates the Ischemia AKI Sensitivity and Oxidative Stress Level. As shown in Figure 4, RES significantly attenuated the AKI sensitivity of STZ-induced diabetic rats as indicated by histology and apoptosis, BUN ($P > 0.05$ versus DS group), and serum creatinine (Figures 4(a)–4(f)).

We also examined the effect of RES on oxidative stress level after I/R 48 hours and found that there was a significant increase of superoxide anion radical scavenging capacity (Figure 4(g)) and SOD content (Figure 4(i)) in RES-treated group as compared to DI/R group. The MDA production in RES-treated group was significantly decreased as compared to DI/R group (Figure 4(h)).

3.6. STZ-Induced Diabetes Stimulates TXNIP Expression and NLRP3 Inflammasome Activation following Renal I/R 48 Hours and Subsequent Effect of RES on TXNIP Expression and Inflammasome Activation. As TXNIP is known to be involved in oxidative stress and diabetic complications, we determined kidney TXNIP expression by IHC (Figure 5(a)) and Western blot (Figures 5(b) and 5(c)) in ND rats and DM rats treated after I/R injury. In the sham groups, the TXNIP protein expression was significantly higher in DS than NS group. After I/R 48, both NI/R group and DI/R group stimulated kidney TXNIP expression as compared to each sham group. Furthermore, DI/R group showed a significant increase in TXNIP content compared with NI/R group (by 1.21-fold). The data suggested that ischemia AKI-induced TXNIP was enhanced by STZ-induced diabetes. Moreover, RES administration (DI/R-RES group) significantly decreased the expression of TXNIP by 24.6% compared to DI/R group. We also examined the effect of TXNIP on NLRP3 activation; after ischemia AKI injury, kidney NLRP3 inflammasome expression was dramatically increased in both DI/R rats and NI/R rats as compared to rats of each sham group. Furthermore, compared to NI/R group, the DI/R group showed significantly elevated levels of NLRP3 (by 1.25-fold) (Figure 5(d)). Meanwhile, increase in NLRP3 protein activation was accompanied by marked induction of cleavage of caspase-1 expression (Figure 5(e)) and IL-1β and IL-18 (Figures 5(f) and 5(g)) release. Moreover, RES treatment attenuated NLRP3 inflammasome protein activation at 48

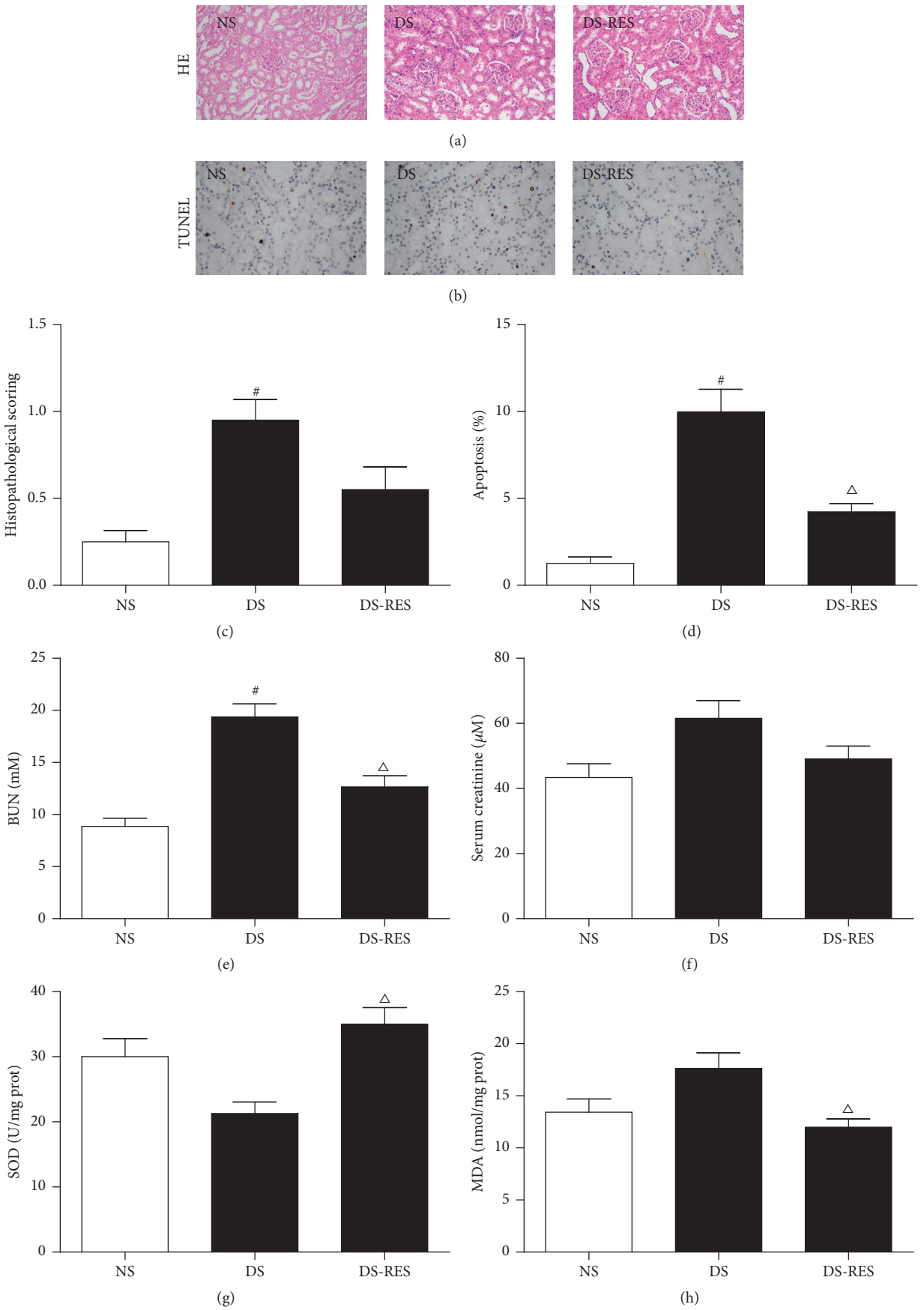

Figure 3: Continued.

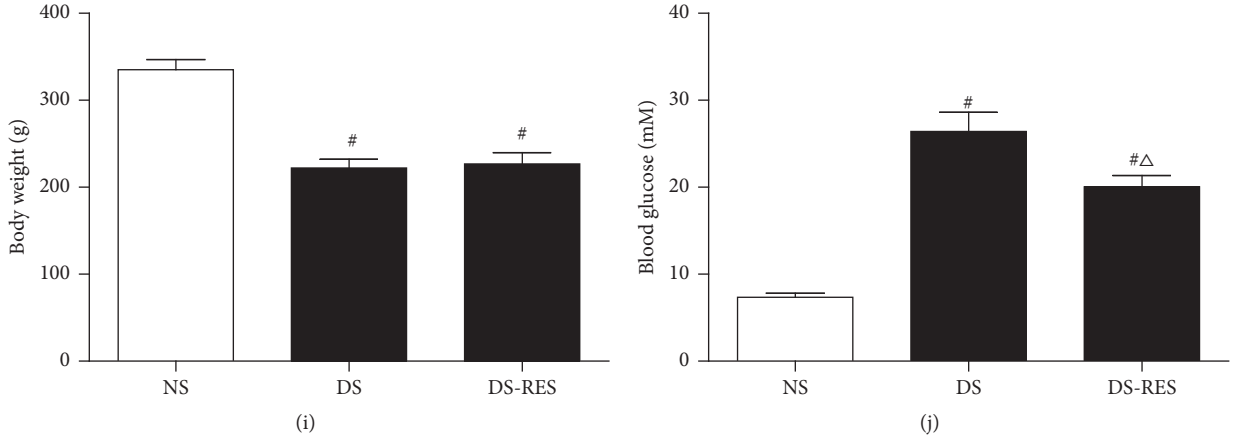

Figure 3: RES treatment of STZ-induced diabetes ameliorates renal dysfunction and oxidative stress level. After RES administration for 7 consecutive days (daily ip 10 mg/kg RES), kidney tissues were collected for H&E staining and the histological damage score (a, c) and TUNEL assay of apoptosis (b, d). Blood samples for measuring BUN (e), serum creatinine (f), kidney tissues for analysis of SOD content (g) and MDA production (h), body weight (i), and plasma glucose (j) were examined. The data in (c–j) are means ± SE ($n = 4$). $^{\#}P < 0.05$ versus NS group; $^{\triangle}P < 0.05$ versus DS group. NS and DS: nondiabetic and STZ-induced diabetic rats were subjected to sham operation. NI/R and DI/R: nondiabetic and STZ-induced diabetic rats were subjected to 25 min ischemia followed by 48 h reperfusion. DS-RES: STZ-induced diabetic rats that underwent sham operation were treated with RES (10 mg/kg, ip daily) for 7 consecutive days.

hours after ischemia in DM rats while concomitantly reducing the expression of caspase-1 and release of IL-1β and IL-18 (Figures 4(b), 4(d), and 4(f)–4(h)). However, pro-caspase-1 (Figure 5(e)) had no significant change among all groups.

3.7. Inhibition of TXNIP Improves the Viability and Injury of HK-2 Cells Impaired by High Glucose (HG) and Hypoxia/Reoxygenation (HH/R). Following 4 hours of hypoxia and 2 hours of reoxygenation, cell viability was significantlyreduced (Figure 6(a)) and cellular LDH activity was increased (Figure 6(b)) in HK-2 cells exposed to high glucose. Both transfection of HK-2 cells with TXNIP siRNA and RES treatment markedly alleviated HH/R-induced reduction of cell viability and elevation of cellular LDH activity.

3.8. Changes of TXNIP/NLRP3 Signaling in HK-2 Cells Exposed to High Glucose (HG) and Hypoxia/Reoxygenation (HR). At first, we chose NG plus mannitol (24.4 mM) as an osmotic control, and there was no significant difference between the NG group and NG plus mannitol group (data not shown). However the expressions of TXNIP protein (Figures 7(a) and 7(c)) and NLRP3 protein (Figures 7(a) and 7(d)) as well as the activity of caspase-1 (Figure 7(e)) and IL-1β level (Figure 7(f)) were upregulated in response to high glucose (30 mM) stimulation for 72 hours. Following 4 hours of hypoxia and 2 hours of reoxygenation, TXNIP protein expression was significantly higher in HK-2 cells exposed to high glucose than normal glucose (by 2-fold) (Figures 7(a) and 7(c)), while NLRP3 (Figures 7(a) and 7(d)) expression and the activity of caspase-1 (Figure 7(e)) and IL-1β level (Figure 7(f)) had similar changes as TXNIP. Transfection of HK-2 cells with specific siRNA decreased TXNIP protein expression by more than 70% (Figure 7(b)). In line with the *in vitro* experiments, following transfection of TXNIP siRNA, TXNIP (Figures 7(a) and 7(c)) and NLRP3 (Figures 7(a) and 7(d)) protein expressions were decreased by 53.1%, and the activity of caspase-1 (Figure 7(e)) and the level of IL-1β were also reduced (Figure 7(f)) in HK-2 cells after exposure to high glucose following H/R. Meanwhile, RES treatment significantly decreased TXNIP protein expression by 35.2% (Figures 7(a) and 7(c)) and correspondingly decreased NLRP3 protein expression by 32.8% (Figures 7(a) and 7(d)) and the activity of caspase-1 (Figure 7(e)) and level of IL-1β (Figure 7(f)) as compared to HH/R group. Subsequently, the expressions of TXNIP (Figure 8(a)) and NLRP3 (Figure 8(b)) were determined by immunofluorescence staining. Obvious increases of TXNIP and NLRP3 expression were induced by both HG and H/R. Moreover, HH/R enhanced the above effects as compared to NH/R group, whereas transfection of TXNIP siRNA and treatment with RES inhibited the expression of TXNIP and NLRP3 under HH/R.

3.9. The Oxidative Stress Status and Apoptosis in HK-2 Cells Exposed to High Glucose (HG) and H/R. To study the mechanism of the AKI sensitivity of HG and H/R, the HK-2 cells were cultured for 72 hours in 30 mM glucose (HG). These cells were then subjected to 4 hours of hypoxia and 2 hours of reoxygenation. Our studies demonstrated that both HG and H/R could induce higher apoptosis levels (Figures 9(a) and 9(b)) and oxidative stress (Figures 9(c)–9(e)); moreover, HH/R induced significantly increased apoptosis levels (Figures 9(a) and 9(b)) and oxidative stress (Figures 9(c)–9(e)) as compared to NH/R. Both knockdown of TXNIP and pretreatment with RES significantly inhibited ROS generation (by 32.1% and 15.7%, resp.) (Figure 9(c)) in HK-2 cells that were exposed to HG combined H/R, while the SOD content (Figure 9(d)) significantly increased (by 1.4-fold and 1.34-fold, resp.) and MDA (Figure 9(e)) significantly decreased

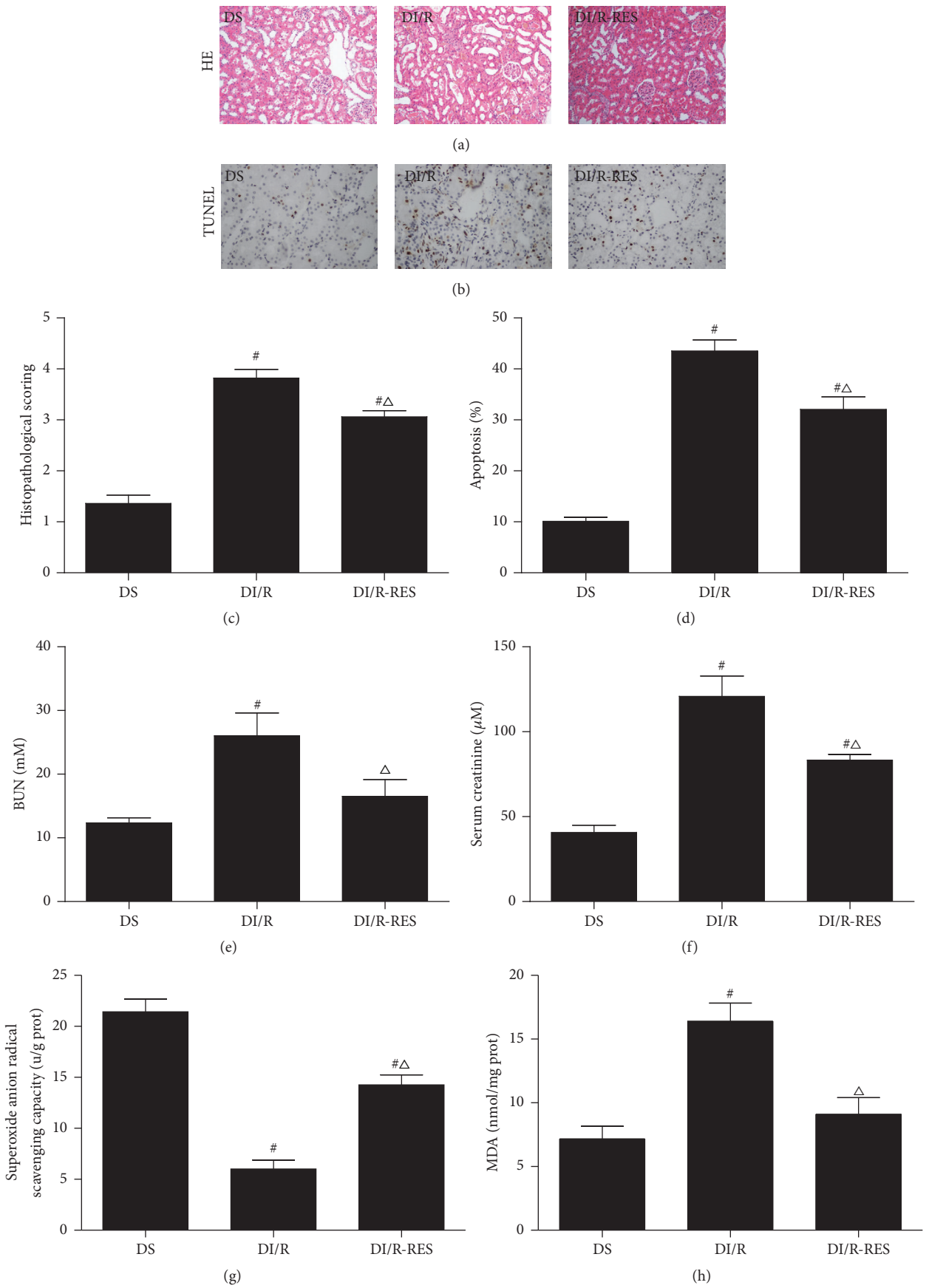

Figure 4: Continued.

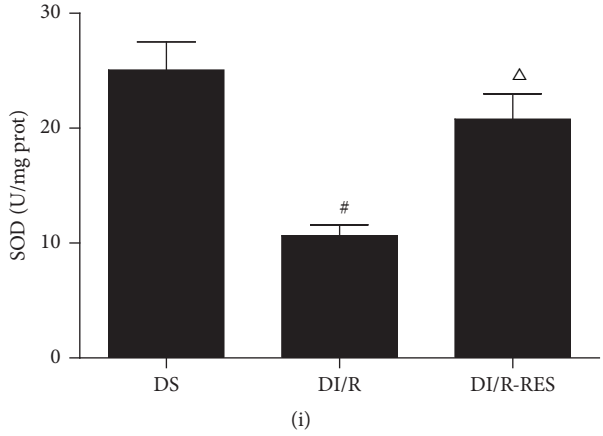

Figure 4: RES treatment of STZ-induced diabetes reduces AKI sensitivity and oxidative stress level. After I/R 48 hours, kidney tissues were collected for H&E staining and the histological damage score (a, c) and TUNEL assay of apoptosis (b, d) were examined; blood samples were used to measure BUN (e), serum creatinine (f) levels, and kidney tissues for analysis of superoxide anion radical scavenging capacity (g), MDA production (h), and SOD content (i). The data in (c–i) are means ± SE ($n = 6$). $^{\#}P < 0.05$ versus DS group; $^{\triangle}P < 0.05$ versus DI/R group. NS and DS: nondiabetic and STZ-induced diabetic rats were subjected to sham operation. NI/R and DI/R: nondiabetic and STZ-induced diabetic rats were subjected to 25 min ischemia followed by 48 h reperfusion. DI/R-RES: STZ-induced diabetic rats that underwent I/R were treated with RES (10 mg/kg, ip daily) for 7 consecutive days before renal ischemia-reperfusion.

(by 45.2% and 32.5%, resp.) as compared to HH/R group. Similarly, after HH/R, both TXNIP siRNA transfection and pretreatment with RES significantly decreased the percentage of apoptotic cells (by 40.5% and 30.9%, resp.) (Figures 9(a) and 9(b)) compared to HH/R group.

4. Discussion

Using STZ-induced diabetic rat models as well as high glucose cultured HK-2 cells, our study provides evidence for increased ischemia AKI sensitivity in DM. Mechanistically, the injury sensitivity involves upregulation expression of TXNIP protein which resulted in activation of NLRP3 inflammasome. Both *in vitro* and *in vivo* decrease of TXNIP expression by RES treatment or RNA interference blocked TXNIP expression and subsequently inhibited NLRP3 inflammasome activation in response to ischemia-induced AKI in DM. These findings demonstrate the critical role of TXNIP which subsequently triggered activation of NLRP3 inflammasome in AKI sensitivity in DM.

Diabetic patients with AKI have an increased risk of advanced CKD, and AKI is an independent risk factor of kidney disease progression [7]. Renal I/R is one of the major causes of AKI, while cardiovascular surgery and renal transplantation may also cause ischemia AKI in clinical settings [39]. In animal models, the exaggerated vulnerability of the diabetic kidney to the ischemic insult could be attributed to activation of proinflammatory cytokine pathways [40]. Previous research revealed that this susceptibility was attributed to the oxidative and nitrosative stress [41]. Furthermore, a recent study demonstrated the role of apoptosis in the susceptibility of diabetic models to AKI [42]. Consistent with a previous study [43], herein, after 4 weeks of STZ-induced diabetic rats, the diabetic rats showed higher levels of BUN, tubule injury score, and apoptosis than nondiabetic rats, indicating that diabetic kidney was already significantly injured before I/R. However, the diabetic rats were also more sensitive to renal I/R injury as compared with nondiabetic rats. Following I/R injury, renal dysfunction and apoptosis level were more severe in diabetic rats than in nondiabetic rats. Our current results suggested that at the cellular level the injury sensitivity may be due to cell viability and the release of LDH. TXNIP gene knockdown by siRNA or RES treatment could inhibit TXNIP and NLRP3 expression and reduce the apoptosis level and decrease the cellular LDH activity. We have demonstrated that diabetic or high glucose further promoted I/R- (H/R-) induced MDA content expression. In addition, both kidney and cell SOD contents were significantly impaired. Meanwhile, the superoxide anion radical scavenging capacity in diabetic kidney was declined. Specifically, in response to hypoxia and reoxygenation, high glucose-conditioned HK-2 cells showed significantly higher expression of TXNIP and NLRP3 inflammasome. Moreover, renal I/R stimulated TXNIP expression which induced higher NLRP3 activation and IL-1β (IL-18) release from diabetic kidneys than nondiabetic tissues. Importantly, we further showed that RES could decrease TXNIP expression and NLRP3 activation both *in vivo* and *in vitro*. To the best of our knowledge, this is the first report of the renal I/R injury sensitization through TXNIP/NLRP3 pathway by high glucose *in vitro* and diabetic *in vivo*.

The activation of NLRP3 inflammasomes has been implicated in various pathological conditions, ranging from metabolic syndrome and kidney diseases [44, 45]. Formation of NLRP3 inflammasome can increase the expression of cleaved caspase-1 and IL-1β (IL-18) and mature IL-1β that participate in the pathological process of renal I/R [15, 16], in addition to revealing its role in apoptosis [46]. Despite studies that have demonstrated that NLRP3 contributes to renal ischemia reperfusion (I/R) injury by a direct effect on renal tubular

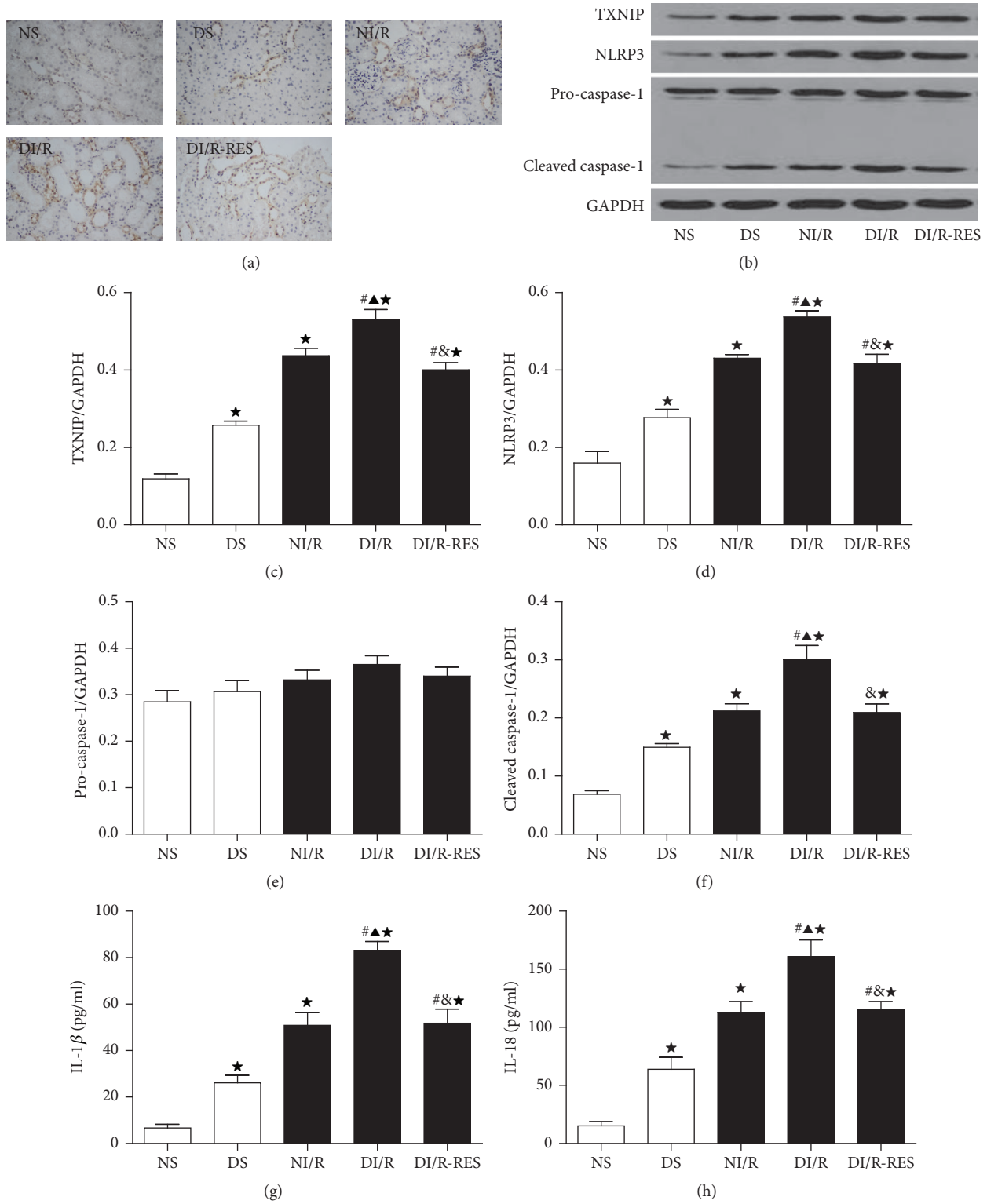

Figure 5: STZ-induced diabetes induces TXNIP expression and NLRP3 inflammasome activation following I/R 48. TXNIP expression was examined by IHC (a), representative blots (b), and quantitative analysis of Western blots for TXNIP (c), NLRP3 (d) and pro-caspase-1 and cleaved caspase-1 (e-f), and release of IL-1β and IL-18 by ELISA (g-h). The data in (c–h) are means ± SE ($n = 5$). $^{\star}P < 0.05$ versus NS group; $^{\#}P < 0.05$ versus DS group; $^{\blacktriangle}P < 0.05$ versus NI/R group; $^{\&}P < 0.05$ versus DI/R group. NS and DS: nondiabetic and STZ-induced diabetic rats were subjected to sham operation. NI/R and DI/R: nondiabetic and STZ-induced diabetic rats were subjected to 25 min ischemia followed by 48 h reperfusion. DI/R-RES: STZ-induced diabetic rats that underwent I/R were treated with RES (10 mg/kg, ip daily) for 7 consecutive days before renal ischemia-reperfusion.

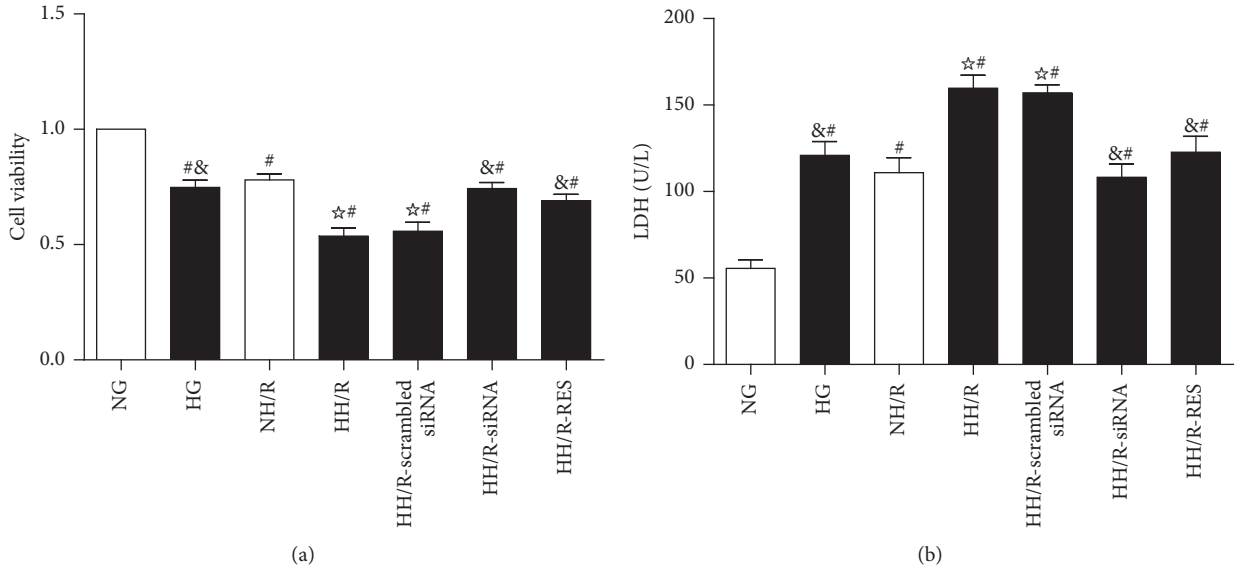

Figure 6: HK-2 cells injury after 4 hours of hypoxia followed by 2 hours of reoxygenation under high glucose stimulation. Effects of TXNIP blockage on cell viability assessed by CCK-8 (a); lactate dehydrogenase (LDH) release (b). The data in (a-b) are means ± SE ($n = 6$). $^{\#}P < 0.05$ versus NG group; $^{\star}P < 0.05$ versus NH/R group; $^{\&}P < 0.05$ versus HH/R-scrambled siRNA group; NG: normal glucose (5.6 mM); HG: high glucose (30 mM). NH/R: hypoxia (4 h)/reoxygenation (2 h) under NG condition; HH/R: hypoxia (4 h)/reoxygenation (2 h) under HG condition. HH/R-RES: HH/R pretreated by RES (50 μM) for 72 h with the high glucose incubation. HH/R-siRNA: TXNIP protein was inhibited by transfection with TXNIP siRNA before HH/R; HH/R-scrambled siRNA: scrambled siRNA used as control before HH/R.

epithelium [17, 18], it remains unclear how NLRP3 is able to sense redox changes, particularly in renal tubular epithelium during ischemia AKI in diabetes. In our study, we reconfirmed that the NLRP3/cleaved caspase-1/IL-1β, IL-18 signal pathway was upregulated in the nondiabetic kidney following I/R and normal-glucose-cultured HK-2 cells following H/R. Moreover, there was significantly increased expression of NLRP3 inflammasome in diabetic kidney and high-glucose-cultured HK-2 cells after I/R and H/R, respectively, accompanied by increased tubular cells apoptosis. These results provide evidence that NLRP3 inflammasome plays a key role in the pathogenesis of ischemia AKI of diabetic models.

To date, some mechanisms concerning the NLRP3 inflammasome activation have been identified, for example, intracellular ROS, which are commonly produced in response to many NLRP3 activators [19], and TXNIP (also known as vitamin D_3upregulated protein-1 [VDUP-1] and thioredoxin-binding protein-2 [TBP-2]), the endogenous inhibitor and regulator of TRX [24]. The TRX-TXNIP system, as a major ROS-scavenging system, maintains intracellular redox balance [27]. Overexpression of TXNIP inhibits the activity of TRX and thereby can modulate the cellular redox state and promote oxidative stress [25, 26]. Liu et al. demonstrated that TXNIP-mediated NLRP3 inflammasome activation was involved in myocardial I/R injury [47]. Hyperglycaemia has been identified as an inducer of TXNIP expression in various cells including HK-2 [21, 22]; meanwhile, enhanced myocardial TXNIP expression that contributes to hyperglycaemia-aggravated oxidative stress and exacerbates cardiac injury following I/R has been reported [48]. TXNIP expression is markedly upregulated in human diabetes and diabetic complications [49, 50], indicating that TXNIP is a potential therapeutic target of diabetes. Recently Zhou et al. confirmed an important role for TXNIP in the pathogenesis of type-2 diabetes and showed that TXNIP binding to NLRP3 was essential for ROS-mediated inflammasome activation [23]. Recent work demonstrated that TXNIP induced NLRP3 expression, activation of caspase-1, and release of IL-1β in a model of hyperhomocysteinemia or hyperglycemia with podocyte injury [51, 52]. In our current study, to our knowledge, this is the first report that shows TXNIP expression was induced in kidney tissue or HK-2 cells under ischemia (hypoxia) and in diabetic (high glucose) combined with ischemia (hypoxia) conditions. Additionally, we sought to determine the effect of TXNIP and elucidated its relationship to NLRP3 inflammasome activation in the susceptibility to ischemic AKI in diabetes.

Several studies have demonstrated that RES exerts protective effects against I/R injury in the kidneys [31], as well as the liver and brain injury by reducing oxidative stress and due to inhibition of TXNIP expression [32, 33]. In the present study, we found that TXNIP protein expression was significantly reduced after siRNA transfection in cultured HK-2 cells. We also found that RES could decrease TXNIP expression both *in vitro* and *in vivo*. Both RES at a dose of 50 μM and TXNIP siRNA markedly attenuated reduction of cell viability and increase of cellular LDH activity in high glucose and H/R treated HK-2 cells. Meanwhile, TRX-TXNIP interaction is an important antioxidant system and TXNIP is the endogenous inhibitor of cellular TRX [24, 27]. Previous researches showed that knockdown of TXNIP prevented high glucose (30 mM)-induced intracellular ROS generation

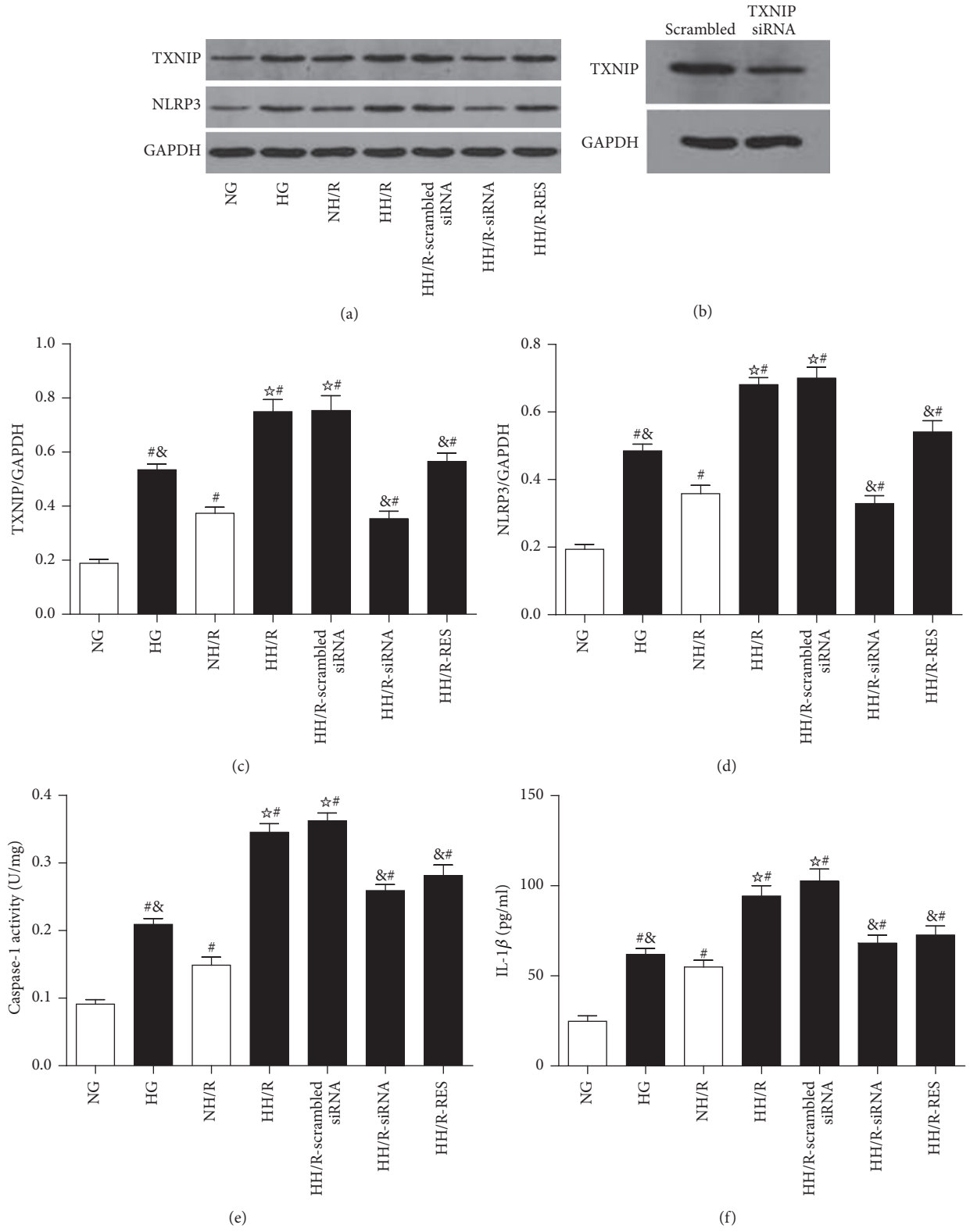

Figure 7: Western blot analysis of TXNIP and NLRP3 protein expression in cultured HK-2 cells treated by normal glucose (5.5 mM), high glucose (30 mM), and NG + mannitol, respectively, for 72 hours, then following 4 hours of hypoxia and 2 hours of reoxygenation in HK-2 cells under high glucose stimulation with or without TXNIP siRNA and RES treatment, respectively. Representative blots (a) and quantitative analysis of Western blots for TXNIP (c) and NLRP3 (d), activity of caspase-1 (e), level of IL-1β (f), and Western blot of TXNIP gene knockdown in HK-2 cells (b). The data in (c–f) are means ± SE ($n = 5$). $^{\#}P < 0.05$ versus NG group; $^{\star}P < 0.05$ versus NH/R group; $^{\&}P < 0.05$ versus HH/R-scrambled siRNA group.

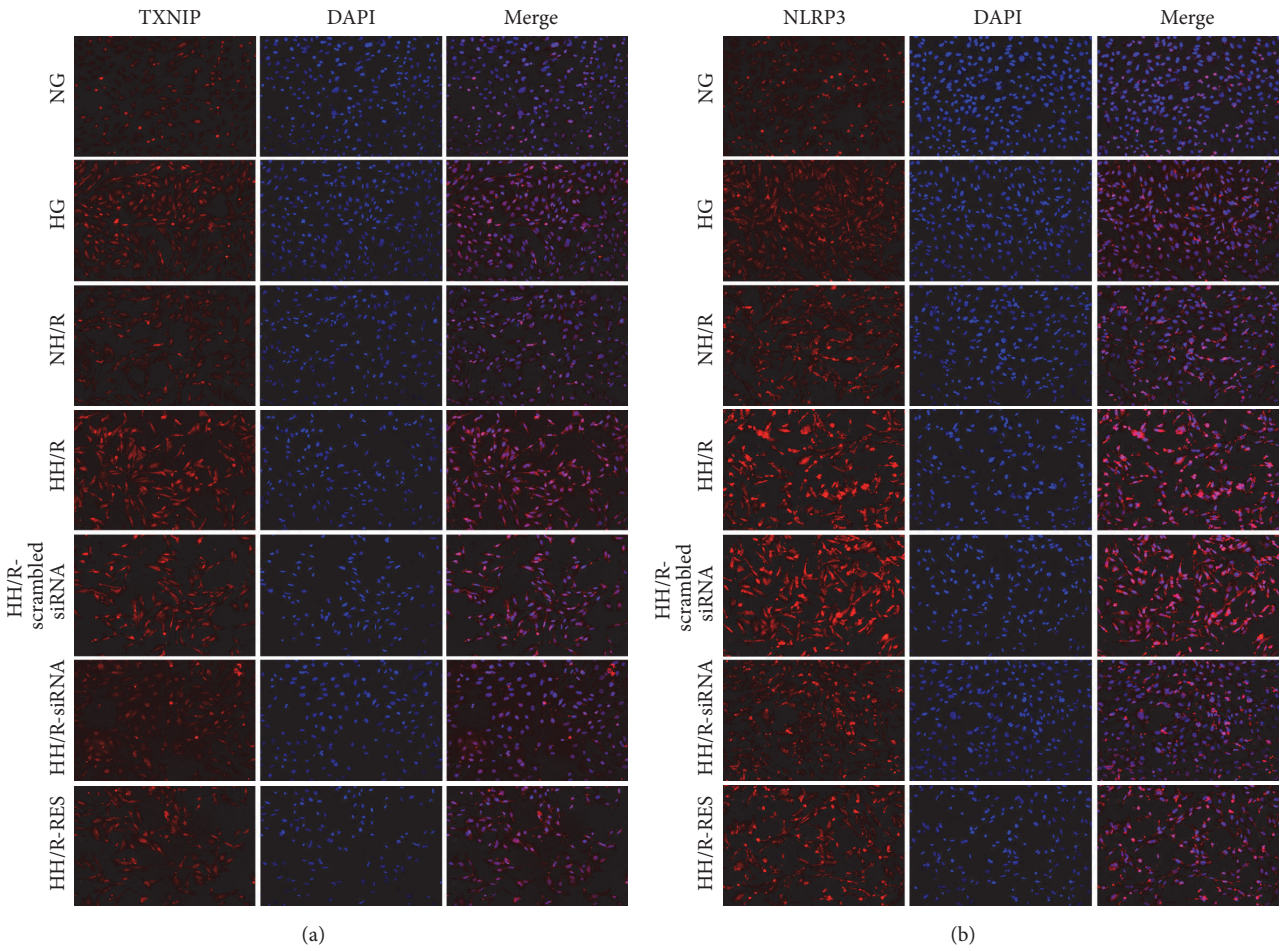

Figure 8: Immunofluorescence staining of TXNIP (a) and NLRP3 (b). NG: normal glucose (5.6 mM); HG: high glucose (30 mM). NH/R: hypoxia (4 h)/reoxygenation (2 h) under NG conditions; HH/R: hypoxia (4 h)/reoxygenation (2 h) under HG conditions. HH/R-RES: HH/R pretreated by RES (50 μM) for 72 h with the high glucose incubation. HH/R-siRNA: TXNIP protein was inhibited by transfection with TXNIP siRNA before HH/R; HH/R-scrambled siRNA: scrambled siRNA used as control before HH/R.

and reversed the high glucose-induced suppression of TRX activity in HK-2 cells [22]. Further, knockdown of TXNIP in mouse mesangial cells also suppressed high glucose-induced apoptosis by the reduction of ROS [53]. Furthermore, gene silencing of TXNIP reduced hyperglycaemia-elevated ROS production and apoptosis in cardiomyocytes within H/R [48]. In our *in vitro* study, both TXNIP siRNA and RES treatment significantly prevented HH/R-induced excessive oxidative stress (indicated by ROS, MDA, and SOD) and apoptosis level in HK-2 cells, subsequently prevented HH/R-induced NLRP3 inflammasome formation, and hindered caspase-1 activation in HK-2 cells. Additionally, RES treatment ameliorated hyperglycemia-mediated renal dysfunction or diabetic nephropathy [30, 36, 54]. In our *in vivo* experiments, we found that RES treatment downregulated the blood glucose level in diabetic rats, which was consistent with previous studies [36, 54]; this insulin-like property protective effect required further exploration. Meanwhile, a recent study showed that TXNIP expression was increased in the glomerular lysate of DN mice [52]. Our study found that the expression of TXNIP was increased in the diabetic kidney about 4 weeks after induction with STZ. Moreover, RES treatment partly normalized renal dysfunction in diabetic rats in addition to attenuating oxidative stress which was indicated by histology score ($P > 0.05$), BUN, apoptosis%, MDA, and SOD activities. Next, STZ-induced diabetic rats were used to establish I/R injury models, and RES further ameliorated renal function and the ability of antioxidative stress, decreased TXNIP-mediated NLRP3 inflammasome activation and expression of cleaved caspase-1 protein, and impeded IL-1β maturation in I/R-induced AKI in diabetic models. Our results indicated that TXNIP-mediated NLRP3 inflammasome activation is a ROS-dependent way.

5. Conclusion

Our results demonstrate that TXNIP inhibition protects the diabetic kidney from I/R injury and diminishes the AKI sensitivity of diabetic kidney tissues by inhibiting oxidative stress and NLRP3 inflammasome activation. Our findings further suggest that TXNIP, an endogenous redox regulator, may represent an important future target to develop newer

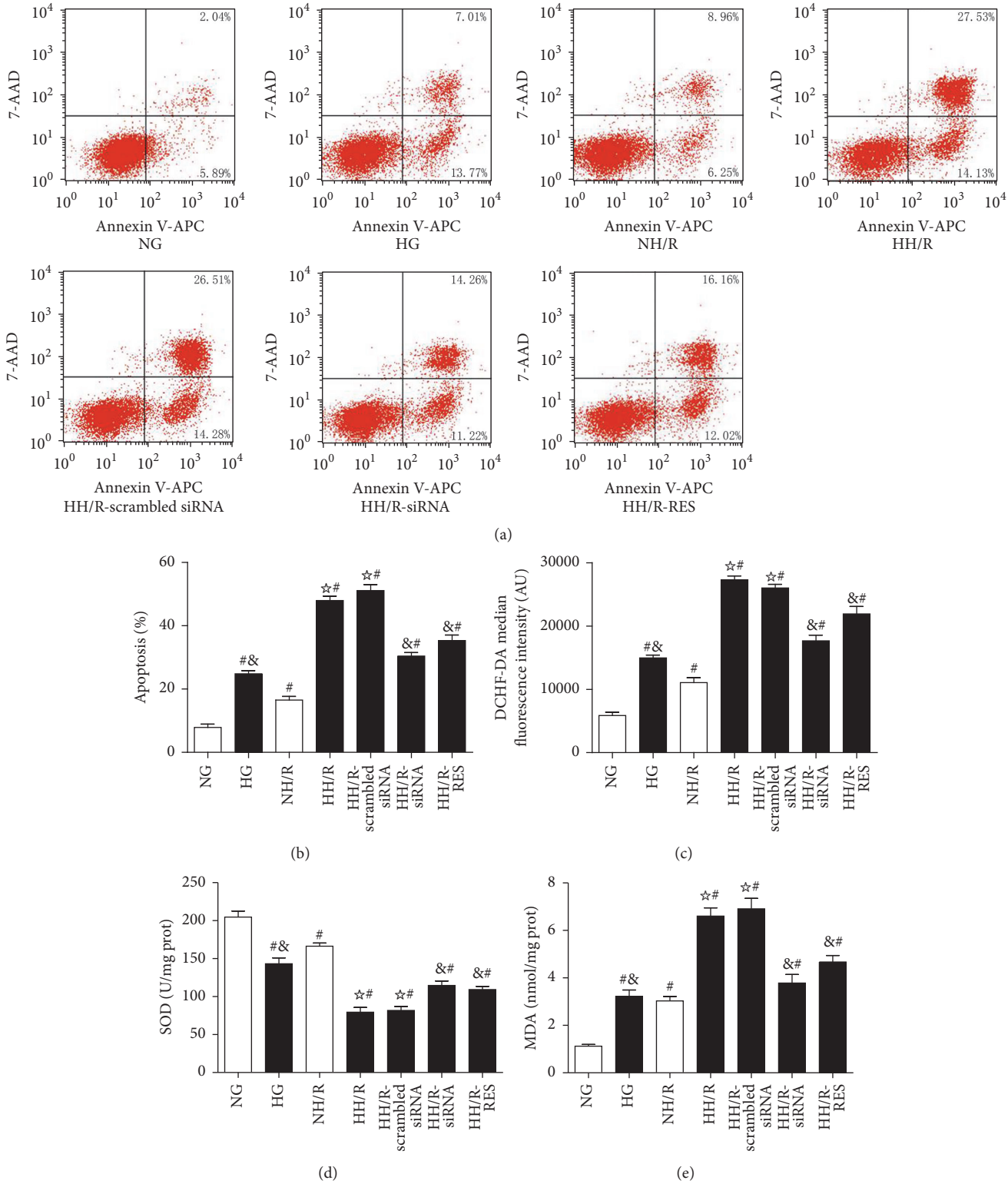

Figure 9: Effect of TXNIP inhibition on the HH/R-induced apoptosis and oxidative stress in HK-2 cells. Apoptotic cells were defined as the cells in the right two quadrants of each plot and the percentages were determined by flow cytometry (a, b); intracellular ROS was detected by flow cytometry (c); SOD (d) and MDA (e) were detected by microplate reader. The data in (b–e) are means ± SE ($n = 5$). $^{\#}P < 0.05$ versus NG group; $^{\star}P < 0.05$ versus NH/R group; $^{\&}P < 0.05$ versus HH/R-scrambled siRNA group. NG: normal glucose (5.6 mM); HG: high glucose (30 mM). NH/R: hypoxia (4 h)/reoxygenation (2 h) under NG condition; HH/R: hypoxia (4 h)/reoxygenation (2 h) under HG condition. HH/R-RES: HH/R pretreated by RES (50 μM) for 72 h with the high glucose incubation. HH/R-siRNA: TXNIP protein was inhibited by transfection with TXNIP siRNA before HH/R; HH/R-scrambled siRNA: scrambled siRNA used as control before HH/R.

therapeutics in diabetic patients that can reduce AKI sensitivity of kidney tissues.

Disclosure

All authors have no financial, personal, or other relationships with other people or organizations that could inappropriately influence the work.

Competing Interests

The authors declare that they have no competing interests.

References

[1] S. M. Sancho-Martínez, J. M. López-Novoa, and F. J. López-Hernández, "Pathophysiological role of different tubular epithelial cell death modes in acute kidney injury," *Clinical Kidney Journal*, vol. 8, no. 5, pp. 548–559, 2015.

[2] E. M. Bucuvic, D. Ponce, and A. L. Balbi, "Risk factors for mortality in acute kidney injury," *Revista da Associação Médica Brasileira*, vol. 57, no. 2, pp. 158–163, 2011.

[3] S. Giunti, D. Barit, and M. E. Cooper, "Diabetic nephropathy: from mechanisms to rational therapies," *Minerva Medica*, vol. 97, no. 3, pp. 241–262, 2006.

[4] Y. S. Kanwar, L. Sun, P. Xie, F.-Y. Liu, and S. Chen, "A glimpse of various pathogenetic mechanisms of diabetic nephropathy," *Annual Review of Pathology*, vol. 6, pp. 395–423, 2011.

[5] J. M. Forbes, M. T. Coughlan, and M. E. Cooper, "Oxidative stress as a major culprit in kidney disease in diabetes," *Diabetes*, vol. 57, no. 6, pp. 1446–1454, 2008.

[6] D. P. Basile, M. D. Anderson, and T. A. Sutton, "Pathophysiology of acute kidney injury," *Comprehensive Physiology*, vol. 2, no. 2, pp. 1303–1353, 2012.

[7] C. V. Thakar, A. Christianson, J. Himmelfarb, and A. C. Leonard, "Acute kidney injury episodes and chronic kidney disease risk in diabetes mellitus," *Clinical Journal of the American Society of Nephrology*, vol. 6, no. 11, pp. 2567–2572, 2011.

[8] J. Melin, O. Hellberg, L. M. Akyürek, Ö. Källskog, E. Larsson, and B. C. Fellström, "Ischemia causes rapidly progressive nephropathy in the diabetic rat," *Kidney International*, vol. 52, no. 4, pp. 985–991, 1997.

[9] J. Melin, O. Hellberg, E. Larsson, L. Zezina, and B. C. Fellström, "Protective effect of insulin on ischemic renal injury in diabetes mellitus," *Kidney International*, vol. 61, no. 4, pp. 1383–1392, 2002.

[10] K. J. Kelly, J. L. Burford, and J. H. Dominguez, "Postischemic inflammatory syndrome: a critical mechanism of progression in diabetic nephropathy," *American Journal of Physiology—Renal Physiology*, vol. 297, no. 4, pp. F923–F931, 2009.

[11] G. Gao, B. Zhang, G. Ramesh et al., "TNF-α mediates increased susceptibility to ischemic AKI in diabetes," *American Journal of Physiology—Renal Physiology*, vol. 304, no. 5, pp. F515–F521, 2013.

[12] P. J. Bakker, L. M. Butter, L. Kors et al., "Nlrp3 is a key modulator of diet-induced nephropathy and renal cholesterol accumulation," *Kidney International*, vol. 85, no. 5, pp. 1112–1122, 2014.

[13] Y. Yin, J. L. Pastrana, X. Li et al., "Inflammasomes: sensors of metabolic stresses for vascular inflammation," *Frontiers in Bioscience*, vol. 18, no. 2, pp. 638–649, 2013.

[14] B. Luo, B. Li, W. Wang et al., "NLRP3 gene silencing ameliorates diabetic cardiomyopathy in a type 2 diabetes rat model," *PLoS ONE*, vol. 9, no. 8, Article ID e104771, 2014.

[15] L. M. Bivol, B. M. Iversen, M. Hultstrom et al., "Unilateral renal ischemia in rats induces a rapid secretion of inflammatory markers to renal lymph and increased peritubular capillary permeability," *The Journal of Physiology*, vol. 594, no. 6, pp. 1709–1726, 2015.

[16] F. Martinon, K. Burns, and J. Tschopp, "The inflammasome: a molecular platform triggering activation of inflammatory caspases and processing of proIL-β," *Molecular Cell*, vol. 10, no. 2, pp. 417–426, 2002.

[17] A. A. Shigeoka, J. L. Mueller, A. Kambo et al., "An inflammasome-independent role for epithelial-expressed Nlrp3 in renal ischemia-reperfusion injury," *Journal of Immunology*, vol. 185, no. 10, pp. 6277–6285, 2010.

[18] P. J. Bakker, L. M. Butter, N. Claessen et al., "A tissue-specific role for Nlrp3 in tubular epithelial repair after renal ischemia/reperfusion," *American Journal of Pathology*, vol. 184, no. 7, pp. 2013–2022, 2014.

[19] A. Abderrazak, T. Syrovets, D. Couchie et al., "NLRP3 inflammasome: from a danger signal sensor to a regulatory node of oxidative stress and inflammatory diseases," *Redox Biology*, vol. 4, pp. 296–307, 2015.

[20] K. Maiese, "New insights for oxidative stress and diabetes mellitus," *Oxidative Medicine and Cellular Longevity*, vol. 2015, Article ID 875961, 17 pages, 2015.

[21] W. Qi, X. Chen, R. E. Gilbert et al., "High glucose-induced thioredoxin-interacting protein in renal proximal tubule cells is independent of transforming growth factor-β1," *The American Journal of Pathology*, vol. 171, no. 3, pp. 744–754, 2007.

[22] J. Wei, Y. Shi, Y. Hou et al., "Knockdown of thioredoxin-interacting protein ameliorates high glucose-induced epithelial to mesenchymal transition in renal tubular epithelial cells," *Cellular Signalling*, vol. 25, no. 12, pp. 2788–2796, 2013.

[23] R. Zhou, A. Tardivel, B. Thorens, I. Choi, and J. Tschopp, "Thioredoxin-interacting protein links oxidative stress to inflammasome activation," *Nature Immunology*, vol. 11, no. 2, pp. 136–140, 2010.

[24] O. N. Spindel, C. World, and B. C. Berk, "Thioredoxin interacting protein: redox dependent and independent regulatory mechanisms," *Antioxidants and Redox Signaling*, vol. 16, no. 6, pp. 587–596, 2012.

[25] E. Junn, S. H. Han, J. Y. Im et al., "Vitamin D_3 up-regulated protein 1 mediates oxidative stress via suppressing the thioredoxin function," *The Journal of Immunology*, vol. 164, no. 12, pp. 6287–6295, 2000.

[26] P. Patwari, L. J. Higgins, W. A. Chutkow, J. Yoshioka, and R. T. Lee, "The interaction of thioredoxin with TXNIP. Evidence for formation of a mixed disulfide by disulfide exchange," *The Journal of Biological Chemistry*, vol. 281, no. 31, pp. 21884–21891, 2006.

[27] P. C. Schulze, J. Yoshioka, T. Takahashi, Z. He, G. L. King, and R. T. Lee, "Hyperglycemia promotes oxidative stress through inhibition of thioredoxin function by thioredoxin-interacting protein," *The Journal of Biological Chemistry*, vol. 279, no. 29, pp. 30369–30374, 2004.

[28] A. A. A. Bertelli and D. K. Das, "Grapes, wines, resveratrol, and heart health," *Journal of Cardiovascular Pharmacology*, vol. 54, no. 6, pp. 468–476, 2009.

[29] M. Kitada and D. Koya, "Renal protective effects of resveratrol," *Oxidative Medicine and Cellular Longevity*, vol. 2013, Article ID 568093, 7 pages, 2013.

[30] M. Kitada, S. Kume, N. Imaizumi, and D. Koya, "Resveratrol improves oxidative stress and protects against diabetic nephropathy through normalization of Mn-SOD dysfunction in AMPK/SIRT1-independent pathway," *Diabetes*, vol. 60, no. 2, pp. 634–643, 2011.

[31] A. Khader, W.-L. Yang, M. Kuncewitch et al., "Novel resveratrol analogues attenuate renal ischemic injury in rats," *Journal of Surgical Research*, vol. 193, no. 2, pp. 807–815, 2015.

[32] V. Nivet-Antoine, C.-H. Cottart, H. Lemaréchal et al., "trans-Resveratrol downregulates TXNIP overexpression occurring during liver ischemia-reperfusion," *Biochimie*, vol. 92, no. 12, pp. 1766–1771, 2010.

[33] T. Ishrat, I. N. Mohamed, B. Pillai et al., "Thioredoxin-interacting protein: a novel target for neuroprotection in experimental thromboembolic stroke in mice," *Molecular Neurobiology*, vol. 51, no. 2, pp. 766–778, 2015.

[34] M.-J. Lee, D. Feliers, K. Sataranatarajan et al., "Resveratrol ameliorates high glucose-induced protein synthesis in glomerular epithelial cells," *Cellular Signalling*, vol. 22, no. 1, pp. 65–70, 2010.

[35] M. Jiang, K. Liu, J. Luo, and Z. Dong, "Autophagy is a renoprotective mechanism during in vitro hypoxia and in vivo ischemia-reperfusion injury," *The American Journal of Pathology*, vol. 176, no. 3, pp. 1181–1192, 2010.

[36] C.-C. Chang, C.-Y. Chang, Y.-T. Wu, J.-P. Huang, T.-H. Yen, and L.-M. Hung, "Resveratrol retards progression of diabetic nephropathy through modulations of oxidative stress, proinflammatory cytokines, and AMP-activated protein kinase," *Journal of Biomedical Science*, vol. 18, no. 1, article 47, 2011.

[37] K. Zeytin, N. S. Çiloğlu, F. Ateş, F. Vardar Aker, and F. Ercan, "The effects of resveratrol on tendon healing of diabetic rats," *Acta Orthopaedica et Traumatologica Turcica*, vol. 48, no. 3, pp. 355–362, 2014.

[38] Q. Wei and Z. Dong, "Mouse model of ischemic acute kidney injury: technical notes and tricks," *American Journal of Physiology—Renal Physiology*, vol. 303, no. 11, pp. F1487–F1494, 2012.

[39] Y. Zhu, M. Blum, U. Hoff et al., "Renal ischemia/reperfusion injury in soluble epoxide hydrolase-deficient mice," *PLoS ONE*, vol. 11, no. 1, Article ID e0145645, 2016.

[40] M. Collino, E. Benetti, G. Miglio et al., "Peroxisome proliferator-activated receptor β/δ agonism protects the kidney against ischemia/reperfusion injury in diabetic rats," *Free Radical Biology and Medicine*, vol. 50, no. 2, pp. 345–353, 2011.

[41] N. Abu-Saleh, H. Awad, M. Khamaisi et al., "Nephroprotective effects of TVP1022, a non-MAO inhibitor S-isomer of rasagiline, in an experimental model of diabetic renal ischemic injury," *American Journal of Physiology—Renal Physiology*, vol. 306, no. 1, pp. F24–F33, 2014.

[42] J. Peng, X. Li, D. Zhang et al., "Hyperglycemia, p53, and mitochondrial pathway of apoptosis are involved in The susceptibility of diabetic models to ischemic acute kidney injury," *Kidney International*, vol. 87, no. 1, pp. 137–150, 2015.

[43] S. Zhu, Y. Yang, J. Hu et al., "WldS ameliorates renal injury in a type 1 diabetic mouse model," *American Journal of Physiology—Renal Physiology*, vol. 306, no. 11, pp. F1348–F1356, 2014.

[44] D. De Nardo and E. Latz, "NLRP3 inflammasomes link inflammation and metabolic disease," *Trends in Immunology*, vol. 32, no. 8, pp. 373–379, 2011.

[45] W. P. Pulskens, L. M. Butter, G. J. Teske et al., "Nlrp3 prevents early renal interstitial edema and vascular permeability in unilateral ureteral obstruction," *PLoS ONE*, vol. 9, no. 1, Article ID e85775, 2014.

[46] V. Sagulenko, S. J. Thygesen, D. P. Sester et al., "AIM2 and NLRP3 inflammasomes activate both apoptotic and pyroptotic death pathways via ASC," *Cell Death and Differentiation*, vol. 20, no. 9, pp. 1149–1160, 2013.

[47] Y. Liu, K. Lian, L. Zhang et al., "TXNIP mediates NLRP3 inflammasome activation in cardiac microvascular endothelial cells as a novel mechanism in myocardial ischemia/reperfusion injury," *Basic Research in Cardiology*, vol. 109, no. 5, article 415, 2014.

[48] H. Su, L. Ji, W. Xing et al., "Acute hyperglycaemia enhances oxidative stress and aggravates myocardial ischaemia/reperfusion injury: role of thioredoxin-interacting protein," *Journal of Cellular and Molecular Medicine*, vol. 17, no. 1, pp. 181–191, 2013.

[49] L. L. Dunn, P. J. L. Simpson, H. C. Prosser et al., "A critical role for thioredoxin-interacting protein in diabetes-related impairment of angiogenesis," *Diabetes*, vol. 63, no. 2, pp. 675–687, 2014.

[50] H. Parikh, E. Carlsson, W. A. Chutkow et al., "TXNIP regulates peripheral glucose metabolism in humans," *PLoS Medicine*, vol. 4, no. 5, article e158, 2007.

[51] J. M. Abais, M. Xia, G. Li et al., "Nod-like receptor protein 3 (NLRP3) inflammasome activation and podocyte injury via thioredoxin-interacting protein (TXNIP) during hyperhomocysteinemia," *Journal of Biological Chemistry*, vol. 289, no. 39, pp. 27159–27168, 2014.

[52] P. Gao, X.-F. Meng, H. Su et al., "Thioredoxin-interacting protein mediates NALP3 inflammasome activation in podocytes during diabetic nephropathy," *Biochimica et Biophysica Acta—Molecular Cell Research*, vol. 1843, no. 11, pp. 2448–2460, 2014.

[53] Y. Shi, Y. Ren, L. Zhao et al., "Knockdown of thioredoxin interacting protein attenuates high glucose-induced apoptosis and activation of ASK1 in mouse mesangial cells," *FEBS Letters*, vol. 585, no. 12, pp. 1789–1795, 2011.

[54] P. Palsamy and S. Subramanian, "Resveratrol protects diabetic kidney by attenuating hyperglycemia-mediated oxidative stress and renal inflammatory cytokines via Nrf2-Keap1 signaling," *Biochimica et Biophysica Acta—Molecular Basis of Disease*, vol. 1812, no. 7, pp. 719–731, 2011.

Hindawi Publishing Corporation
Oxidative Medicine and Cellular Longevity
Volume 2016, Article ID 6032306, 11 pages
http://dx.doi.org/10.1155/2016/6032306

Review Article

Targeting Glial Mitochondrial Function for Protection from Cerebral Ischemia: Relevance, Mechanisms, and the Role of MicroRNAs

Le Li[1,2] and Creed M. Stary[1]

[1]*Department of Anesthesiology, Perioperative & Pain Medicine, Stanford University School of Medicine, 300 Pasteur Drive, Stanford, CA 94305-5117, USA*
[2]*Department of Anesthesiology, Zhujiang Hospital, Southern Medical University, 253 Industrial Road, Guangzhou, Guangdong Province 510280, China*

Correspondence should be addressed to Creed M. Stary; cstary@stanford.edu

Received 24 June 2016; Revised 21 August 2016; Accepted 31 August 2016

Academic Editor: Adriana M. Cassina

Astrocytes and microglia play crucial roles in the response to cerebral ischemia and are effective targets for stroke therapy in animal models. MicroRNAs (miRs) are important posttranscriptional regulators of gene expression that function by inhibiting the translation of select target genes. In astrocytes, miR expression patterns regulate mitochondrial function in response to oxidative stress *via* targeting of Bcl2 and heat shock protein 70 family members. Mitochondria play an active role in microglial activation, and miRs regulate the microglial neuroinflammatory response. As endogenous miR expression patterns can be altered with exogenous mimics and inhibitors, miR-targeted therapies represent a viable intervention to optimize glial mitochondrial function and improve clinical outcome following cerebral ischemia. In the present article, we review the role that astrocytes and microglia play in neuronal function and fate following ischemic stress, discuss the relevance of mitochondria in the glial response to injury, and present current evidence implicating miRs as critical regulators in the glial mitochondrial response to cerebral ischemia.

1. Introduction

Ischemic stroke remains a leading cause of death and long-term disability worldwide [1]. Despite hundreds of promising preclinical trials demonstrating efficacy of neuron-targeted therapies in animal models of stroke, the only clinical treatment remains early restoration of blood flow with thrombolysis [2]. The failure to translate neuron-targeted approaches to useful clinical therapy suggests that alternative cellular targets in the brain may more effectively coordinate the complex intra- and intercellular signaling cascades that contribute to neuronal injury. Astrocytes comprise the most numerous type of cell in the brain and play a crucial role in neuronal homeostasis both for normal physiologic functioning and in response to cell stress [3]. Microglia coordinate growth and remodeling of the neural network and regulate the neuroinflammatory response to stroke [4, 5]. In both astrocytes and microglia, mitochondria play a central role in determining local neuronal cell fate. Therapeutic strategies aimed at maintaining mitochondrial function in glia following stroke may therefore provide a novel approach to reduce the degree of injury and improve neurobehavioral outcome.

MicroRNAs (miRs) are a class of small noncoding RNAs that regulate gene expression by binding to the 3′ untranslated region (UTR) of target genes and destabilizing or inhibiting their translation [6]. In glia, miRs have been shown to play an important role in the cellular response to ischemic injury (for reviews, see [7–9]). In particular, miRs can alter the expression of proteins that both directly and indirectly modulate glial mitochondrial function. The purpose of this review is to (1) provide an overview of astrocyte and microglia-mediated regulation of neuronal cell function and fate following ischemic injury; (2) discuss the relevance of glial mitochondrial function in response to ischemic injury; (3) review coordination of mitochondrial homeostasis by B-cell lymphoma 2 (Bcl2) and heat shock protein 70 (Hsp70) family

members; and (4) present current evidence demonstrating the critical role miRs play in regulating glial mitochondrial function in response to cerebral ischemic injury.

2. Glia in Health and in Response to Ischemia

2.1. Astrocytes. Neuronal maintenance, neurite outgrowth, and repair of the neuronal network are coordinated by resident astrocytes [10–12]. As an essential component of the neurovascular unit (a dynamic structure also composed of endothelial cells, pericytes, basement membrane, and surrounding neurons), astrocytes control blood circulation, extracellular ion homeostasis, and release of energy substrates and growth factors in the central nervous system. In addition to their role in neuronal housekeeping and protection, astrocytes play a significant role in neurotransmission [11, 13]. Astrocytes are central to synapse formation and stabilization in development and disease [3, 14, 15] and modulate synaptic transmission *via* glutamate uptake [16]. Astrocytes extend many fine branching processes, putting them in direct contact with cell bodies, dendrites, and synaptic terminals, such that an individual astrocyte may contact up to 100,000 neurons [17]. Moreover, astrocytes communicate with adjacent astrocytes *via* intercellular gap junctions to function as a coordinated syncytium [18, 19]. As a consequence, astrocytes actively regulate and organize local and distant synaptic activity, excitability, transmission, and plasticity of the neuronal network [20–23].

Ischemic stroke remains the most common and debilitating source of cerebral ischemia [1]. However, acute cerebral ischemia can occur *via* a number of mechanisms, including hemorrhagic stroke, subdural and epidural hematoma, subarachnoid hemorrhage, traumatic brain injury, cerebral edema, vascular compression from brain masses, cardiac arrest, or any physiologic condition resulting in low cardiac output. Following cerebral ischemia, astrocytes perform multiple functions beneficial for neuronal survival. One common pathway for neuronal cell death following cerebral ischemia is the accumulation of extrasynaptic glutamate, which triggers mitochondrial dysfunction characterized by imbalances in intracellular Ca^{2+} handling and excessive production of oxidants, eventually leading to neuronal cell death (Figure 1). Astrocytes have been shown to protect neurons from glutamate excitotoxicity during pathophysiologic stresses such as stroke [24], traumatic brain injury [25], and spinal cord injury [26]. However, the astrocyte response to oxidative stress also induces morphologic and phenotypic changes that can paradoxically exacerbate injury, a process termed reactive gliosis or astrogliosis [24, 27]. Reactive astrocytes are identified by increases in cytoplasmic mass and branching processes and increased production of cytoplasmic filaments, most notably glial fibrillary acidic protein. Reactive astrogliosis and subsequent development of an astrocytic scar surrounding the area of injury are essential for isolating the injury site and protecting neurons against harmful substances released from the infarct core. However, this process can also contribute to limiting neuronal regeneration by inhibiting axonal sprouting *via* secretion of chondroitin sulfate proteoglycans [28, 29].

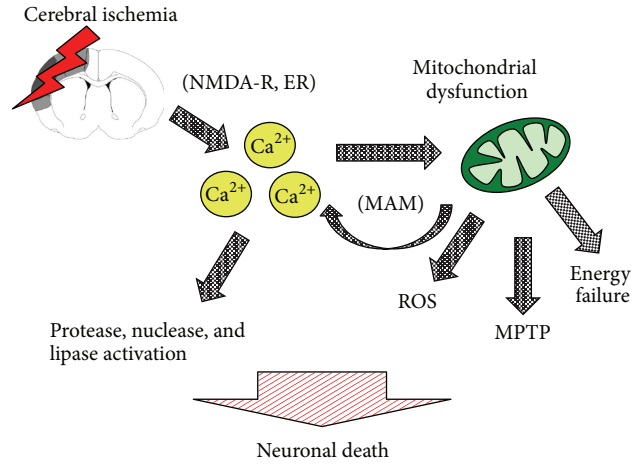

Figure 1: Cerebral ischemia induces mitochondrial dysfunction and neuronal cell death. Ischemia-reperfusion induces elevations in cytosolic Ca^{2+} *via* glutamate binding extrasynaptic NMDA receptors (NMDA-R) and/or mitochondrial-associated membrane (MAM) mediated release from the endoplasmic reticulum (ER). As mitochondrial Ca^{2+} buffering capacity is exceeded and mitochondrial dysfunction ensues, mitochondria produce excessive reactive oxygen species (ROS), decrease capacity for ATP production, and activate the mitochondrial permeability transition pore (MPTP), which can trigger cytochrome c mediated apoptosis. Sustained elevations in cytosolic Ca^{2+} can activate proteases, lipases, and nucleases triggering autophagy or necrotic cell death. NMDA: N-methyl-D-aspartate.

The astrocytic syncytium may also influence neuronal survival by coordinating the spatial delivery of metabolic fuels, thereby maintaining both mitochondrial and cellular integrity. Gap junctions are permeable to both glucose and lactate [30], regulate the development of postinjury edema [31], and have the potential to facilitate delivery of substrates to metabolically active neurons in local areas of decreased perfusion. However, the role of astrocytic gap junctions in stroke remains controversial [32]. For example, astrocytic gap junctions remaining open following ischemia [33] can allow proapoptotic factors and other molecules to spread through the syncytium, expanding the size of the infarct [34]. Moreover, persistently open gap junctions can allow Ca^{2+} waves to propagate throughout the syncytium and induce remote neuronal cell death [35].

Astrocyte-targeted therapies have been shown to protect against neurotoxicity in animal models of neurodegeneration. For example, in astrocytes with an amyotrophic lateral sclerosis- (ALS-) linked mutation in mitochondrial superoxide dismutase ($SOD1^{G93A}$) that disrupts mitochondrial function and results in motor neuron cell death, pretreatment of astrocytes with mitochondrial-targeted antioxidants (ubiquinone and carboxy-proxyl nitroxide coupled to triphenylphosphonium) or with dichloroacetate (DCA, an activator of the pyruvate dehydrogenase complex that improves oxidative phosphorylation coupling) mitigated neuronal cell death in cocultures [36, 37]. Studies specifically targeting astrocytes for improving outcome following

cerebral ischemia are limited but have shown promise in rodent models. Augmenting astrocyte extrasynaptic glutamate sequestration by increasing the activity of astrocytic glutamate transporter GLT-1 has been effective at decreasing glutamate excitotoxicity, thereby indirectly maintaining mitochondrial function [38, 39]. However, targeting of the astrocyte response to oxidative stress has also been effective: overexpression of superoxide dismutase 2 (SOD2) in astrocytes reduced evidence of oxidative stress in the hippocampus from transient global ischemia [40] and was also accompanied by preservation of GLT-1. Additionally, increasing astrocytic pyruvate preserved mitochondrial function and improved neuronal survival *via* a glutathione-dependent mechanism [41]. Utilizing direct mitochondrial-targeted approaches in astrocytes may serve to outweigh the negative consequences of reactive gliosis, a necessary astrocyte response for minimizing the degree of injury from cerebral ischemia [42].

2.2. Microglia. Microglia constitute 10–15% of all cells in the brain and play an important role in neuronal migration, axonal growth, and synaptic remodeling and in response to ischemic injury (for reviews, see [4, 5, 43]). Microglia share a common myeloid lineage with monocytes and macrophages and similarly act as the primary form of tissue immune defense. The primary functions of microglia are (1) pathogen recognition; (2) phagocytosis of damaged cells, inactive synapses, debris, and infectious agents; and (3) regulation of T-cell responses and induction of inflammation. Under normal physiological conditions, microglia exist in a "resting" state, although they remain highly dynamic with continuous extension and retraction of processes that survey the local microenvironment. Cerebral ischemia induces microglial activation [43], characterized by a change from a ramified to amoeboid shape, loss of branching processes, and production of lysosomes and phagosomes. Mitochondrial function (and dysfunction) appears to play a direct role in microglial activation [44]. Similar to astrocytes, activated microglia have been observed to exert both injurious and protective effects subsequent to cerebral ischemia [45]. This ambiguity has been partially resolved by the observation that microglial activation in response to stroke is a polarized process, described as M1 and M2 activation states (for review, see [5]).

Morphologically, microglia of both M1 and M2 activation states become spherical and retract their processes. Differentiation between the two states is therefore based on antigen expression and cytokine secretion patterns. In M1 or "classical" activation, microglia are characterized by upregulation of proinflammatory surface antigens that can be induced by bacterial lipopolysaccharides or the proinflammatory cytokine interferon-γ. M1 activation triggers the production of proinflammatory factors such as tumor necrosis factor-α (TNF-α), interleukin-1β (IL-1β), nitric oxide, and reactive oxygen species (ROS), which, in excess, can exacerbate brain injury. TNF-α is a critical proinflammatory cytokine released from M1 microglial cells following ischemia, which serves as an activator of receptor-mediated proapoptotic pathways within the neuron, and can further stimulate microglia *via* inducible nitric oxide synthase (iNOS) and cyclooxygenase 2 [46].

Activation of the M2 phenotype by IL-4, IL-10, and/or IL-13 induces surface-receptor expression of several distinct antigens, such as arginase, heparin-binding lectin Ym-1, CD206, and CD36. M2 polarization may also result in a greater capacity for phagocytosis [47–49], important for sequestration of cytotoxic material and in activation of the adaptive immune response. Observations suggest that the time course of polarization and the relative abundance of the two phenotypes depend on the severity, location, and duration of ischemia and reperfusion [43]. Although the precise poststroke temporal kinetics of microglial polarization and mechanisms that determine polarization remain to be determined, current evidence suggests that oxidative stress and mitochondrial function play a central regulatory role [50]. However, more recently, the M1 and M2 classification scheme has been brought into question [51], with the suggestion that, with the advent of novel technologies that better define the complexities of the immunological landscape, the present dichotomy will likely be replaced by a spectrum of activation states that will more accurately reflect the microglial response to ischemic injury.

3. Mitochondrial Function in Response to Ischemic Injury

3.1. Calcium and Oxidative Stress. Therapeutic strategies that optimize mitochondrial homeostasis may offer a unifying approach to simultaneously target multiple deleterious pathways: mitochondria are central regulators of apoptosis, ROS, and intracellular Ca^{2+} handling. Depletion of energy reserves as occurs during ischemia leads to a massive rise in free cytosolic Ca^{2+} (Figure 1), both from the endoplasmic reticulum (ER) and from the extracellular space, which can then be transmitted to the matrix of mitochondria *via* the mitochondrial-associated membrane (MAM) (for review, see [52]). When mitochondrial matrix Ca^{2+} exceeds buffering capacity, mitochondrial function becomes compromised and results in increased generation of free radicals and formation of the mitochondrial permeability transition pore (MPTP, [53]). Activation and opening on the MPTP can cause release of cytochrome c [54, 55] and other proapoptotic factors into the cytoplasm. The combination of Ca^{2+} accumulation in cytosolic and mitochondrial compartments and excessive ROS levels from reperfusion can induce alterations in protein folding homoeostasis, leading to MAM-mediated amplification in cytosolic Ca^{2+}, which can then activate protease, nuclease, and lipase pathways, ultimately contributing to necrotic cell death [52, 56]. Oxidative stress mediated by nitric oxide (e.g., peroxynitrate, $ONOO^-$) can also induce reactive gliosis and induce neuronal cell death, an effect mitigated by coadministration of nitric acid synthase (NOS) inhibitors or peroxynitrite scavengers [57].

3.2. Glia Mitochondrial Function Regulates Neuronal Survival. Astrocytic mitochondrial function plays several direct and indirect roles in maintaining neuronal survival from

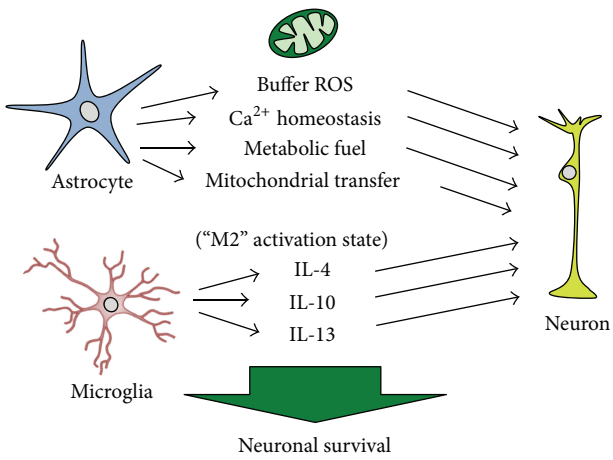

Figure 2: Glia mitochondrial function is essential to neuronal survival following cerebral ischemia. Astrocytes provide protection to neurons by a number of mitochondrial-associated mechanisms, including buffering excessive reactive oxygen species (ROS), maintaining Ca^{2+} homeostasis, and providing metabolic substrate and ATP to neurons. Astrocytes may also regulate neuronal homeostasis and the neuronal bioenergetic response to injury by direct transfer of mitochondria from astrocytes to neurons. Microglial activation polarity determines neuronal fate, with M2 activation state associated with anti-inflammatory cytokine production. Microglial activation is coordinated by microglial and astrocyte mitochondrial function. IL-4: interleukin-4; IL-10: interleukin-10; IL-13: interleukin-13.

ischemic injury (Figure 2). Davis et al. [58] previously observed sequestration of degraded neuronal mitochondria by local astrocytes, suggesting a role for astrocytes in neuronal mitochondrial recycling and biogenesis. More recently, Hayakawa et al. [59] demonstrated that astrocytes are capable of direct transfer of functional mitochondria to neurons and that suppression of this process worsens injury and neurologic outcome from cerebral ischemia. Together, these observations demonstrate a role for mitochondria as a novel medium for neuronal-astrocyte communication and position astrocytes as central to maintenance of neuronal metabolism and bioenergetics in response to cell stress. For example, in addition to coordinating apoptosis, mitochondria are fundamental to maintaining ATP levels *via* oxidative phosphorylation. Neurons, with a relatively higher rate of ATP consumption compared with glia, require a constant source of reducing equivalents to rephosphorylate ATP from ADP and AMP. ATP is required to establish and maintain resting electrochemical gradients and repolarize membranes after depolarization and synaptic transmission and is essential for a host of intracellular signaling and biosynthetic functions. During ischemia, substrate for oxidative phosphorylation (i.e., oxygen and glucose) is reduced, and energy deprivation results in impaired cellular function and eventually cell death (for review, see [60]). Neurons do not normally store glucose as glycogen and must rely on exogenous delivery of substrate [61, 62]. Astrocytes can store glycogen and are therefore critical in maintaining a steady source of metabolic fuel to neurons during ischemic conditions [61, 62]. Lactate generated by astrocytes is transported into neurons *via* the monocarboxylate transporter-2 (MCT-2, [63]), which can serve as a metabolic fuel to maintain basal neuronal activity, particularly when the blood supply of glucose is interrupted [64, 65]. Triggering astrocytic glycolysis is at least in part due to neuronal-astrocyte energy coupling *via* activation of adenosine monophosphate-activated protein kinase (AMPK), an evolutionarily conserved enzyme that functions as an energy sensor by coupling changes in ATP supply to ATP production [66]. Neuronal release of tissue plasminogen activator (tPA), a strong activator of AMPK in astrocytes, induces a switch to glycolysis and subsequent release of lactate, which is then transported into neurons *via* MCT-2 [67]. However, in the nonstressed state, particularly in the poststroke recovery phase when energy requirements are high, a return to oxidative phosphorylation is preferred [60].

Astrocytes are therefore predictably more tolerant to injury than neurons: similar exposure times to oxygen-glucose deprivation (OGD) result in greater injury to primary neuronal cultures *versus* primary astrocyte cultures [68]. Neurons also have limited antioxidant capacity and rely heavily on the antioxidant capacity of astrocyte cytosolic and mitochondrial superoxide dismutase, catalase, glutathione reductase, and glutathione peroxidase to combat oxidative stress [69, 70]. By these and other mechanisms, astrocyte mitochondrial dysfunction can lead to increased neuronal death [70]. For example, disruptions in astrocyte mitochondrial function have been shown to play a direct role in neurotoxicity in animal models of neurodegeneration. Nagai et al. [71] observed that the ALS-linked mutation $SOD1^{G93A}$ was associated with increased neurotoxicity and cell death of motor neurons. Cassina et al. [36] observed that astrocytes with the $SOD1^{G93A}$ mutation demonstrate severe disruptions in oxidative phosphorylation coupling and enhanced mitochondrial superoxide production and recapitulated their neurotoxic effect by pretreatment of astrocytes in neuronal-astrocyte cocultures with mitochondrial inhibitors (rotenone, antimycin A, sodium azide, or fluorocitrate). A further example is that the mitochondrial Ca^{2+} buffering capacity of astrocytes determines astrocyte GLT-1 expression [72], and therefore astrocyte mitochondrial function is intimately tied to the capacity of astrocytes to buffer excessive (extrasynaptic) glutamate and prevent excitotoxicity [73, 74].

In microglia, the role of mitochondrial function in neuronal survival can be considered direct, as neuronal survival is a function of microglial ROS production [75], and indirect, *via* polarization of activation state and subsequent downstream production of cytokines (Figure 2). Cytotoxic M1 activation of microglia is associated with neuronal loss and decline of cognitive and neurobehavioral function [76]. Conversely, M2 activated microglia secrete neurotrophic factors and neuroprotective cytokines. NF-κB, a transcription factor that activates genes regulating cellular survival, growth, differentiation, inflammation, and cell death, plays a central role in regulating the effect of microglia by participating both in protective and in deleterious responses. High concentrations of ROS inactivate NF-κB, inhibiting its binding to DNA, while moderate levels of ROS lead to the sequential phosphorylation, polyubiquitination, and degradation of IκB

(inhibitor of κB), allowing activation of NF-κB. Once activated, NF-κB plays a prosurvival role by inhibiting caspase cell death pathways and upregulating transcriptional activation of antiapoptotic proteins and genes involved in decreasing mitochondrial ROS, such as manganese superoxide dismutase [77]. NF-κB also activates antiapoptotic responses regulated by mitochondria, thereby protecting neurons from ischemic brain injury [78]. Therefore, mitochondrial function and microglial activation serve reciprocal roles: targeting cytokines that promote the microglial M2 activation state may result in protecting mitochondrial homeostasis, while direct approaches to augment microglial mitochondrial function may promote M2 activation.

4. Hsp70 and Bcl2 in Mitochondrial Homeostasis

Two families of well-known cytoprotective proteins, the Hsp70 family of chaperones and the Bcl2 apoptosis-regulating family, have been shown to be integral to maintaining mitochondrial homeostasis. The Hsp70 family of chaperones is a functionally related group of proteins that assist in the folding or unfolding of proteins, sequestration of denatured proteins, and assembly of protein complexes. Two relevant Hsp70 family members known to regulate glial mitochondrial function are cytosolic Hsp70/Hsp72 and glucose-related binding protein 78 (Grp78)/binding immunoglobulin protein (BiP). The Bcl2 protein family is a central regulator of cell survival by helping to maintain mitochondrial membrane integrity and function and coordinating apoptotic signaling [79, 80].

4.1. Bcl2. The Bcl2 family is known to play an important role in the evolution of injury following cerebral ischemia [81]. Overexpressing prosurvival Bcl2 family members protects against cerebral ischemia *in vivo* [82, 83] and *in vitro* [84]. Cytosolic Bcl2 was shown to contribute to MAM formation by localizing to both the ER and the mitochondrial outer membranes [85] and to coordinate ER and mitochondrial Ca^{2+} homeostasis following cerebral ischemia [8, 86]. In addition to regulating induction of apoptosis by controlling mitochondrial outer membrane permeabilization, Bcl2 protein family members have been shown to regulate calcium handling [87] and modulate intercompartmental cross talk between mitochondria and the endoplasmic reticulum [88, 89].

4.2. Hsp70/Hsp72. Hsp72, a cytosolic member of the Hsp70 family, participates in protein import and sorting at MAM [90] and regulates downstream Bcl2 expression [91]. Hsp72 is induced in response to a variety of stresses, particularly oxidative stress, and is protective from both necrotic and apoptotic cell death [92, 93].

Hsp72 has been shown to preserve mitochondrial function, reduce oxidative stress, regulate inflammation, and protect from cerebral ischemia [40, 92, 94]. Overexpression protected hippocampus neurons from global cerebral ischemia, mediated in part by increased Bcl2 expression [91]. Overexpression of Hsp72 has been shown to protect both animal and cell models of cerebral ischemia [92]. Astrocyte-specific overexpression of Hsp72 was shown to preserve GLT-1 activity and reduce oxidative stress in the hippocampus following transient global cerebral ischemia [40]. Specifically increasing Hsp72 level in astrocytes demonstrated a reduction in oxidative stress and reduced neuronal vulnerability to global cerebral ischemia [40], as well as improving long-term recovery following focal cerebral ischemia [95]. Evidence suggests that Hsp72 also modulates inflammation from cerebral ischemia [96]. Regulation of NF-κB by Hsp72 can occur *via* inhibition of IκB phosphorylation by IKK and NF-κB dissociation [97] and *via* binding IKK to impair NF-κB signaling [98]. Increased levels of Hsp72 have been shown to decrease the negative effects of NF-κB activation in astrocytes *via* reductions in iNOS expression [98]. Activation of NF-κB was inhibited significantly in Hsp72-overexpressing microglia and transgenic mice [97].

4.3. Grp78. Grp78, a regulator of the ER unfolded protein response [52, 99], is largely localized to the endoplasmic reticulum [100] but has been shown to translocate to mitochondria [101], suggesting a role in MAM-dependent Ca^{2+} transport between ER and mitochondria. Studies utilizing a green fluorescent/Grp78 fusion protein reported targeting to mitochondria within a short period of ischemia-like stress [86]. Overexpression of Grp78 in BV2 mouse microglial cell lines [102] and astrocytes protected against ischemic injury and preserved respiratory activity and mitochondrial membrane potential after ischemic stress [103]. Pharmacological induction of Grp78 reduced neuronal loss in both forebrain and focal cerebral ischemia [104, 105]. Grp78 appears to play an important role in ischemia associated with oxidative stress: increased levels of Grp78 were observed in astrocytes and microglia associated with overproduction of ROS [106, 107].

In addition to effects on oxidative stress and mitochondrial function, Grp78 also mediates the inflammatory response. Grp78 was shown to stimulate the production of the anti-inflammatory cytokines IL-4 and IL-10 through specific T lymphocytes [108, 109]. Interestingly, IL-10 deprivation in mice brains also induced Grp78 expression [110], suggesting a negative-feedback mechanism. Conversely, lower levels of Grp78 inhibited upregulation of IL-6 under glucose-deprived conditions [111]. Though the precise regulatory role of Grp78 in the inflammatory cascade remains to be elucidated, the critical role of astrocytes and microglia in the neuroinflammatory response to cerebral ischemia suggests that pharmacologic manipulation of Hsp72 family members in glia may be a powerful therapeutic approach.

5. MicroRNAs Regulate the Mitochondrial Response to Ischemia

Studies investigating the role of miRs in cerebral ischemia have largely focused on changes in miR expression patterns with ischemia [112]. To define the role of a given miR of interest, predicted molecular targets that have complementarity to the binding sequence of the miR are identified using a bioinformatic approach. Efficacy of translational inhibition

can be tested when the 3′UTR of the putative target mRNA is placed downstream of a luciferase reporter construct. Using this approach, two brain-enriched miRs, miR-181a and miR-29a, were identified as important mediators in the evolution of injury and in determining outcome following stroke (see [113]). A recent microarray analysis of miR expression in the four principal cell types of the CNS (neurons, astrocytes, oligodendrocytes, and microglia) delineated a preferential cellular expression pattern of individual miRs [114]. Notably, miR-181a and miR-29a were more highly expressed in astrocytes, corroborating previous observations [115, 116].

5.1. miR-181. The brain-enriched miR-181 family contains four highly conserved members, miR-181a, miR-181b, miR-181c, and miR-181d, which play a role in mitochondrial function, redox state, and inflammatory pathways [7]. Bioinformatics and dual luciferase assays were used to identify and validate miR-181a as a regulator of several Hsp70 [117, 118] and Bcl2 family members [118]. Increased miR-181a exacerbated injury both *in vitro* and *in vivo*, while reduced levels were associated with reduced injury and increased Grp78 protein levels [118]. Overexpression of miR-181a in astrocytes enhanced disruption of mitochondrial membrane potential and increased ROS formation and cell death from glucose deprivation [118]. Intracerebroventricular infusion and intravenous injection of 181a antagomir, a chemically modified 181a inhibitor optimized for *in vivo* use, were used to treat mice after ischemic injury. miR-181a antagomir was effective at abolishing endogenous expression of miR-181a and showed substantial neuroprotective effects against ischemic neuronal damage and neurological impairment in mice. This protective effect, including recovery of motor function and coordination, persisted over 28 days [119], concordant with decreased expression of Bcl2 and X-linked inhibitor of apoptosis protein (XIAP). Interestingly in primary neurons miR-181a failed to significantly alter levels of Bcl2 and did not improve survival after ischemia-like injury [120]. The difference in effects of miR-181a suppression between different brain cell types may be the result of differences in baseline levels of expression or changes in expression in response to ischemia.

Another member of this family, miR-181c, was identified as directly targeting tumor necrosis factor-alpha (TNF-α) following ischemia, thereby regulating microglial activation and microglial-mediated neuronal injury [121]. Ectopic expression of miR-181c was also shown to suppress expression of iNOS, leading to decreased production of NO following OGD [121]. Additionally, the microglial activator Toll-like receptor 4 (TLR4) was shown to be a target of miR-181c in microglial cells. miR-181c inhibited NF-κB activation induced by OGD and the downstream production of proinflammatory mediators by suppressing TLR4 expression [122].

5.2. miR-29. The miR-29 family, composed of miR-29a, miR-29b, and miR-29c, is distributed across the central nervous system and enriched in astrocytes [123, 124]. All members have been shown to regulate various facets of inflammation [125]. Inhibition of miR-29b significantly reduced expression of activated microglial proinflammatory mediators such as TNF-α, IL-1b, IL-6, and monocyte chemoattractant protein-1 [126]. Recently, miR-29b has been recognized as a survival factor in neuronal cells by silencing the proapoptotic BH3-only family [127]. Interestingly, Shi et al. reported that increasing miR-29b had the effect of *promoting* neuronal cell death in focal ischemia by inhibiting Bcl2l2 (protein BCL-w), an antiapoptotic member of the Bcl2 protein family [128]. Whether the same effect occurs in astrocytes or microglia has not been investigated; however, computational algorithms (i.e., TargetScan5.1, http://www.targetscan.org/) predict that miR-29b targets several members of the Bcl2 family known to be both protective and harmful. The multiple functions of miR-29b are therefore likely due to which Bcl2 family member exerts the more dominant effect in a given cell type and in response to a given injury paradigm.

Ischemic stroke induced by middle-cerebral artery occlusion (MCAO) in mice caused loss of miR-29b and higher 12-lipoxygenase activity in infarcted tissue [129]; delivery of miR-29b mimic markedly attenuated the infarct size. Ouyang et al. observed that miR-29a expression significantly increased in the more ischemia-resistant hippocampal subregion dentate gyrus but decreased in the more ischemia-sensitive cornu ammonis 1 subregion following transient global ischemia [115]. In the setting of *in vitro* ischemia, Ouyang et al. observed that miR-29a mimic protected and miR-29a inhibitor aggravated astrocyte injury and mitochondrial function by targeting the Bcl2 family member p53 upregulated modulator of apoptosis (PUMA, [115]). PUMA binds and antagonizes all known antiapoptotic Bcl2 family members and activates two key multidomain proapoptotic Bcl2 family proteins, BAX and BAK, leading to mitochondrial dysfunction and caspase activation [130]. Most recently [131], we observed in astrocytes cultured from CA1 and DG hippocampal subregions that CA1 astrocytes exhibited more cell death and a greater decrease in miR-29a subsequent to glucose deprivation injury. We identified the mitochondrial voltage-dependent cation channel 1 (VDAC1) as a target of miR-29a in these astrocytes. Located in the outer mitochondrial membrane, VDACs mediate intercompartmental transport of anions, cations, and ATP between the cytosol and mitochondria (for review, see [132]). VDAC1 is the most abundantly expressed and is thought to regulate mitochondrial function and cell survival in response to injury [133]. We observed that increasing miR-29a in CA1 astrocytes decreased VDAC1 and improved cell survival, while knockdown of VDAC1 improved survival. Moreover, the protective effect of miR-29a was eliminated by inhibition of miR-29a/VDAC1 binding *via* cotreatment with a target-site blocker. Together, these findings suggest that the selective vulnerability of the CA1 to injury may be due in part to a limited miR-29a response in CA1 astrocytes, thereby allowing a greater increase in VDAC1-mediated cellular dysfunction in CA1 astrocytes.

6. Conclusions and Future Directions

As targets for stroke therapy, miR-based strategies provide the advantage of rapid onset of action, a critical element in developing effective clinical treatments for stroke, and

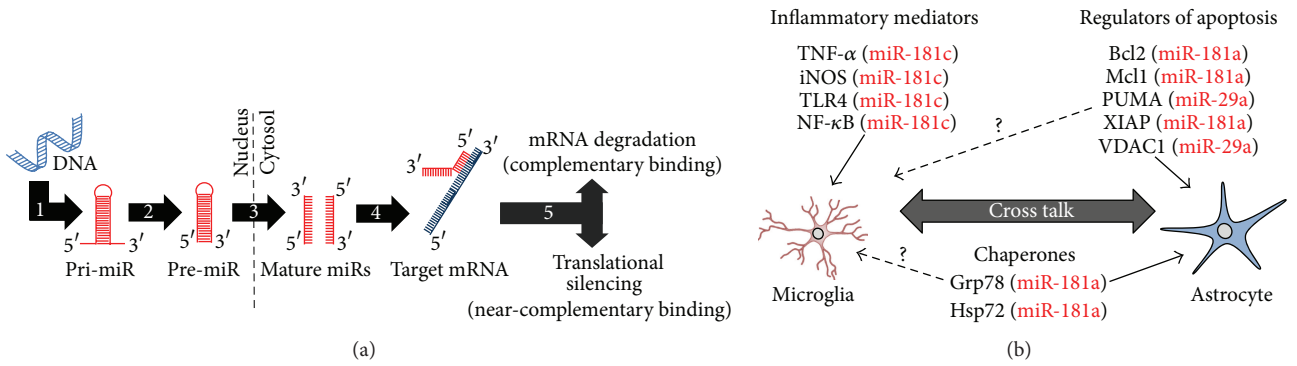

Figure 3: MicroRNAs (miRs) regulate mitochondrial function in glia. (a) miR biogenesis begins in the nucleus with genomic transcription of pri-miR (1). Drosha-mediated cleavage results in pre-miR (2), which is then exported to the cytosol by Exportin-5 and processed to the final mature miR forms by Dicer (3). In the cytosol, either the leading or the reverse complementary mature miR strand is then free to interact with the 3′ untranslated region of target messenger RNAs (mRNAs, (4)). miR/mRNA complexes are then targeted by the RNA-induced silencing complex (5) for either mRNA degradation or translational silencing, depending on the degree of miR/mRNA binding complementarity. (b) miR-mediated control of microglial mitochondrial function and activation state occurs secondary to miR targeting of cytokines and inflammatory mediators. miRs directly affect mitochondrial function in astrocytes by targeting Bcl2 family members and chaperones. Whether the same miR targets are relevant in microglia has not yet been determined (dashed arrows), yet astrocyte/microglial cross talk suggests at least an indirect role. Bcl2: B-cell lymphoma 2; DNA: deoxyribonucleic acid; Grp78: glucose-related protein 78; Hsp75: heat shock protein 75; iNOS: inducible nitric oxide synthase; Mcl1: myeloid cell leukemia 1; NF-κB: nuclear factor kappa B; PUMA: p53 upregulated modulator of apoptosis; TLR4: Toll-like receptor 4; TNF-α: tumor necrosis factor-alpha; VDAC1: voltage-dependent anion channel 1; XIAP: X-linked inhibitor of apoptosis protein.

endogenous miR expression levels can be pharmacologically manipulated. A successful phase 2 trial of the first miR-targeted drug, a locked nucleic acid targeting miR-122 to treat hepatitis C, has recently been completed [134], demonstrating that rapid translation of miR-based therapies from bench to clinic may be possible once candidate targets are identified.

Astrocytes and microglia play critical roles in neuronal survival following stroke and are ideal cellular targets for novel therapeutic approaches. miRs target proteins directly involved in maintaining astrocyte mitochondrial homeostasis in response to stress and neuroinflammatory mediators that regulate microglial activation with downstream effects on mitochondrial function (Figure 3). Recent findings [58, 59] demonstrating a novel role for mitochondria as a potential transduction pathway for neuronal-astrocyte cross talk and the emerging relevance of astrocytes as regulators of the neuronal bioenergetic response to cell stress [59] suggest that future studies investigating the role of miRs in these processes may provide a novel angle to overcome prior translational hurdles in the search for new clinical therapies for cerebral ischemia. Moreover, microglial activation can depend on astrocytic release of ATP in response to local injury, suggesting that astrocyte mitochondrial function plays a direct role in microglial activation state [24]. Therefore, miR-based therapeutic interventions targeting mechanisms that mediate cross talk between astrocytes and microglia may provide an alternative approach to simultaneously coordinate both glial mitochondrial function and microglial activation polarization.

The short (only 5–7-nucleotide-long) sequence in the mature miR determines binding specificity to target mRNAs; as a consequence, a single miR can bind multiple mRNAs, and a single mRNA can be bound by multiple miRs, creating a new and complex layer of posttranscriptional control. Identifying glial-enriched miRs that target multiple mitochondria-regulating genes and gene families may produce a substantial effect *versus* single gene silencing techniques, for example, with small interfering RNA or short hairpin RNA. However, the combinatorial effect of the short binding sequence can also offset any protective effects if the same miR simultaneously binds gene family members with opposite functions, as has been demonstrated with miR-29 and Bcl2 family members. Therefore, it remains critical to identify glial mitochondrial targets, test and verify the predicted miR/mRNA interaction, and investigate the effect of varying miR levels both *in vitro* and *in vivo* on mitochondrial function and injury in response to cerebral ischemia.

Competing Interests

The authors declare that there are no competing interests regarding the publication of this paper.

Acknowledgments

This study was supported by American Heart Association Grant FTF19970029 awarded to Dr. Creed M. Stary and National Institutes of Health Grant R01 NS084396 awarded to Dr. Rona G. Giffard.

References

[1] V. L. Roger, A. S. Go, D. M. Lloyd-Jones et al., "Heart disease and stroke statistics-2011 update: a report from the American Heart Association," *Circulation*, vol. 123, no. 4, pp. e18–e19, 2011.

[2] J. O. Blakeley and R. H. Llinas, "Thrombolytic therapy for acute ischemic stroke," *Journal of the Neurological Sciences*, vol. 261, no. 1-2, pp. 55–62, 2007.

[3] C. Eroglu and B. A. Barres, "Regulation of synaptic connectivity by glia," *Nature*, vol. 468, no. 7321, pp. 223–231, 2010.

[4] M. A. Yenari, T. M. Kauppinen, and R. A. Swanson, "Microglial activation in stroke: therapeutic targets," *Neurotherapeutics*, vol. 7, no. 4, pp. 378–391, 2010.

[5] J.-Y. Kim, N. Kim, and M. A. Yenari, "Mechanisms and potential therapeutic applications of microglial activation after brain injury," *CNS Neuroscience and Therapeutics*, vol. 21, no. 4, pp. 309–319, 2015.

[6] J. H. Park and C. Shin, "MicroRNA-directed cleavage of targets: mechanism and experimental approaches," *BMB Reports*, vol. 47, no. 8, pp. 417–423, 2014.

[7] Y.-B. Ouyang, C. M. Stary, R. E. White, and R. G. Giffard, "The use of microRNAs to modulate redox and immune response to stroke," *Antioxidants and Redox Signaling*, vol. 22, no. 2, pp. 187–202, 2015.

[8] Y.-B. Ouyang, C. M. Stary, G.-Y. Yang, and R. Giffard, "microRNAs: innovative targets for cerebral ischemia and stroke," *Current Drug Targets*, vol. 14, no. 1, pp. 90–101, 2013.

[9] C. M. Stary and R. G. Giffard, "Advances in astrocyte-targeted approaches for stroke therapy: an emerging role for mitochondria and microRNAS," *Neurochemical Research*, vol. 40, no. 2, pp. 301–307, 2015.

[10] E. E. Benarroch, "Neuron-astrocyte interactions: partnership for normal function and disease in the central nervous system," *Mayo Clinic Proceedings*, vol. 80, no. 10, pp. 1326–1338, 2005.

[11] A. Araque, R. P. Sanzgiri, V. Parpura, and P. G. Haydon, "Astrocyte-induced modulation of synaptic transmission," *Canadian Journal of Physiology and Pharmacology*, vol. 77, no. 9, pp. 699–706, 1999.

[12] Z. Liu and M. Chopp, "Astrocytes, therapeutic targets for neuroprotection and neurorestoration in ischemic stroke," *Progress in Neurobiology*, vol. 144, pp. 103–120, 2016.

[13] E. Blanco-Suarez, A. L. Caldwell, and N. J. Allen, "Role of astrocyte-synapse interactions in CNS disorders," *The Journal of Physiology*, 2016.

[14] L. E. Clarke and B. A. Barres, "Emerging roles of astrocytes in neural circuit development," *Nature Reviews Neuroscience*, vol. 14, no. 5, pp. 311–321, 2013.

[15] J. B. Zuchero and B. A. Barres, "Glia in mammalian development and disease," *Development*, vol. 142, no. 22, pp. 3805–3809, 2015.

[16] A. Schousboe, N. Westergaard, U. Sonnewald, S. B. Petersen, A. C. H. Yu, and L. Hertz, "Regulatory role of astrocytes for neuronal biosynthesis and homeostasis of glutamate and GABA," *Progress in Brain Research*, vol. 94, pp. 199–211, 1992.

[17] E. A. Bushong, M. E. Martone, Y. Z. Jones, and M. H. Ellisman, "Protoplasmic astrocytes in CA1 stratum radiatum occupy separate anatomical domains," *The Journal of Neuroscience*, vol. 22, no. 1, pp. 183–192, 2002.

[18] N. Rouach, J. Glowinski, and C. Giaume, "Activity-dependent neuronal control of gap-junctional communication in astrocytes," *Journal of Cell Biology*, vol. 149, no. 7, pp. 1513–1526, 2000.

[19] G. Cheung, O. Chever, and N. Rouach, "Connexons and pannexons: newcomers in neurophysiology," *Frontiers in Cellular Neuroscience*, vol. 8, article 348, 2014.

[20] G. Arcuino, J. H.-C. Lin, T. Takano et al., "Intercellular calcium signaling mediated by point-source burst release of ATP," *Proceedings of the National Academy of Sciences of the United States of America*, vol. 99, no. 15, pp. 9840–9845, 2002.

[21] S. Y. Gordleeva, S. V. Stasenko, A. V. Semyanov, A. E. Dityatev, and V. B. Kazantsev, "Bi-directional astrocytic regulation of neuronal activity within a network," *Frontiers in Computational Neuroscience*, vol. 6, article 92, 2012.

[22] V. Parpura and P. G. Haydon, "Physiological astrocytic calcium levels stimulate glutamate release to modulate adjacent neurons," *Proceedings of the National Academy of Sciences of the United States of America*, vol. 97, no. 15, pp. 8629–8634, 2000.

[23] A. Pérez-Alvarez and A. Araque, "Astrocyte-neuron interaction at tripartite synapses," *Current Drug Targets*, vol. 14, no. 11, pp. 1220–1224, 2013.

[24] T. Takano, N. A. Oberheim, M. L. Cotrina, and M. Nedergaard, "Astrocytes and ischemic injury," *Stroke*, vol. 40, no. 3, pp. S8–S12, 2009.

[25] J. Shields, D. E. Kimbler, W. Radwan, N. Yanasak, S. Sukumari-Ramesh, and K. M. Dhandapani, "Therapeutic targeting of astrocytes after traumatic brain injury," *Translational Stroke Research*, vol. 2, no. 4, pp. 633–642, 2011.

[26] A. Falnikar, K. Li, and A. C. Lepore, "Therapeutically targeting astrocytes with stem and progenitor cell transplantation following traumatic spinal cord injury," *Brain Research*, vol. 1619, pp. 91–103, 2015.

[27] J. L. Zamanian, L. Xu, L. C. Foo et al., "Genomic analysis of reactive astrogliosis," *The Journal of Neuroscience*, vol. 32, no. 18, pp. 6391–6410, 2012.

[28] P. Gris, A. Tighe, D. Levin, R. Sharma, and A. Brown, "Transcriptional regulation of scar gene expression in primary astrocytes," *Glia*, vol. 55, no. 11, pp. 1145–1155, 2007.

[29] J. R. Faulkner, J. E. Herrmann, M. J. Woo, K. E. Tansey, N. B. Doan, and M. V. Sofroniew, "Reactive astrocytes protect tissue and preserve function after spinal cord injury," *The Journal of Neuroscience*, vol. 24, no. 9, pp. 2143–2155, 2004.

[30] C. R. Rose and B. R. Ransom, "Gap junctions equalize intracellular Na^+ concentration in astrocytes," *Glia*, vol. 20, no. 4, pp. 299–307, 1997.

[31] J. Vella, C. Zammit, G. Di Giovanni, R. Muscat, and M. Valentino, "The central role of aquaporins in the pathophysiology of ischemic stroke," *Frontiers in Cellular Neuroscience*, vol. 9, article 108, 2015.

[32] T. Nakase, G. Söhl, M. Theis, K. Willecke, and C. C. G. Naus, "Increased apoptosis and inflammation after focal brain ischemia in mice lacking connexin43 in astrocytes," *The American Journal of Pathology*, vol. 164, no. 6, pp. 2067–2075, 2004.

[33] A. D. Martínez and J. C. Sáez, "Regulation of astrocyte gap junctions by hypoxia-reoxygenation," *Brain Research Reviews*, vol. 32, no. 1, pp. 250–258, 2000.

[34] J. H.-C. Lin, H. Weigel, M. L. Cotrina et al., "Gap-junction-mediated propagation and amplification of cell injury," *Nature Neuroscience*, vol. 1, no. 6, pp. 494–500, 1998.

[35] Q.-P. Dong, J.-Q. He, and Z. Chai, "Astrocytic Ca^{2+} waves mediate activation of extrasynaptic NMDA receptors in hippocampal neurons to aggravate brain damage during ischemia," *Neurobiology of Disease*, vol. 58, pp. 68–75, 2013.

[36] P. Cassina, A. Cassina, M. Pehar et al., "Mitochondrial dysfunction in SOD1G93A-bearing astrocytes promotes motor neuron degeneration: prevention by mitochondrial-targeted antioxidants," *The Journal of Neuroscience*, vol. 28, no. 16, pp. 4115–4122, 2008.

[37] E. Miquel, A. Cassina, L. Martínez-Palma et al., "Modulation of astrocytic mitochondrial function by dichloroacetate improves

survival and motor performance in inherited amyotrophic lateral sclerosis," *PLoS ONE*, vol. 7, no. 4, Article ID e34776, 2012.

[38] Y.-B. Ouyang, L. A. Voloboueva, L.-J. Xu, and R. G. Giffard, "Selective dysfunction of hippocampal CA1 astrocytes contributes to delayed neuronal damage after transient forebrain ischemia," *The Journal of Neuroscience*, vol. 27, no. 16, pp. 4253–4260, 2007.

[39] M. L. Weller, I. M. Stone, A. Goss, T. Rau, C. Rova, and D. J. Poulsen, "Selective overexpression of excitatory amino acid transporter 2 (EAAT2) in astrocytes enhances neuroprotection from moderate but not severe hypoxia-ischemia," *Neuroscience*, vol. 155, no. 4, pp. 1204–1211, 2008.

[40] L. Xu, J. F. Emery, Y.-B. Ouyang, L. A. Voloboueva, and R. G. Giffard, "Astrocyte targeted overexpression of Hsp72 or SOD2 reduces neuronal vulnerability to forebrain ischemia," *Glia*, vol. 58, no. 9, pp. 1042–1049, 2010.

[41] Y. Miao, Y. Qiu, Y. Lin, Z. Miao, J. Zhang, and X. Lu, "Protection by pyruvate against glutamate neurotoxicity is mediated by astrocytes through a glutathione-dependent mechanism," *Molecular Biology Reports*, vol. 38, no. 5, pp. 3235–3242, 2011.

[42] H. Nawashiro, M. Brenner, S. Fukui, K. Shima, and J. M. Hallenbeck, "High susceptibility to cerebral ischemia in GFAP-null mice," *Journal of Cerebral Blood Flow and Metabolism*, vol. 20, no. 7, pp. 1040–1044, 2000.

[43] C. Benakis, L. Garcia-Bonilla, C. Iadecola, and J. Anrather, "The role of microglia and myeloid immune cells in acute cerebral ischemia," *Frontiers in Cellular Neuroscience*, vol. 8, article 461, 2015.

[44] J. Ye, Z. Jiang, X. Chen, M. Liu, J. Li, and N. Liu, "Electron transport chain inhibitors induce microglia activation through enhancing mitochondrial reactive oxygen species production," *Experimental Cell Research*, vol. 340, no. 2, pp. 315–326, 2016.

[45] S. Gordon, "Alternative activation of macrophages," *Nature Reviews Immunology*, vol. 3, no. 1, pp. 23–35, 2003.

[46] M. K. McCoy and M. G. Tansey, "TNF signaling inhibition in the CNS: Implications for normal brain function and neurodegenerative disease," *Journal of Neuroinflammation*, vol. 5, article 45, 2008.

[47] T. S. Kapellos, L. Taylor, H. Lee et al., "A novel real time imaging platform to quantify macrophage phagocytosis," *Biochemical Pharmacology*, vol. 116, pp. 107–119, 2016.

[48] M. Leidi, E. Gotti, L. Bologna et al., "M2 macrophages phagocytose rituximab-opsonized leukemic targets more efficiently than M1 cells in vitro," *Journal of Immunology*, vol. 182, no. 7, pp. 4415–4422, 2009.

[49] W. Li, B. P. Katz, and S. M. Spinola, "*Haemophilus ducreyi*-induced interleukin-10 promotes a mixed M1 and M2 activation program in human macrophages," *Infection and Immunity*, vol. 80, no. 12, pp. 4426–4434, 2012.

[50] E. A. Bordt and B. M. Polster, "NADPH oxidase- and mitochondria-derived reactive oxygen species in proinflammatory microglial activation: a bipartisan affair?" *Free Radical Biology and Medicine*, vol. 76, no. 1, pp. 34–46, 2014.

[51] R. M. Ransohoff, "A polarizing question: do M1 and M2 microglia exist?" *Nature Neuroscience*, vol. 19, no. 8, pp. 987–991, 2016.

[52] N. Chaudhari, P. Talwar, A. Parimisetty, C. L. d'Hellencourt, and P. Ravanan, "A molecular web: endoplasmic reticulum stress, inflammation, and oxidative stress," *Frontiers in Cellular Neuroscience*, vol. 8, article 213, 2014.

[53] A. Ruiz, C. Matute, and E. Alberdi, "Endoplasmic reticulum Ca^{2+} release through ryanodine and IP_3 receptors contributes to neuronal excitotoxicity," *Cell Calcium*, vol. 46, no. 4, pp. 273–281, 2009.

[54] D. R. Green, L. Galluzzi, and G. Kroemer, "Mitochondria and the autophagy-inflammation-cell death axis in organismal aging," *Science*, vol. 333, no. 6046, pp. 1109–1112, 2011.

[55] S. W. G. Tait and D. R. Green, "Mitochondria and cell death: outer membrane permeabilization and beyond," *Nature Reviews Molecular Cell Biology*, vol. 11, no. 9, pp. 621–632, 2010.

[56] K. A. Webster, "Mitochondrial membrane permeabilization and cell death during myocardial infarction: roles of calcium and reactive oxygen species," *Future Cardiology*, vol. 8, no. 6, pp. 863–884, 2012.

[57] P. Cassina, H. Peluffo, M. Pehar et al., "Peroxynitrite triggers a phenotypic transformation in spinal cord astrocytes that induces motor neuron apoptosis," *Journal of Neuroscience Research*, vol. 67, no. 1, pp. 21–29, 2002.

[58] C.-H. O. Davis, K.-Y. Kim, E. A. Bushong et al., "Transcellular degradation of axonal mitochondria," *Proceedings of the National Academy of Sciences of the United States of America*, vol. 111, no. 26, pp. 9633–9638, 2014.

[59] K. Hayakawa, E. Esposito, X. Wang et al., "Transfer of mitochondria from astrocytes to neurons after stroke," *Nature*, vol. 535, no. 7613, pp. 551–555, 2016.

[60] L. Hertz, "Bioenergetics of cerebral ischemia: a cellular perspective," *Neuropharmacology*, vol. 55, no. 3, pp. 289–309, 2008.

[61] R. Wender, A. M. Brown, R. Fern, R. A. Swanson, K. Farrell, and B. R. Ransom, "Astrocytic glycogen influences axon function and survival during glucose deprivation in central white matter," *The Journal of Neuroscience*, vol. 20, no. 18, pp. 6804–6810, 2000.

[62] L. Hertz and G. A. Dienel, "Energy metabolism in the brain," *International Review of Neurobiology*, vol. 51, pp. 1–102, 2002.

[63] I. A. Simpson, A. Carruthers, and S. J. Vannucci, "Supply and demand in cerebral energy metabolism: the role of nutrient transporters," *Journal of Cerebral Blood Flow & Metabolism*, vol. 27, no. 11, pp. 1766–1791, 2007.

[64] P. T. Fox, M. E. Raichle, M. A. Mintun, and C. Dence, "Nonoxidative glucose consumption during focal physiologic neural activity," *Science*, vol. 241, no. 4864, pp. 462–464, 1988.

[65] L. Pellerin and P. J. Magistretti, "Glutamate uptake into astrocytes stimulates aerobic glycolysis: a mechanism coupling neuronal activity to glucose utilization," *Proceedings of the National Academy of Sciences of the United States of America*, vol. 91, no. 22, pp. 10625–10629, 1994.

[66] S. Amato and H.-Y. Man, "Bioenergy sensing in the brain: the role of AMP-activated protein kinase in neuronal metabolism, development and neurological diseases," *Cell Cycle*, vol. 10, no. 20, pp. 3452–3460, 2011.

[67] J. An, W. B. Haile, F. Wu, E. Torre, and M. Yepes, "Tissue-type plasminogen activator mediates neuroglial coupling in the central nervous system," *Neuroscience*, vol. 257, pp. 41–48, 2014.

[68] M. P. Goldberg and D. W. Choi, "Combined oxygen and glucose deprivation in cortical cell culture: calcium-dependent and calcium-independent mechanisms of neuronal injury," *The Journal of Neuroscience*, vol. 13, no. 8, pp. 3510–3524, 1993.

[69] G. E. Barreto, J. Gonzalez, Y. Torres, and L. Morales, "Astrocytic-neuronal crosstalk: implications for neuroprotection from brain injury," *Neuroscience Research*, vol. 71, no. 2, pp. 107–113, 2011.

[70] M. W. Greve and B. J. Zink, "Pathophysiology of traumatic brain injury," *Mount Sinai Journal of Medicine*, vol. 76, no. 2, pp. 97–104, 2009.

[71] M. Nagai, D. B. Re, T. Nagata et al., "Astrocytes expressing ALS-linked mutated SOD1 release factors selectively toxic to motor neurons," *Nature Neuroscience*, vol. 10, no. 5, pp. 615–622, 2007.

[72] R. C. Reyes and V. Parpura, "Mitochondria modulate Ca^{2+}-dependent glutamate release from rat cortical astrocytes," *The Journal of Neuroscience*, vol. 28, no. 39, pp. 9682–9691, 2008.

[73] F. Zhang, X. L. Ma, Y. X. Wang et al., "TPEN, a specific Zn^{2+} chelator, inhibits Sodium Dithionite and Glucose Deprivation (SDGD)-induced neuronal death by modulating apoptosis, glutamate signaling, and voltage-gated K^+ and Na^+ channels," *Cellular and Molecular Neurobiology*, 2016.

[74] K. Inoue, T. Leng, T. Yang, Z. Zeng, T. Ueki, and Z. Xiong, "Role of serum- and glucocorticoid-inducible kinases in stroke," *Journal of Neurochemistry*, vol. 138, no. 2, pp. 354–361, 2016.

[75] J. Zhang, A. Malik, H. B. Choi, R. W. Y. Ko, L. Dissing-Olesen, and B. A. MacVicar, "Microglial CR3 activation triggers long-term synaptic depression in the hippocampus via NADPH oxidase," *Neuron*, vol. 82, no. 1, pp. 195–207, 2014.

[76] M. L. Block, L. Zecca, and J.-S. Hong, "Microglia-mediated neurotoxicity: uncovering the molecular mechanisms," *Nature Reviews Neuroscience*, vol. 8, no. 1, pp. 57–69, 2007.

[77] D. A. Patten, M. Germain, M. A. Kelly, and R. S. Slack, "Reactive oxygen species: stuck in the middle of neurodegeneration," *Journal of Alzheimer's Disease*, vol. 20, supplement 2, pp. S357–S367, 2010.

[78] M. P. Mattson, "NF-κB in the survival and plasticity of neurons," *Neurochemical Research*, vol. 30, no. 6-7, pp. 883–893, 2005.

[79] J. M. Adams and S. Cory, "Bcl-2-regulated apoptosis: mechanism and therapeutic potential," *Current Opinion in Immunology*, vol. 19, no. 5, pp. 488–496, 2007.

[80] M. J. Parsons and D. R. Green, "Mitochondria in cell death," *Essays in Biochemistry*, vol. 47, pp. 99–114, 2010.

[81] Y.-B. Ouyang and R. G. Giffard, "MicroRNAs affect BCL-2 family proteins in the setting of cerebral ischemia," *Neurochemistry International*, vol. 77, pp. 2–8, 2014.

[82] K. Kitagawa, M. Matsumoto, Y. Tsujimoto et al., "Amelioration of hippocampal neuronal damage after global ischemia by neuronal overexpression of BCL-2 in transgenic mice," *Stroke*, vol. 29, no. 12, pp. 2616–2621, 1998.

[83] H. Zhao, M. A. Yenari, D. Cheng, R. M. Sapolsky, and G. K. Steinberg, "Bcl-2 overexpression protects against neuron loss within the ischemic margin following experimental stroke and inhibits cytochrome c translocation and caspase-3 activity," *Journal of Neurochemistry*, vol. 85, no. 4, pp. 1026–1036, 2003.

[84] Y.-B. Ouyang, S. G. Carriedo, and R. G. Giffard, "Effect of Bcl-x_L overexpression on reactive oxygen species, intracellular calcium, and mitochondrial membrane potential following injury in astrocytes," *Free Radical Biology and Medicine*, vol. 33, no. 4, pp. 544–551, 2002.

[85] E. Szegezdi, D. C. MacDonald, T. N. Chonghaile, S. Gupta, and A. Samali, "Bcl-2 family on guard at the ER," *American Journal of Physiology—Cell Physiology*, vol. 296, no. 5, pp. C941–C953, 2009.

[86] Y.-B. Ouyang and R. G. Giffard, "ER-mitochondria crosstalk during cerebral ischemia: molecular chaperones and ER-mitochondrial calcium transfer," *International Journal of Cell Biology*, vol. 2012, Article ID 493934, 8 pages, 2012.

[87] B. Bonneau, J. Prudent, N. Popgeorgiev, and G. Gillet, "Non-apoptotic roles of Bcl-2 family: the calcium connection," *Biochimica et Biophysica Acta (BBA)—Molecular Cell Research*, vol. 1833, no. 7, pp. 1755–1765, 2013.

[88] S. Grimm, "The ER-mitochondria interface: the social network of cell death," *Biochimica et Biophysica Acta (BBA)—Molecular Cell Research*, vol. 1823, no. 2, pp. 327–334, 2012.

[89] D. Rodriguez, D. Rojas-Rivera, and C. Hetz, "Integrating stress signals at the endoplasmic reticulum: the BCL-2 protein family rheostat," *Biochimica et Biophysica Acta (BBA)—Molecular Cell Research*, vol. 1813, no. 4, pp. 564–574, 2011.

[90] G. Szabadkai and R. Rizzuto, "Chaperones as parts of organelle networks," *Advances in Experimental Medicine and Biology*, vol. 594, pp. 64–77, 2007.

[91] S. Kelly, Z. J. Zhang, H. Zhao et al., "Gene transfer of HSP72 protects cornu ammonis 1 region of the hippocampus neurons from global ischemia: influence of Bcl-2," *Annals of Neurology*, vol. 52, no. 2, pp. 160–167, 2002.

[92] R. G. Giffard, R.-Q. Han, J. F. Emery, M. Duan, and J. F. Pittet, "Regulation of apoptotic and inflammatory cell signaling in cerebral ischemia: the complex roles of heat shock protein 70," *Anesthesiology*, vol. 109, no. 2, pp. 339–348, 2008.

[93] S. Kesaraju, G. Nayak, H. M. Prentice, and S. L. Milton, "Upregulation of Hsp72 mediates anoxia/reoxygenation neuroprotection in the freshwater turtle via modulation of ROS," *Brain Research*, vol. 1582, pp. 247–256, 2014.

[94] X. Sun, R. Crawford, C. Liu, T. Luo, and B. Hu, "Development-dependent regulation of molecular chaperones after hypoxia-ischemia," *Neurobiology of Disease*, vol. 82, pp. 123–131, 2015.

[95] L. Xu, X. Xiong, Y. Ouyang, G. Barreto, and R. Giffard, "Heat shock protein 72 (Hsp72) improves long term recovery after focal cerebral ischemia in mice," *Neuroscience Letters*, vol. 488, no. 3, pp. 279–282, 2011.

[96] Z. Zheng, J. Y. Kim, H. Ma, J. E. Lee, and M. A. Yenari, "Anti-inflammatory effects of the 70 kDa heat shock protein in experimental stroke," *Journal of Cerebral Blood Flow and Metabolism*, vol. 28, no. 1, pp. 53–63, 2008.

[97] M. A. Yenari, S. L. Fink, G. H. Sun et al., "Gene therapy with HSP72 is neuroprotective in rat models of stroke and epilepsy," *Annals of Neurology*, vol. 44, no. 4, pp. 584–591, 1998.

[98] D. L. Feinstein, E. Galea, D. A. Aquino, G. C. Li, H. Xu, and D. J. Reis, "Heat shock protein 70 suppresses astroglial-inducible nitric-oxide synthase expression by decreasing NFκB activation," *The Journal of Biological Chemistry*, vol. 271, no. 30, pp. 17724–17732, 1996.

[99] M. Ni, Y. Zhang, and A. S. Lee, "Beyond the endoplasmic reticulum: atypical GRP78 in cell viability, signalling and therapeutic targeting," *Biochemical Journal*, vol. 434, no. 2, pp. 181–188, 2011.

[100] M. K. E. Schäfer, A. Pfeiffer, M. Jaeckel, A. Pouya, A. M. Dolga, and A. Methner, "Regulators of mitochondrial Ca^{2+} homeostasis in cerebral ischemia," *Cell and Tissue Research*, vol. 357, no. 2, pp. 395–405, 2014.

[101] F.-C. Sun, S. Wei, C.-W. Li, Y.-S. Chang, C.-C. Chao, and Y.-K. Lai, "Localization of GRP78 to mitochondria under the unfolded protein response," *Biochemical Journal*, vol. 396, no. 1, pp. 31–39, 2006.

[102] G.-H. Lee, H.-R. Kim, S.-Y. Han et al., "Gastrodia elata Blume and its pure compounds protect BV-2 microglial-derived cell lines against β-amyloid: the involvement of GRP78 and CHOP," *Biological Research*, vol. 45, no. 4, pp. 403–410, 2012.

[103] Y.-B. Ouyang, L.-J. Xu, J. F. Emery, A. S. Lee, and R. G. Giffard, "Overexpressing GRP78 influences Ca^{2+} handling and function of mitochondria in astrocytes after ischemia-like stress," *Mitochondrion*, vol. 11, no. 2, pp. 279–286, 2011.

[104] Y. Oida, H. Izuta, A. Oyagi et al., "Induction of BiP, an ER-resident protein, prevents the neuronal death induced by transient forebrain ischemia in gerbil," *Brain Research*, vol. 1208, pp. 217–224, 2008.

[105] T. Kudo, S. Kanemoto, H. Hara et al., "A molecular chaperone inducer protects neurons from ER stress," *Cell Death & Differentiation*, vol. 15, no. 2, pp. 364–375, 2008.

[106] D. P. K. Wong, J. M. T. Chu, V. K. L. Hung et al., "Modulation of endoplasmic reticulum chaperone GRP78 by high glucose in hippocampus of streptozotocin-induced diabetic mice and C6 astrocytic cells," *Neurochemistry International*, vol. 63, no. 6, pp. 551–560, 2013.

[107] B. Chantong, D. V. Kratschmar, A. Lister, and A. Odermatt, "Inhibition of metabotropic glutamate receptor 5 induces cellular stress through pertussis toxin-sensitive G_i-proteins in murine BV-2 microglia cells," *Journal of Neuroinflammation*, vol. 11, article 190, 2014.

[108] Z. Dong, P. Wu, Y. Li et al., "Myocardial infarction worsens glomerular injury and microalbuminuria in rats with preexisting renal impairment accompanied by the activation of ER stress and inflammation," *Molecular Biology Reports*, vol. 41, no. 12, pp. 7911–7921, 2014.

[109] G. S. Panayi and V. M. Corrigall, "BiP regulates autoimmune inflammation and tissue damage," *Autoimmunity Reviews*, vol. 5, no. 2, pp. 140–142, 2006.

[110] S. Koriauli, N. Natsvlishvili, T. Barbakadze, and D. Mikeladze, "Knockdown of interleukin-10 induces the redistribution of sigma1-receptor and increases the glutamate-dependent NADPH-oxidase activity in mouse brain neurons," *Biological Research*, vol. 48, article 55, 2015.

[111] T. Hosoi, T. Oba, and K. Ozawa, "ER stress-mediated regulation of immune function under glucose-deprived condition in glial cells: up- and down-regulation of PGE2 + IFNγ-induced IL-6 and iNOS expressions," *Biochemical and Biophysical Research Communications*, vol. 441, no. 2, pp. 525–528, 2013.

[112] A. Dharap, K. Bowen, R. Place, L.-C. Li, and R. Vemuganti, "Transient focal ischemia induces extensive temporal changes in rat cerebral microRNAome," *Journal of Cerebral Blood Flow and Metabolism*, vol. 29, no. 4, pp. 675–687, 2009.

[113] Y.-B. Ouyang, L. Xu, S. Yue, S. Liu, and R. G. Giffard, "Neuroprotection by astrocytes in brain ischemia: importance of microRNAs," *Neuroscience Letters*, vol. 565, pp. 53–58, 2014.

[114] A. Jovičić, R. Roshan, N. Moisoi et al., "Comprehensive expression analyses of neural cell-type-specific miRNAs identify new determinants of the specification and maintenance of neuronal phenotypes," *The Journal of Neuroscience*, vol. 33, no. 12, pp. 5127–5137, 2013.

[115] Y.-B. Ouyang, L. Xu, Y. Lu et al., "Astrocyte-enriched miR-29a targets PUMA and reduces neuronal vulnerability to forebrain ischemia," *Glia*, vol. 61, no. 11, pp. 1784–1794, 2013.

[116] E. R. Hutchison, E. M. Kawamoto, D. D. Taub et al., "Evidence for miR-181 involvement in neuroinflammatory responses of astrocytes," *Glia*, vol. 61, no. 7, pp. 1018–1028, 2013.

[117] Y.-B. Ouyang, Y. Lu, S. Yue et al., "MiR-181 regulates GRP78 and influences outcome from cerebral ischemia *in vitro* and *in vivo*," *Neurobiology of Disease*, vol. 45, no. 1, pp. 555–563, 2012.

[118] Y.-B. Ouyang, Y. Lu, S. Yue, and R. G. Giffard, "miR-181 targets multiple Bcl-2 family members and influences apoptosis and mitochondrial function in astrocytes," *Mitochondrion*, vol. 12, no. 2, pp. 213–219, 2012.

[119] L.-J. Xu, Y.-B. Ouyang, X. Xiong, C. M. Stary, and R. G. Giffard, "Post-stroke treatment with miR-181 antagomir reduces injury and improves long-term behavioral recovery in mice after focal cerebral ischemia," *Experimental Neurology*, vol. 264, pp. 1–7, 2015.

[120] J.-M. Moon, L. Xu, and R. G. Giffard, "Inhibition of microRNA-181 reduces forebrain ischemia-induced neuronal loss," *Journal of Cerebral Blood Flow and Metabolism*, vol. 33, no. 12, pp. 1976–1982, 2013.

[121] L. Zhang, L.-Y. Dong, Y.-J. Li, Z. Hong, and W.-S. Wei, "The microRNA miR-181c controls microglia-mediated neuronal apoptosis by suppressing tumor necrosis factor," *Journal of Neuroinflammation*, vol. 9, article 211, 2012.

[122] L. Zhang, Y.-J. Li, X.-Y. Wu, Z. Hong, and W.-S. Wei, "MicroRNA-181c negatively regulates the inflammatory response in oxygen-glucose-deprived microglia by targeting Toll-like receptor 4," *Journal of Neurochemistry*, vol. 132, no. 6, pp. 713–723, 2015.

[123] L. Smirnova, A. Gräfe, A. Seiler, S. Schumacher, R. Nitsch, and F. G. Wulczyn, "Regulation of miRNA expression during neural cell specification," *European Journal of Neuroscience*, vol. 21, no. 6, pp. 1469–1477, 2005.

[124] X. Cao, G. Yeo, A. R. Muotri, T. Kuwabara, and F. H. Gage, "Noncoding RNAs in the mammalian central nervous system," *Annual Review of Neuroscience*, vol. 29, pp. 77–103, 2006.

[125] J. W. Graff, A. M. Dickson, G. Clay, A. P. McCaffrey, and M. E. Wilson, "Identifying functional microRNAs in macrophages with polarized phenotypes," *The Journal of Biological Chemistry*, vol. 287, no. 26, pp. 21816–21825, 2012.

[126] M. C. Thounaojam, D. K. Kaushik, K. Kundu, and A. Basu, "MicroRNA-29b modulates Japanese encephalitis virus-induced microglia activation by targeting tumor necrosis factor alpha-induced protein 3," *Journal of Neurochemistry*, vol. 129, no. 1, pp. 143–154, 2014.

[127] A. J. Kole, V. Swahari, S. M. Hammond, and M. Deshmukh, "miR-29b is activated during neuronal maturation and targets BH3-only genes to restrict apoptosis," *Genes & Development*, vol. 25, no. 2, pp. 125–130, 2011.

[128] G. Shi, Y. Liu, T. Liu et al., "Upregulated miR-29b promotes neuronal cell death by inhibiting Bcl2L2 after ischemic brain injury," *Experimental Brain Research*, vol. 216, no. 2, pp. 225–230, 2012.

[129] S. Khanna, C. Rink, R. Ghoorkhanian et al., "Loss of miR-29b following acute ischemic stroke contributes to neural cell death and infarct size," *Journal of Cerebral Blood Flow & Metabolism*, vol. 33, no. 8, pp. 1197–1206, 2013.

[130] J. Yu and L. Zhang, "PUMA, a potent killer with or without p53," *Oncogene*, vol. 27, supplement 1, pp. S71–S83, 2008.

[131] C. M. Stary, X. Sun, Y. B. Ouyang, L. Li, and R. G. Giffard, "miR-29a differentially regulates cell survival in astrocytes from cornu ammonis 1 and dentate gyrus by targeting VDAC1," *Mitochondrion*, vol. 30, pp. 248–254, 2016.

[132] V. Shoshan-Barmatz and D. Ben-Hail, "VDAC, a multifunctional mitochondrial protein as a pharmacological target," *Mitochondrion*, vol. 12, no. 1, pp. 24–34, 2012.

[133] H. Huang, K. Shah, N. A. Bradbury, C. Li, and C. White, "Mcl-1 promotes lung cancer cell migration by directly interacting with VDAC to increase mitochondrial Ca^{2+} uptake and reactive oxygen species generation," *Cell Death and Disease*, vol. 5, no. 10, Article ID e1482, 2014.

[134] H. L. A. Janssen, H. W. Reesink, E. J. Lawitz et al., "Treatment of HCV infection by targeting microRNA," *The New England Journal of Medicine*, vol. 368, no. 18, pp. 1685–1694, 2013.

Hindawi Publishing Corporation
Oxidative Medicine and Cellular Longevity
Volume 2016, Article ID 1015390, 13 pages
http://dx.doi.org/10.1155/2016/1015390

Research Article

Soluble Receptor for Advanced Glycation End Product Ameliorates Chronic Intermittent Hypoxia Induced Renal Injury, Inflammation, and Apoptosis via P38/JNK Signaling Pathways

Xu Wu,[1,2] Wenyu Gu,[3] Huan Lu,[1,2] Chengying Liu,[4] Biyun Yu,[5] Hui Xu,[5] Yaodong Tang,[5] Shanqun Li,[1,2] Jian Zhou,[1,2] and Chuan Shao[5]

[1]*Department of Pulmonary Medicine, Zhongshan Hospital, Fudan University, Shanghai 200032, China*
[2]*Clinical Center for Sleep Breathing Disorder and Snoring, Zhongshan Hospital, Fudan University, Shanghai 200032, China*
[3]*Department of Urology, Shanghai Tenth People's Hospital, Tongji University School of Medicine, Shanghai 200072, China*
[4]*Department of Respiratory Medicine, Affiliated Jiangyin Hospital of Southeast University, Jiangyin 214400, China*
[5]*Department of Respiratory Medicine, Ningbo Medical Center Lihuili Eastern Hospital, Taipei Medical University Ningbo Medical Center, Ningbo 315040, China*

Correspondence should be addressed to Shanqun Li; li.shanqun@zs-hospital.sh.cn, Jian Zhou; zhou.jian@fudan.edu.cn, and Chuan Shao; shaochuan1984@sina.cn

Received 18 April 2016; Revised 12 July 2016; Accepted 25 July 2016

Academic Editor: Hariom Yadav

Obstructive sleep apnea (OSA) associated chronic kidney disease is mainly caused by chronic intermittent hypoxia (CIH) triggered tissue damage. Receptor for advanced glycation end product (RAGE) and its ligand high mobility group box 1 (HMGB1) are expressed on renal cells and mediate inflammatory responses in OSA-related diseases. To determine their roles in CIH-induced renal injury, soluble RAGE (sRAGE), the RAGE neutralizing antibody, was intravenously administered in a CIH model. We also evaluated the effect of sRAGE on inflammation and apoptosis. Rats were divided into four groups: (1) normal air (NA), (2) CIH, (3) CIH+sRAGE, and (4) NA+sRAGE. Our results showed that CIH accelerated renal histological injury and upregulated RAGE-HMGB1 levels involving inflammatory (NF-κB, TNF-α, and IL-6), apoptotic (Bcl-2/Bax), and mitogen-activated protein kinases (phosphorylation of P38, ERK, and JNK) signal transduction pathways, which were abolished by sRAGE but p-ERK. Furthermore, sRAGE ameliorated renal dysfunction by attenuating tubular endothelial apoptosis determined by immunofluorescence staining of CD31 and TUNEL. These findings suggested that RAGE-HMGB1 activated chronic inflammatory transduction cascades that contributed to the pathogenesis of the CIH-induced renal injury. Inhibition of RAGE ligand interaction by sRAGE provided a therapeutic potential for CIH-induced renal injury, inflammation, and apoptosis through P38 and JNK pathways.

1. Introduction

Obstructive sleep apnea (OSA) is characterized by repetitive upper airway collapse and recurrent hypoxia during sleep. Emerging evidence indicates that chronic kidney disease (CKD) is highly prevalent complication of untreated OSA with symptoms of polyuria and proteinuria [1, 2]. Meanwhile, the prevalence of OSA in CKD patients ranges severalfold higher than the general population [3]. Two mechanisms are responsible for the loss of kidney function in OSA patients: chronic nocturnal intrarenal hypoxia and activation of sympathetic nervous system in response to oxidative stress, resulting in tubulointerstitial injury and ultimately leading common pathway to end-stage renal disease (ESKD) [4, 5]. As the foremost pathophysiological change in the process of OSA, chronic intermittent hypoxia (CIH) often causes oxidative stress and inflammations, contributing to damage of various tissue and organs [6].

The receptor for advanced glycation end products (RAGE), first identified as a member of the immunoglobulin superfamily, is a pattern-recognition receptor that interacts with multiligands, such as advanced glycation end products (AGEs), high mobility group box 1 (HMGB1), S-100 calcium-binding protein (S100B), and Mac-1 [7]. Multiple descriptive studies have demonstrated RAGE and its ligands are potentially related to OSA. Regarding RAGE ligands, a previous study had evaluated levels of HMGB1 and their relation to endothelial function in OSA patients [8]. S100B levels, identified as a useful biochemical marker, have also been found increased in OSA [9]. Broadly speaking, RAGE and its ligands are almost expressed in all tissues and on a wide range of cell types, also including renal (proximal) tubules, mesangial cells, and podocytes [10]. More recently, accumulations of RAGE and its ligands are recognized to be upregulated in various types of renal disorders. A review investigated that RAGE was associated not only with diabetic nephropathy, but also with obesity-related glomerulopathy, hypertensive nephropathy, and ischemic renal injury, all of which were closely related to OSA-associated-renal injury [11]. Considering chronic kidney disease is an immune inflammatory condition [12], it is natural to link chronic kidney disease to RAGE-HMGB1 and to identify them as key mediators in inflammatory responses as well as potential signaling molecules in progression to ESKD [13, 14]. As expected, HMGB1 is elevated significantly in CKD patients and correlates with GFR as well as markers of inflammation [15]. In particular, serum levels of HMGB1 in CKD patients were also significantly higher than those in control subjects [16]. These findings raise the possibility of RAGE-HMGB1 in the pathogenesis of OSA-associated chronic kidney disease, but their contribution in CIH-induced renal injury has not yet been elucidated.

Furthermore, it is well documented that RAGE is an inverse marker in CKD patients [17], thus inhibition of RAGE constituting a possible strategy for the treatment of CKD [18, 19]. Soluble RAGE (sRAGE), which possesses the RAGE ligand binding positions but lacks the cytoplasmic and transmembrane domains, secretes out of the cells and acts as decoys to prevent RAGE signal transduction directly [20]. In clinical settings, serum sRAGE showed increased levels in patients with ESKD [21], but whether it could protect against toxic effects of RAGE remains to be known. Recent study found that RAGE and nuclear factor kappa B (NF-κB) downstream signaling were centrally involved in sleep apnea obtained from the intermittent hypoxia (IH) experimental model [22]. In this study we establish a CIH model to investigate the participation of RAGE-HMGB1 and the therapeutic effect of recombinant soluble RAGE. The possible mechanism involved was also elucidated.

2. Material and Methods

2.1. Animal Model of CIH. Male Sprague-Dawley rats at age of 4 weeks and body weight 140–150 g, obtained from the Experimental Animal Centre of Fudan University (China) and allowed free access to laboratory chow and tap water in day-night quarters at 25°C, were used in this study. The animal protocol was approved by the Animal Care Committee of Fudan University, in accordance with the National Institutes of Health Guide for the Care and Use of Laboratory Animals. All effects were made to minimize animal suffering. Rats were randomly divided into the following four experimental groups of 6 animals each: the normal air (NA) control group; the CIH group; the CIH plus sRAGE group; normal air plus sRAGE group (NA+sRAGE). The CIH protocol was modeled according to the study of Fu et al. [23]. Rats were placed in four identical designed chambers. Nitrogen (100%) was delivered to the chambers for 30 s to reduce the ambient fraction of inspired oxygen to 6-7% for 10 s. Then, oxygen was infused for 20 s so that the oxygen concentration returned to 20~21%. This cycle took one minute, 8 h/day for 7 d/week for 5 weeks. The oxygen concentration was measured automatically using an oxygen analyzer (Chang Ai Electronic Science & Technology Company, Shanghai, China). The CIH plus sRAGE treatment group received the same CIH protocol as for comparison with the CIH model group. Rats in the sRAGE treatment group were subsequently injected with recombinant sRAGE protein 150 μg/per rat (diluted in 1 mL phosphate-buffered saline) intraperitoneally every 48 h for 5 weeks before each hypoxia cycle. This dose of rats was converted based on previous work where daily dose of sRAGE in a mouse model of chronic hypoxia was 20 μg/day [24]. Control rats included NA and NA+sRAGE group rats, all of which were subjected to normal air and administered with phosphate-buffered saline (PBS) as a vehicle control and 150 μg/per rat of recombinant sRAGE, respectively. During this exposure, all rats were kept under pathogen-free conditions and allowed to access to food and water. At the end of 5 weeks of CIH model, all the rats were euthanized 15 h after last hypoxia circle. Their blood and kidneys were collected. Blood samples were obtained from the inferior vena cava. Renal function was calculated as serum creatinine and blood urea nitrogen (BUN), which were measured in the core laboratory of Zhongshan Hospital (Shanghai, China).

2.2. Kidney Histology. After being euthanized, kidneys were fixed with 4% paraformaldehyde and embedded in paraffin. Paraffin-embedded specimens were cut into 4 μm thick sections and stained with hematoxylin-eosin. Kidney injury was examined using the modified 0–5 Jablonski grading scale under a light microscope: 0 represents normal; 1 represents occasional degeneration and necrosis of individual cells; 2 represents degenerative cells and necrosis of individual tubules; 3 represents degeneration and necrosis of all cells in adjacent proximal convoluted tubules with survival of surrounding tubules; 4 represents necrosis confined to the distal third of the proximal convoluted tubules, with a band of necrosis extending across the inner cortex; and 5 represents necrosis affecting all the three segments of the proximal convoluted tubules, as described previously [25].

2.3. HMGB1 Immunohistochemistry. For HMGB1 detection, the samples were dewaxed in xylene and dehydrated in a graded ethanol series. Endogenous peroxidase activity was

inhibited by incubating the slides with 0.3% H_2O_2 for 5 min, followed by washing thrice with PBS; the sections were incubated with the primary antibodies to HMGB1 (1 : 1000 dilution, ab18256; Abcam, Cambridge, UK) and incubated at 4°C overnight, washed in PBS, and incubated at 37°C for 1 h with biotinylated anti-rabbit/rat IgG (1 : 200; Maixin-Bio, Shanghai, China) according to manufacturer's instructions. The tissue was incubated with Streptavidin Peroxidase (Maixin-Bio) reagents at 37°C for 30 min, stained with freshly prepared DAB (Maixin-Bio). Morphometric quantification of the stained sections was performed with a customized digital image analysis system (IMAGE-Pro plus 4.5). Analysis of the kidney and capturing images was performed.

2.4. Immunofluorescent Triple Staining for CD31, TUNEL, DAPI, and Apoptotic Determination. To visualize apoptotic changes during CIH-induced renal injury, 4 μm paraffin-embedded tissue slides were deparaffinized, rehydrated, and prepared as described in immunohistochemistry. Antigen was retrieved by microwave-citrate buffer antigen retrieval method. The slides were blocked with 5% goat serum (Invitrogen) for 1 hour at room temperature, permeabilized with 0.2% Triton X-100, incubated overnight at 4°C with mouse anti-rat CD31 antibody (1 : 50 dilution, No. ab64543; Abcam, Cambridge, UK). After the samples were rinsed 4 times (3 min each) with PBS, the slides were then incubated for 30 minutes at room temperature with Alexa Fluor 488-conjugated goat anti-mouse IgG (1 : 400; B40941, Invitrogen). For detection of apoptotic cells, TUNEL staining was carried out using a Promega apoptosis detection kit. Immunofluorescence for TUNEL staining was performed with Alexa Fluor 594-conjugated goat anti-mouse IgG (1 : 400; A11020, Invitrogen). The glass was mounted with cover slips containing Vectashield mounting medium with 4′,6-diamidino-2-phenylindole (DAPI; Vector Laboratories) and imaged under an fluorescent microscope (Leica). Endothelial cells (CD31+) stained green fluorescence and DAPI stained blue fluorescence. TUNEL-positive apoptotic cells were detected by localized red fluorescence within cell nuclei. TUNEL-positive ($TUNEL^+$) and DAPI positive ($DAPI^+$) cells were counted at ×100 magnification with a fluorescence microscopy, respectively. The number of apoptotic cells was calculated as $TUNEL^+/DAPI^+$ cells in random 10 fields per section for quantification.

2.5. Western Blot Analysis for Target Protein. Proteins were extracted from animal kidney tissues using NucleoSpin (REF 740933.50; Macherey-Nagel), after which they were separated with SDS-PAGE on 8% gels and transferred to PVDF membranes which were then incubated overnight at 4°C with the primary antibody diluted in blocking solution. The primary antibodies and the dilutions were as follows: p-ERK [1/2] No. 9101 (1 : 1000), p-JNK No. 9255 (1 : 2000), t-JNK No. 9252 (1 : 1000), p-p38 No. 9211 (1 : 1000), and t-p38 No. 9212 (1 : 1000) (Cell Signaling Technology, Danvers, MA); Bax No. ab5714 (1 : 500), Bcl-2 No. ab136285 (1 : 500), NF-κB p65 No. ab16502 (1 : 1000), HMGB1 No. ab18256 (1 : 1000), (Abcam, Cambridge, UK), and RAGE (1 : 500, No. R3611, Sigma, USA). Horseradish peroxidase-coupled rabbit and mouse IgG (1 : 2000) were used as secondary antibodies. The blots were incubated with horseradish peroxidase-conjugated anti-IgG for 1 h at 37°C. Nonspecific binding sites were blocked for 1 h with 0.05 g/mL nonfat milk powder in Tris-buffered saline (pH 7.4) and 0.05% (v/v) Tween 20 (Bio-Rad) followed by overnight incubations with primary antibody. Blots were probed with anti-glyceraldehyde 3-phosphate dehydrogenase (GAPDH) antibody (sc-25778, Santa Cruz, USA) to ensure equal loading and detected using ECL chemiluminescent system (Amersham Biosciences, Piscataway, NJ, USA). Band intensity was quantified by scanning densitometry. Each measurement was made 3 times.

2.6. Enzyme-Linked Immunosorbent Assay (ELISA). Serum was isolated from the blood after centrifugation at 14 000 rpm for 20 min at 4°C. After centrifugation, serum was frozen at −80°C until enzyme-linked immunosorbent assay (ELISA) analyses were performed. HMGB1 (IBL International) and the levels of inflammatory mediators (TNF-a, IL-6, and IL-17 from R&D Systems) in the serum samples were measured in triplicate following the procedures supplied by the manufacturer.

2.7. Statistical Analysis. Data were presented as mean ± SEM and analyzed using SPSS 18.0. Comparisons between multiple groups were performed using ANOVA with the Bonferroni test. $P < 0.05$ was considered statistically significant between groups.

3. Results

3.1. Protective Effect of sRAGE on Kidney Function and Histopathological Assessment. In histological examination of kidney stained with hematoxylin-eosin, NA group rats showed normal glomerular and tubular structures, while CIH resulted in prominent tubular atrophy and inflammatory cell infiltration (Figure 1(a)). Injury score was further evaluated by the modified 0–5 Jablonski grading scale (Figure 1(b)). Consistent with desquamation of renal tubules epithelium in CIH group rats, the serum creatinine as well as BUN levels significantly elevated (58.59 ± 5.84 μmol/L and 17.54 ± 1.97 mmol/L, $P < 0.001$) as compared to the NA control group (37.29 ± 5.07 μmol/L and 6.12 ± 2.47 mmol/L; Figures 1(c) and 1(d)). However, animals treated with sRAGE before each hypoxia circle seldom displayed extensive features of tubule epithelial swelling and narrowed tubular lumens, without significant changes in distal convoluted tubule (Figure 1(a)). Contrast to CIH-incurred renal damage, sRAGE attenuated dysfunction and inflammation, as reflected by improvements in serum parameters (creatinine decreased by 24.41%, $P = 0.0043$; BUN decreased by 14.59%, $P = 0.041$) and histological grade ($P = 0.002$).

3.2. Soluble RAGE Attenuated CIH-Induced Renal Tubular Endothelial Cell Apoptosis. Indeed, the renal tubular endothelial cell injury has been a key to the pathogenesis of CKD. Since CD31 was recognized to be a specific marker

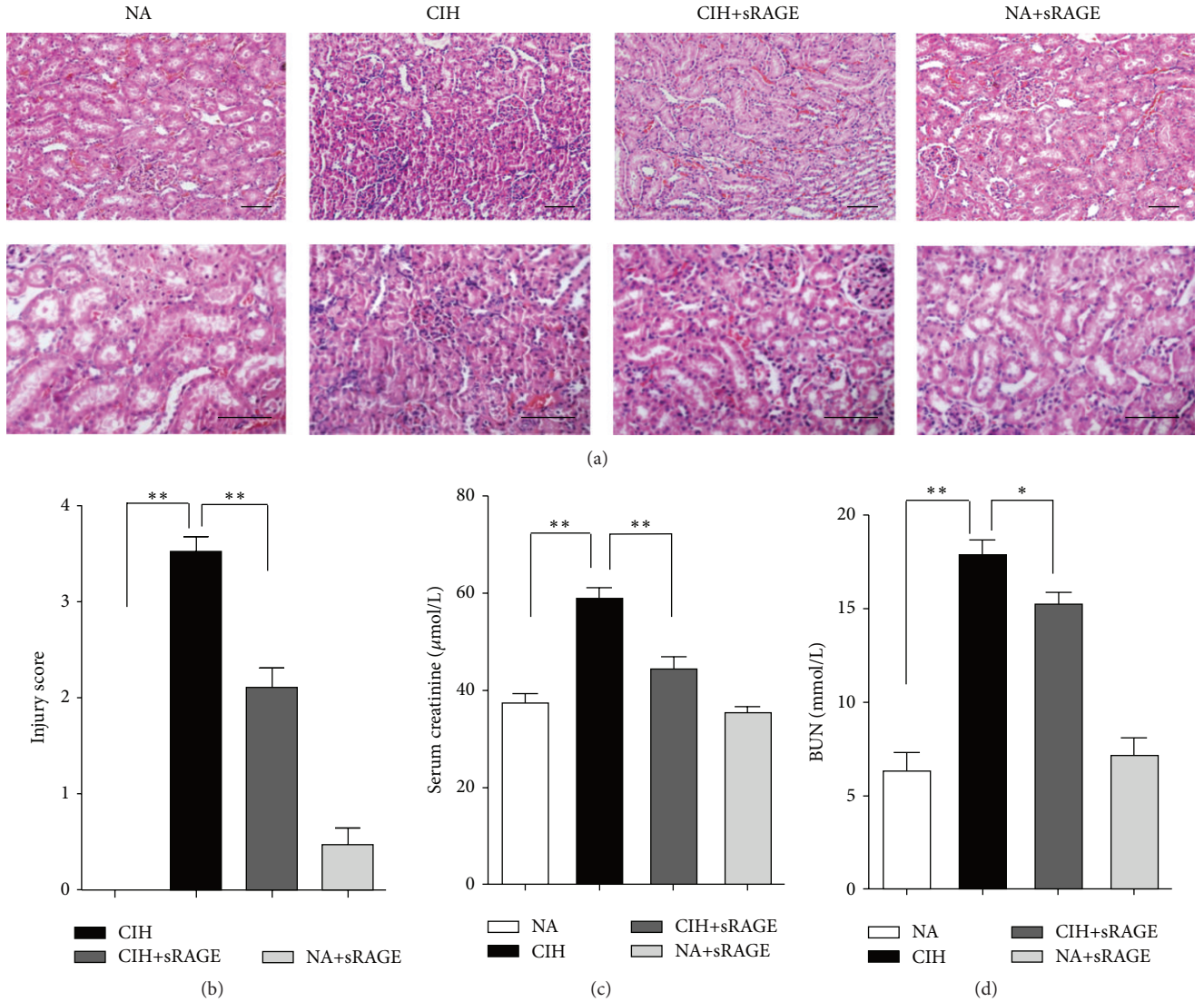

Figure 1: Effect of sRAGE on CIH-induced histological damage and renal dysfunction. (a) Representative kidney sections from normal air (NA) group, CIH group, CIH+sRAGE group, and negative control (NA+sRAGE) group are stained by H&E (scale bar: 50 μm). In light microscopic examination, tubular degeneration, interstitial neutrophil infiltration, and massive desquamation of renal epithelium are more remarkable in the kidney tissues of CIH rats compared to NA group, while pretreatment of sRAGE apparently shows almost normal tubules and mild dilatation of tubular lumen absence of severe inflammatory infiltrations. (b) Sections are graded based on the 0–5 Jablonski grading scale averaging the values from 10 fields per kidney under microscopy. Renal function is determined by serum creatinine (c) and BUN (d). Data are presented as the mean ± SEM. $^{*}P < 0.05$, $^{**}P < 0.01$; $n = 6$/group.

of endothelial cells [26], we performed immunofluorescence staining of CD31 and TUNEL to evaluate the degree of renal tubular endothelial cell apoptosis. DAPI was used to visualize cell nuclei; thus merged immunofluorescent TUNEL/DAPI staining depicted the proportion of apoptosis. In normal kidneys, $CD31^{+}$ cells clearly stained in the wall of renal proximal and distal tubules did not express $TUNEL^{+}$ cells. In contrast, CIH significantly reduced CD31 expression in corticomedullary junction and peritubular capillary endothelium, indicating that chronic hypoxia caused severe endothelial injury (Figure 2(a)). In addition, $TUNEL^{+}$ cells were widely noted at the corticomedullary section in the CIH group. Colocalization of CD31/TUNEL immunofluorescent staining yielded that endothelial cells were undergoing apoptosis and the percentage of apoptotic endothelial cells was greatest following CIH exposure (Figure 2(a)). Upon pretreatment with sRAGE during CIH, only some faint, nonspecific, red background TUNEL staining was observed, whereas endothelial CD31 staining remained relatively apparent. The specific costaining for CD31 and lessened $TUNEL^{+}$ cells in the merged picture suggested sRAGE ameliorated CIH-induced endothelial injury. In line with this, the percentage of apoptosis was significantly reduced 37% by sRAGE compared with the CIH group ($P = 0.002$, Figure 2(b)).

Oxidative stress affects the endothelial cell apoptosis by regulation of the balance between Bax and Bcl-2 proteins [27].

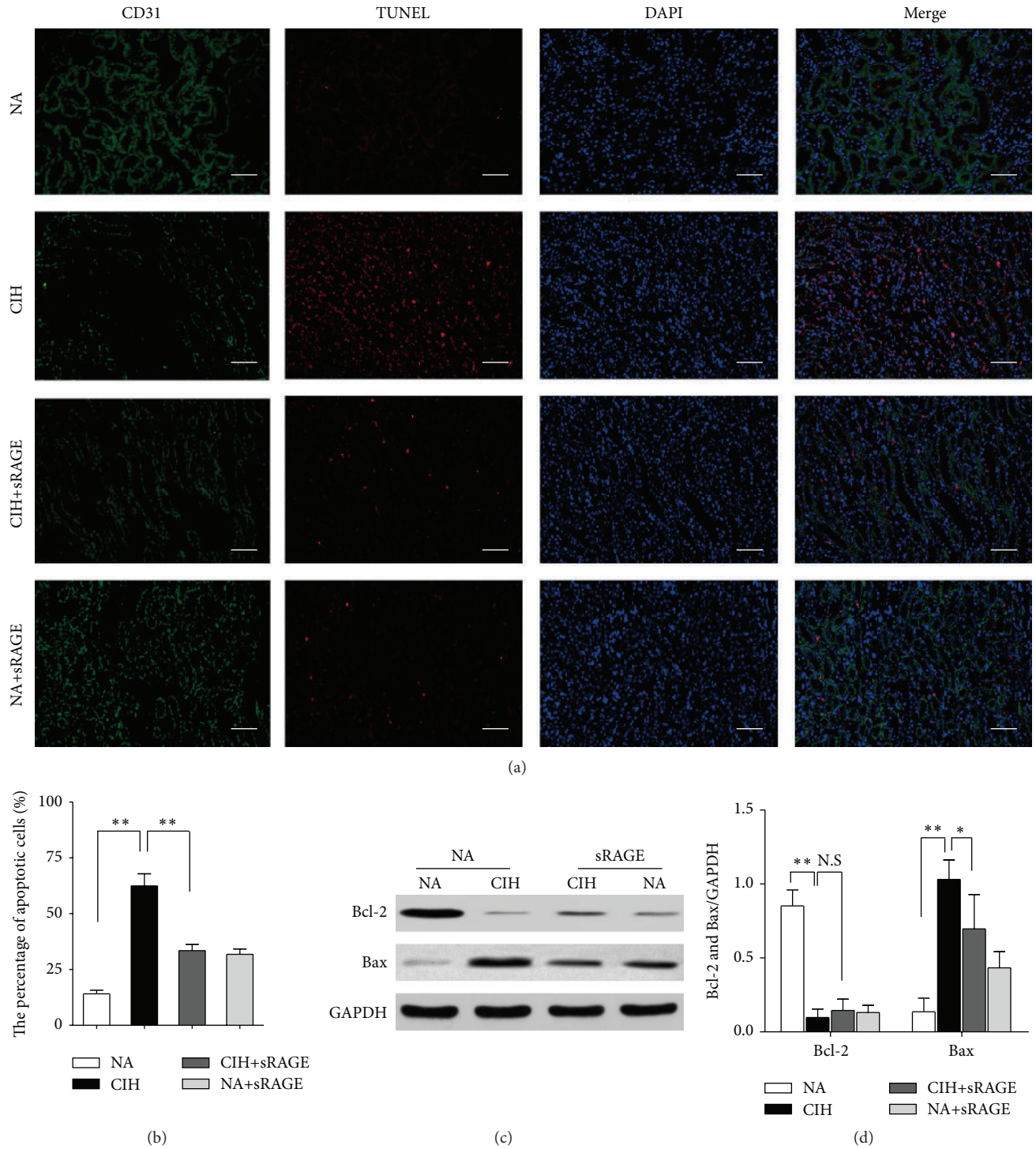

Figure 2: Effect of sRAGE on renal tubular endothelial cell apoptosis. (a) Representative immunofluorescence staining for CD31 (green), TUNEL (red), DAPI (blue), and the merged pictures from kidney tissues of each group. The scale bars represent 50 μm. (b) Quantitative assessment of the percentage of apoptosis by counting the TUNEL$^+$/DAPI$^+$ cells in 10 random fields (100x) for each section. (c) Western blots analysis of Bcl-2 and Bax protein in comparison with GAPDH used as a loading control. (d) Representative bar diagram showing quantitative relative levels of Bcl-2 and Bax in NA, CIH, CIH+sRAGE, and NA plus sRAGE treated groups. Data are presented as the mean ± SEM. NS: no significance. $^*P < 0.05$, $^{**}P < 0.01$; $n = 6$/group.

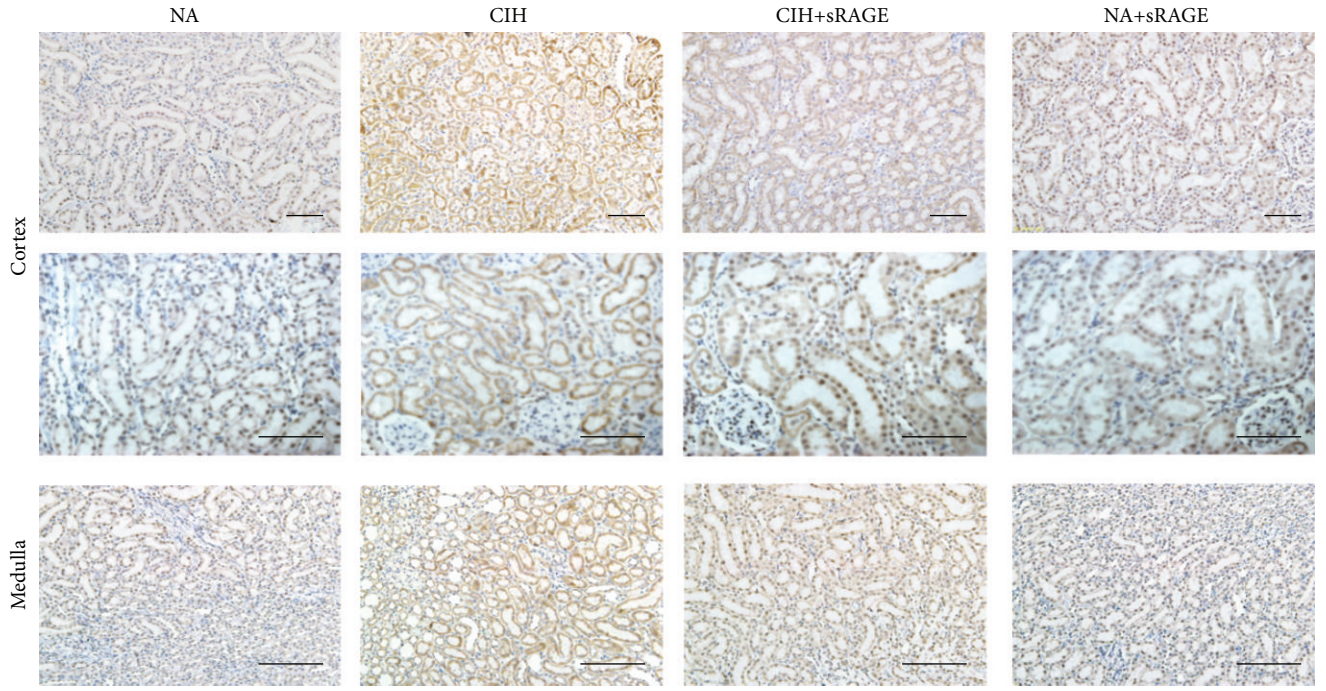

Figure 3: Representative immunohistochemistry of renal cortex (the top panel including glomeruli and proximal tubule) and medulla (the bottom panel including peritubular capillaries and distal tubule) for localization of HMGB1 (scale bar: 50 μm). HMGB1 is abundant in cytoplasmic renal tubules of CIH group, compared with nuclear patterns of HMGB1 in NA group. sRAGE gradually attenuates HMGB1 cytoplasmic deposition, intraluminal infiltration, and nuclear staining in expanded renal tubules.

In contrast to NA group, expression of the proapoptotic protein Bax was upregulated during CIH process, whereas the magnitude of antiapoptotic protein Bcl-2 was significantly decreased as shown in Figure 2(c). Our histological results were further supported by Bcl-2/Bax protein ratio. Bcl-2/Bax ratio decreased from 1.49 ± 1.18 to 0.26 ± 0.43, suggestive of CIH-promoted propensity to apoptosis. But pretreatment of sRAGE exhibited a significant improvement of 125.11% in Bcl-2/Bax protein ratio compared with CIH alone. These data indicated that tubular endothelial cell apoptosis played a critical role in CIH-induced renal injury. Therefore, administration of sRAGE alleviated the renal endothelial cell death through a Bcl-2/Bax-dependent mechanism, thus improving functional recovery.

3.3. Effect of sRAGE on CIH-Induced HMGB1 Expression. During oxidative stress provoked necrotic process, cells invariably lose membrane integrity and eventually lyse, resulting in intracellular contents release such as HMGB1. To ascertain it, immunohistochemistry was performed to determine the location of HMGB1 in each group. Results showed that HMGB1 expression was predominantly detected in cortical areas in contrast to medulla, meaning that proximal tubular cells were likely to be a prominent source of HMGB1. In CIH group, HMGB1 was expressed diffusely in the distended tubular cytoplasms as well as the nuclei of renal tubular epithelial cells, whereas HMGB1 was not or modestly expressed in the nuclei of proximal and distal convoluted tubules in NA group (Figure 3). In addition, the increased extracellular and cytoplasmic HMGB1 in CIH rats was gradually attenuated upon pretreatment of sRAGE, as depicted by lessened but mild expression in proximal and distal convoluted tubule (Figure 3). Negative control group (NA+sRAGE) excluded the possibility of nonspecific staining of sRAGE.

3.4. Effect of sRAGE on RAGE-HMGB1 Downstream Inflammatory Cytokines and Molecules. To distinguish the deleterious contribution of RAGE-HMGB1 in the pathogenesis of CIH-induced kidney injury, western blot technique was used to detect RAGE-HMGB1 and associated inflammatory molecules. Results demonstrated significant differences in RAGE-HMGB1 expression between NA and CIH control (RAGE: 0.466 ± 0.090 versus 2.368 ± 0.931, HMGB1: 0.038 ± 0.026 versus 1.118 ± 0.335, $P < 0.001$, Figure 4). Also, we found that NF-κB was significantly increased in CIH group as compared to normal condition (0.071 ± 0.056 versus 1.056 ± 0.376, $P < 0.001$, Figure 4). In contrast to CIH alone, sRAGE-pretreatment group exhibited a significant suppression on RAGE (1.643 ± 0.581, $P < 0.01$, Figure 4) and also on HMGB1 (0.566 ± 0.341, $P < 0.01$, Figure 4). Besides, sRAGE played a pivotal role in the inhibition of NF-κB activation (0.713 ± 0.628, $P < 0.05$, Figure 4). Conversely, treatment with sRAGE alone did not elicit apparent changes in RAGE-HMGB1 or NF-κB activation. In this regard, engagement of RAGE-HMGB1 may accompany transcription factor NF-κB activation that regulated the induction of multiple proinflammatory cytokines.

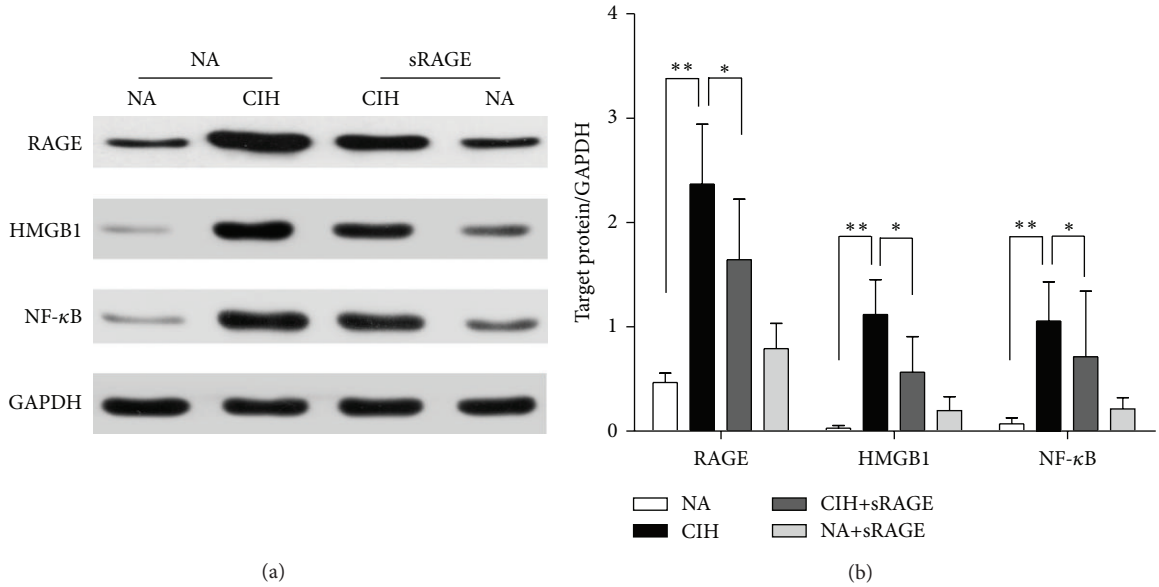

Figure 4: Effect of sRAGE on expressions of RAGE, HMGB1, and NF-κB. (a) Representative western blot images (upper panel) and GAPDH (lower panel) used as the endogenous control are shown in each group. (b) Quantification densitometric analysis summarizes the fold changes of protein levels normalized to GAPDH. Data are expressed as means ± SEM. $^{*}P < 0.05$, $^{**}P < 0.01$; $n = 6$/group.

Following 5 weeks of CIH exposure, serum inflammatory cytokines of IL-6 and TNF-a increased significantly (118.28 ± 18.98 pg/mL and 125.16 ± 13.04 pg/mL resp., $P < 0.0001$; Figures 5(a) and 5(b)) but were lowly detectable in control (24.03±6.77 pg/mL and 38.72±9.36 pg/mL) and CIH+sRAGE group (84.75 ± 11.99 pg/mL and 69.29 ± 10.49 pg/mL). As expected, elevated serum levels of HMGB1 and IL-17 indeed occurred in the CIH rats (32.88 ± 2.69 ng/mL and 119.49 ± 18.77 pg/mL, $P < 0.01$; Figures 5(c) and 5(d)). Importantly, the results obtained from serum corresponded to the expression of RAGE signaling and inflammation response in tissues. Furthermore, as showed in Figures 5(a) and 5(b), the inhibitory effect of sRAGE on amplified inflammatory cytokine productions of IL-6 and TNF-α under CIH condition was obvious. However, it should be noteworthy that sRAGE had an adverse effect on the circulatory HMGB1 in CIH+sRAGE group rats compared with CIH alone (34.58 ± 4.32 ng/mL, $P = 0.43$; Figure 5(c)). Another negative result was observed in subsequent decreased levels of IL-17 in CIH+sRAGE group rats (105.49 ± 30.21 pg/mL, $P = 0.061$; Figure 5(d)). In this in vivo study, we confirmed the potential therapeutic effect of sRAGE on RAGE mediated inflammatory molecular signaling accompanied by reduced cytokines without the presence of circulatory HMGB1 and IL-17.

3.5. Soluble RAGE Modulates P-P38 and P-JNK but Not P-ERK Signaling. Mitogen-activated protein kinases (MAPKs) are well accepted upstream modulators of apoptosis and inflammatory cytokines. They also have crucial roles in signal transduction from the cell surface to the nucleus, which are required for subsequent NF-κB transcriptional activation. As shown in Figure 6(a), the phosphorylated JNK and p38, measured as phospho/total-JNK and phospho/total-p38 level, both reached maximal kinase activities after 5 weeks of CIH exposure (JNK: 1.75 ± 0.81 and p38: 1.11 ± 0.49, $P < 0.01$). Also, CIH tended to enhance the phosphorylation of ERK1/2 approximately twofold over basal levels (0.24 ± 0.16 versus 0.12 ± 0.11, $P = 0.013$, Figure 6(b)). Regarding these, MAPKs family including p38, JNK, and ERK1/2 were investigated to be activated in response to oxidative stress. To address whether sRAGE could modulate MAPK activity, we further used specific antibodies to establish the active forms of the kinases activities. In contrast to CIH alone, the levels of phosphorylated JNK and p38 along with sRAGE treatment were decreased (JNK: 0.87 ± 0.31 and p38: 0.69 ± 0.61, $P < 0.01$; Figures 6(c) and 6(d)), whereas the phosphorylation levels of p-ERK1/2 were not significantly affected (0.25 ± 0.09, $P > 0.05$, Figure 6(b)). sRAGE treatment abrogated t-p38 activation, but no changes in the total levels of ERK1/2 or JNK were detectable.

Accordingly, we identify RAGE ligand as key mediators of MAPK downstream molecules leading to CIH-activated inflammation and apoptosis, while signaling proteins such as p38 and JNK MAP kinases are potentially regulators involved in the renal protection of sRAGE.

4. Discussion

Accumulating evidences indicated that RAGE contributed, at least in part, to the development of OSA complications, such as diabetes and nephropathy, cardiovascular disease, and chronic inflammation [28]. Recent studies provided insight into sRAGE in competing with cell surface RAGE for ligand binding, thus potentially representing a novel molecular target for OSA-associated chronic kidney disease. The present

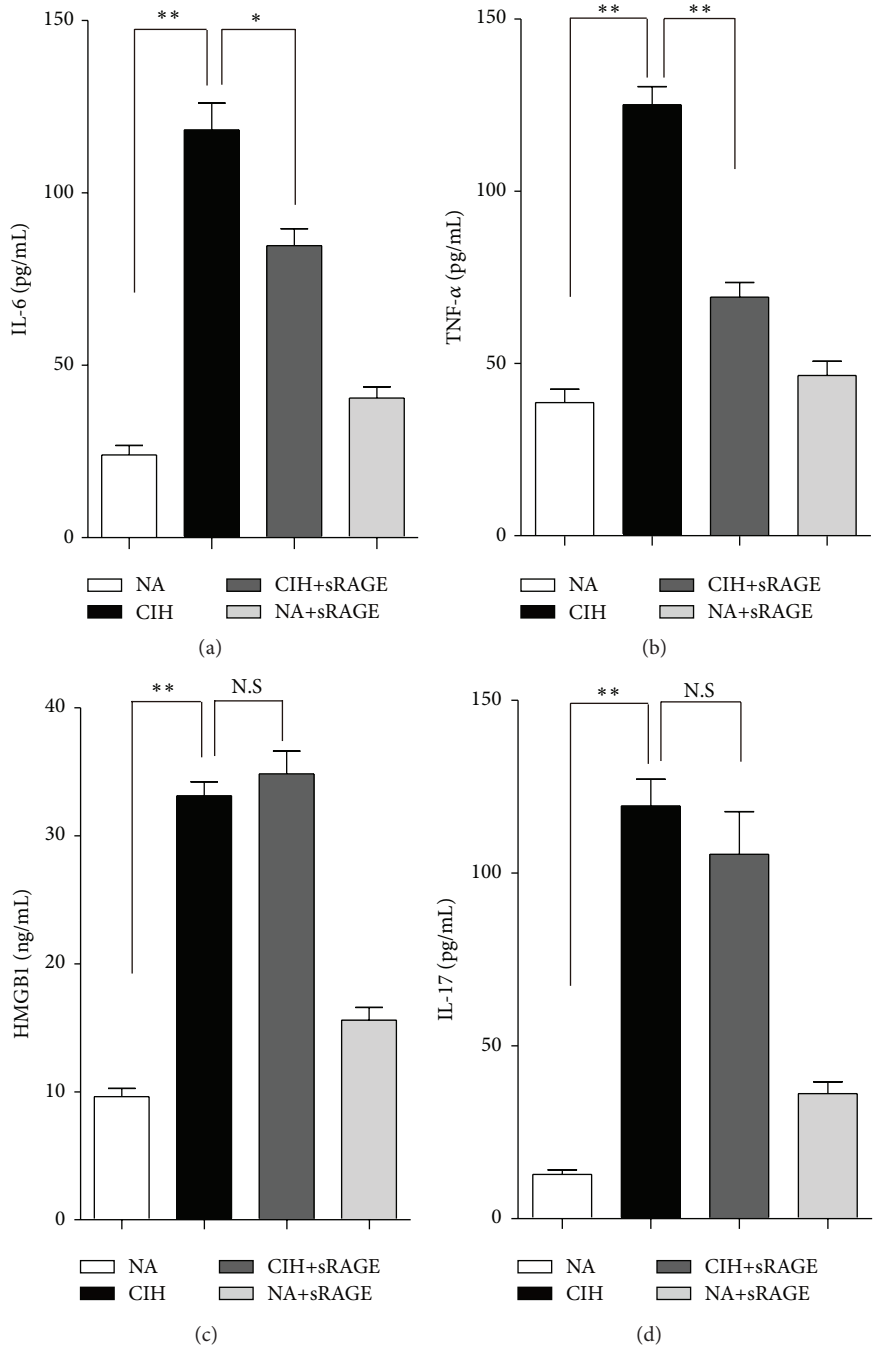

Figure 5: Effect of sRAGE on proinflammatory cytokines IL-6 (a), TNF-a (b), HMGB1 (c), and IL-17 (d) in serum of rats. Data are expressed as means ± SEM. NS: no significance. $^{*}P < 0.05$, $^{**}P < 0.01$; $n = 6$/group.

study shows that RAGE-HMGB1 plays a pivotal role in a CIH model. Furthermore, it is the first evidence that sRAGE demonstrates its anti-inflammatory and antiapoptotic effects by altering p38 and JNK signaling pathways.

Histological examination confirmed that our CIH protocol was sufficient to trigger renal damage. It has been shown that HIF1-α is the main molecular effector of hypoxia signaling and able to combine the HIF-1α binding site present in the RAGE promoter region [29]. Thereby hypoxia may activate RAGE mRNA gene transcription and stimulate RAGE production. Renal interstitial and tubular endothelial cells express specific RAGEs, ongoing generation of which may amplify chronic cellular perturbation and oxidant stress damage by engagement of these receptors on the endothelial surfaces [30]. Our observations in colocalization of CD31/TUNEL immunofluorescent staining revealed that activation of RAGE accelerated tubular endothelial apoptosis. Apart from a possible adaptive response to chronic hypoxia,

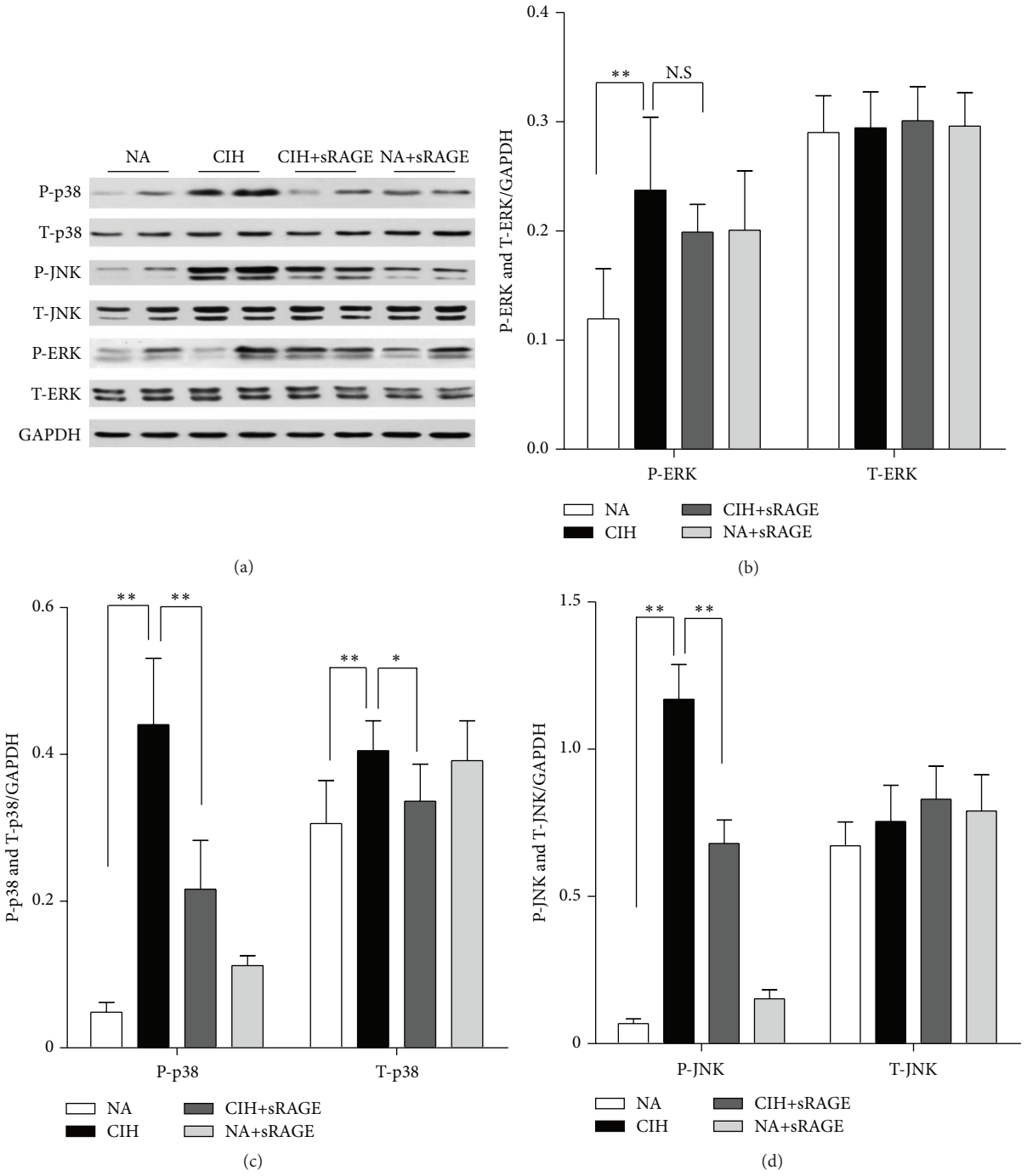

Figure 6: Representative western blot images show the effect of sRAGE on phosphorylated (P) and total (T) ERK, p38, and JNK expression (a). Histograms represent the quantitative densitometric ratio of MAPK signaling molecules ERK (b), p38 (c), and JNK (d) normalized to GAPDH in each group. Data are expressed as means ± SEM. NS: no significance. $^{*}P < 0.05$, $^{**}P < 0.01$; $n = 6$/group.

activation of RAGE observed in our CIH model probably contributed to the CIH-induced injury according to western blot analysis. Of special interest is the finding of extracellular and abundant cytoplasmic accumulations of HMGB1 following CIH. Our results demonstrated that HMGB1 was limited in the nucleus of renal parenchyma cells under normal condition, but dramatically translocated into the cytoplasm and extracellular matrix upon hypoxia insult. For one reason, HMGB1 is passively released in response to inflammatory stress or necrosis [31]. For another, translocation of HMGB1 from the nucleus to cytoplasm requires inflammasome and caspase activity, thus facilitating the chronic inflammation and apoptosis [32, 33]. Furthermore, HMGB1 can behave as a secreted cytokine promoting neutrophil accumulating [34]

and activate macrophages/monocytes to release more proinflammatory cytokines [35, 36]. Consistently, both ELISA and immunohistochemistry results showed that HMGB1 secreted from serum and tissue was collectively elevated and correlated with upregulated TNF-α and IL-6 after CIH. In addition, as a widely acknowledged cytokine for regulating inflammatory reaction and leukocyte migration, IL-17 was reported to be upregulated in RAGE-HMGB1 associated injury [37]. Report from Akirav et al. also indicated the association of RAGE expression and increased IL-17 [38]. Moreover, HMGB1 contributed to lymphocyte infiltration and the release of the Th17 cell specific cytokine IL-17 [39]. In our research, we confirmed previous results, exactly supporting the positive feedback loops of RAGE-HMGB1 activation and proinflammatory mediators.

RAGE-mediated cascades of signal transduction could promote the proinflammatory NF-κB and the MAPK pathway in endothelial cells and monocytes. Importantly, the pathogenic role of RAGE appears to depend on the level of NF-κB transcriptional activity [40]. Inhibition of NF-κB decreased cardiomyocyte apoptosis and recruitment of neutrophils accompanied with HMGB1 suppression [41], indicative of the reciprocal modulation of NF-κB and HMGB1. A range of animal models in vitro and in vivo have demonstrated the involvement of RAGE in pathophysiologic processes, using a receptor decoy such as sRAGE [42]. Phosphorylated levels of p38, JNK, and ERK in present study were higher after CIH exposure and subsequently affected by sRAGE to different extent, implicating RAGE ligand as key mediators in MAPKs signaling. In line with our results, there was evidence in rat renal tubular epithelial cells that indicated the critical importance of HMGB1 in inducing circulating cyto/chemokines secretion through MAP kinase pathways [43]. Similar results were also observed in early reports that RAGE induced NF-κB activation and IL-1 and TNF-α production were dependent on p38 phosphorylation in diabetic glomerular injury [44, 45]. In addition, RAGE ligand interaction may directly induce generation of ERK and reactive oxygen species [46]. Specially, in our studies, these responses of MAPKs to sRAGE lack the participation of p-ERK1/2. Consistent with our results, Taguchi et al. found blockage of RAGE-amphoterin interaction also suppressed p38 and SAP/JNK MAPKs [47]. On the contrary, inhibition of RAGE by siRNA could reduce phosphorylated-ERK in cyst formation [48]. This ambiguity regarding MAPK molecular mechanisms perhaps depends on the cell and RAGE ligand types in vivo and in vitro.

sRAGE can be used as a biomarker in RAGE-dependent inflammations as well as a therapeutic agent to neutralize hypoxia induced inflammation [49]. Moreover, sRAGE can cancel the effects of AGEs on cells in culture [50]. In another hypoxia/reoxygenation model, sRAGE significantly decreased cellular lactic dehydrogenase leakage and increased cell viability in neonatal rat cardiomyocytes [51]. The published data suggest that application of sRAGE is identified to intercept RAGE ligand interaction and subsequent downstream signaling [52]. Since sustained MAPK activation has been associated with oxidative stress and cell apoptosis [53], through histologic and western blot analysis, we reasoned that sRAGE protected against renal inflammation and apoptosis by suppression of p38 and JNK MAPK signaling molecules.

Previous studies revealed the decreased sRAGE levels increased the propensity toward chronic inflammation such as hypertension [54] and coronary artery disease [55]. Serum sRAGE levels were elevated significantly in patients with decreased renal function and inversely related to inflammation [21]. These observations lead us to propose that subsequent production of sRAGE potentially protects against the decreased renal function, but Kalousová et al. found it was not related to mortality of haemodialysis patients [56]. Whether sRAGE represents only an epiphenomenon or a compensatory protective mechanism is still unknown. Although the protective effect of sRAGE is not as effective as the RAGE-deletion [57], the property of long half-life after intraperitoneal injection into normal rats renders the sustained effect in each hypoxia cycle until the end of the observation [58]. Considering RAGE is a multiligand receptor, the accurate blocking target of sRAGE remains to be elucidated. For example, sRAGE is found to interact with Mac-1 in an HMGB1-induced arthritis model [59]. In terms of proinflammatory and proapoptotic effects, HMGB1 is likely to be a main target of sRAGE [60]. Since S100 proteins and HMGB1 certainly do not exclusively bind to RAGE [61], sRAGE did not only result from intercepting the interaction of ligands with cell surface RAGE, but with other possible receptors. That was why that we only observed upregulated circulatory HMGB1 in serum without suddenly degraded levels by sRAGE. It is reasonably speculated that HMGB1 passively released from nucleus to circulation might not be efficiently scavenged. However, in accordance with immunohistochemistry results, western blot analysis of total renal cellular lysates detected the difference of HMGB1 between CIH and exogenous administration of sRAGE groups, suggesting that sRAGE exerted its effect by downregulation of HMGB1. Remarkably, Lee et al. determined that sRAGE exhibited no toxic effects on the liver by testing the activity of ALT [10], providing additional support for this potential therapeutic strategy.

A limitation of this study was the lack of verification that whether the decreased RAGE expression induced by sRAGE treatment was abrogated with exogenous HMBG1 administration. We did not observe such endogenous sRAGE level in renal insufficiency following the chronic hypoxia. To confirm its exact blockage target of RAGE ligand interaction, the capacity of sRAGE in inflammatory responses from diverse models remains to be elucidated.

5. Conclusions

Taken together, RAGE and its ligand HMGB1 activate chronic inflammatory transduction cascades that contribute to the pathogenesis of CIH-induced renal injury. The consequences of amplifying inflammatory response include the recruitment of inflammatory cytokines and effector molecules (sustained expression of NF-κB, TNF-α, IL-6, and MAPK signaling), leading to apoptosis and accelerated renal dysfunction. Interruption of RAGE interaction by administration of

sRAGE has been shown to attenuate these detrimental effects. According to a decoy mechanism, blockade of RAGE ligand interaction could provide a new therapeutic approach in the development and progression of OSA-associated chronic kidney disease.

Competing Interests

None of the authors have conflict of interests to declare.

Authors' Contributions

Wenyu Gu and Shanqun Li conceived and designed the experiments. Jian Zhou, Chengying Liu, Huan Lu, Yaodong Tang, and Chuan Shao performed the experiments. Biyun Yu and Hui Xu analyzed the data. Xu Wu has contributed to manuscript preparation. Xu Wu and Wenyu Gu contributed equally to this work and share the first authorship.

Acknowledgments

The authors thank Wenjing Li and Hong Jiang for their assistance with the model of CIH. This study was funded by Ningbo Natural Science Foundation of China (no. 2013A610236), Shanghai Committee of Science and Technology (no. 13420720500 and no. 15411961500), and National Natural Science Foundation of China (no. 81472175, no. 81400043, no. 81400018, no. 81570081, and no. 81500058).

References

[1] D. D. M. Nicholl, S. B. Ahmed, A. H. S. Loewen et al., "Clinical presentation of obstructive sleep apnea in patients with chronic kidney disease," *Journal of Clinical Sleep Medicine*, vol. 8, no. 4, pp. 381–387, 2012.

[2] P. L. Kimmel, G. Miller, and W. B. Mendelson, "Sleep apnea syndrome in chronic renal disease," *The American Journal of Medicine*, vol. 86, pp. 308–314, 1989.

[3] J. J. Sim, S. A. Rasgon, D. A. Kujubu et al., "Sleep apnea in early and advanced chronic kidney disease: Kaiser Permanente Southern California cohor," *Chest*, vol. 135, no. 3, pp. 710–716, 2009.

[4] P. J. Hanly and S. B. Ahmed, "Sleep apnea and the kidney: is sleep apnea a risk factor for chronic kidney disease?" *Chest*, vol. 146, no. 4, pp. 1114–1122, 2014.

[5] J. M. Beecroft, A. Pierratos, and P. J. Hanly, "Clinical presentation of obstructive sleep apnea in patients with end-stage renal disease," *Journal of Clinical Sleep Medicine*, vol. 5, no. 2, pp. 115–121, 2009.

[6] A. A. Chiang, "Obstructive sleep apnea and chronic intermittent hypoxia: a review," *Chinese Journal of Physiology*, vol. 49, no. 5, pp. 234–243, 2006.

[7] D. Stern, S. D. Yan, S. F. Yan, and A. M. Schmidt, "Receptor for advanced glycation endproducts: a multiligand receptor magnifying cell stress in diverse pathologic settings," *Advanced Drug Delivery Reviews*, vol. 54, no. 12, pp. 1615–1625, 2002.

[8] K.-M. Wu, C.-C. Lin, C.-H. Chiu, and S.-F. Liaw, "Effect of treatment by nasal continuous positive airway pressure on serum high mobility group box-1 protein in obstructive sleep apnea," *Chest*, vol. 137, no. 2, pp. 303–309, 2010.

[9] S. Duru, I. Hikmet Firat, N. Colak, Z. Giniş, T. Delibaşi, and S. Ardiç, "Serum S100B protein: a useful marker in obstructive sleep apnea syndrome," *Neurologia i Neurochirurgia Polska*, vol. 46, no. 5, pp. 450–455, 2012.

[10] E. J. Lee, E. Y. Park, H. Mun et al., "Soluble receptor for advanced glycation end products inhibits disease progression in autosomal dominant polycystic kidney disease by down-regulating cell proliferation," *The FASEB Journal*, vol. 29, no. 8, pp. 3506–3514, 2015.

[11] V. D'Agati and A. M. Schmidt, "RAGE and the pathogenesis of chronic kidney disease," *Nature Reviews Nephrology*, vol. 6, no. 6, pp. 352–360, 2010.

[12] Y.-S. Bao, S.-P. Na, P. Zhang et al., "Characterization of interleukin-33 and soluble ST2 in serum and their association with disease severity in patients with chronic kidney disease," *Journal of Clinical Immunology*, vol. 32, no. 3, pp. 587–594, 2012.

[13] P. Zhu, L. Xie, H.-S. Ding, Q. Gong, J. Yang, and L. Yang, "High mobility group box 1 and kidney diseases (Review)," *International Journal of Molecular Medicine*, vol. 31, no. 4, pp. 763–768, 2013.

[14] A. M. Schmidt, S. D. Yan, S. F. Yan, and D. M. Stern, "The multiligand receptor RAGE as a progression factor amplifying immune and inflammatory responses," *The Journal of Clinical Investigation*, vol. 108, no. 7, pp. 949–955, 2001.

[15] A. Bruchfeld, A. R. Qureshi, B. Lindholm et al., "High mobility group box protein-1 correlates with renal function in chronic kidney disease (CKD)," *Molecular Medicine*, vol. 14, no. 3-4, pp. 109–115, 2008.

[16] T.-B. Zhou, "Role of high mobility group box 1 and its signaling pathways in renal diseases," *Journal of Receptors and Signal Transduction*, vol. 34, no. 5, pp. 348–350, 2014.

[17] D. Leonardis, G. Basta, F. Mallamaci et al., "Circulating soluble receptor for advanced glycation end product (sRAGE) and left ventricular hypertrophy in patients with chronic kidney disease (CKD)," *Nutrition, Metabolism and Cardiovascular Diseases*, vol. 22, no. 9, pp. 748–755, 2012.

[18] E. Y. Park, B. H. Kim, E. J. Lee et al., "Targeting of receptor for advanced glycation end products suppresses cyst growth in polycystic kidney disease," *The Journal of Biological Chemistry*, vol. 289, no. 13, pp. 9254–9262, 2014.

[19] J. Li, Q. Gong, S. Zhong et al., "Neutralization of the extracellular HMGB1 released by ischaemic damaged renal cells protects against renal ischaemia-reperfusion injury," *Nephrology Dialysis Transplantation*, vol. 26, no. 2, pp. 469–478, 2011.

[20] N. Vazzana, F. Santilli, C. Cuccurullo, and G. Davì, "Soluble forms of RAGE in internal medicine," *Internal and Emergency Medicine*, vol. 4, no. 5, pp. 389–401, 2009.

[21] M. Kalousová, M. Hodková, M. Kazderová et al., "Soluble receptor for advanced glycation end products in patients with decreased renal function," *American Journal of Kidney Diseases*, vol. 47, no. 3, pp. 406–411, 2006.

[22] M. F. Angelo, A. Aguirre, R. X. A. Reyes et al., "The proinflammatory RAGE/NF-κB pathway is involved in neuronal damage and reactive gliosis in a model of sleep apnea by intermittent hypoxia," *PLoS ONE*, vol. 9, no. 9, Article ID e107901, 2014.

[23] C. Fu, L. Jiang, F. Zhu et al., "Chronic intermittent hypoxia leads to insulin resistance and impaired glucose tolerance through dysregulation of adipokines in non-obese rats," *Sleep and Breathing*, vol. 19, no. 4, pp. 1467–1473, 2015.

[24] D. G. S. Farmer, M.-A. Ewart, K. M. Mair, and S. Kennedy, "Soluble receptor for advanced glycation end products (sRAGE)

attenuates haemodynamic changes to chronic hypoxia in the mouse," *Pulmonary Pharmacology and Therapeutics*, vol. 29, no. 1, pp. 7–14, 2014.

[25] C. F. Islam, R. T. Mathie, M. D. Dinneen, E. A. Kiely, A. M. Peters, and P. A. Grace, "Ischaemia-reperfusion injury in the rat kidney: the effect of preconditioning," *British Journal of Urology*, vol. 79, no. 6, pp. 842–847, 1997.

[26] A. Nakao, J. S. Neto, S. Kanno et al., "Protection against ischemia/reperfusion injury in cardiac and renal transplantation with carbon monoxide, biliverdin and both," *American Journal of Transplantation*, vol. 5, no. 2, pp. 282–291, 2005.

[27] E. Z. Bagci, Y. Vodovotz, T. R. Billiar, G. B. Ermentrout, and I. Bahar, "Bistability in apoptosis: roles of Bax, Bcl-2, and mitochondrial permeability transition pores," *Biophysical Journal*, vol. 90, no. 5, pp. 1546–1559, 2006.

[28] A. Bierhaus, P. M. Humpert, M. Morcos et al., "Understanding RAGE, the receptor for advanced glycation end products," *Journal of Molecular Medicine*, vol. 83, no. 11, pp. 876–886, 2005.

[29] P. Pichiule, J. C. Chavez, A. M. Schmidt, and S. J. Vannucci, "Hypoxia-inducible factor-1 mediates neuronal expression of the receptor for advanced glycation end products following hypoxia/ischemia," *The Journal of Biological Chemistry*, vol. 282, no. 50, pp. 36330–36340, 2007.

[30] G. Basta, G. Lazzerini, M. Massaro et al., "Advanced glycation end products activate endothelium through signal-transduction receptor RAGE: a mechanism for amplification of inflammatory responses," *Circulation*, vol. 105, no. 7, pp. 816–822, 2002.

[31] G. Faraco, S. Fossati, M. E. Bianchi et al., "High mobility group box 1 protein is released by neural cells upon different stresses and worsens ischemic neurodegeneration *in vitro* and *in vivo*," *Journal of Neurochemistry*, vol. 103, no. 2, pp. 590–603, 2007.

[32] G.-Y. Gwak, T. G. Moon, D. H. Lee, and B. C. Yoo, "Glycyrrhizin attenuates HMGB1-induced hepatocyte apoptosis by inhibiting the p38-dependent mitochondrial pathway," *World Journal of Gastroenterology*, vol. 18, no. 7, pp. 679–684, 2012.

[33] J.-B. Kim, S. C. Joon, Y.-M. Yu et al., "HMGB1, a novel cytokine-like mediator linking acute neuronal death and delayed neuroinflammation in the postischemic brain," *The Journal of Neuroscience*, vol. 26, no. 24, pp. 6413–6421, 2006.

[34] Y. Oyama, T. Hashiguchi, N. Taniguchi et al., "High-mobility group box-1 protein promotes granulomatous nephritis in adenine-induced nephropathy," *Laboratory Investigation*, vol. 90, no. 6, pp. 853–866, 2010.

[35] U. Andersson, H. Wang, K. Palmblad et al., "High mobility group 1 protein (HMG-1) stimulates proinflammatory cytokine synthesis in human monocytes," *The Journal of Experimental Medicine*, vol. 192, no. 4, pp. 565–570, 2000.

[36] A. Lau, S. Wang, W. Liu, A. Haig, Z.-X. Zhang, and A. M. Jevnikar, "Glycyrrhizic acid ameliorates HMGB1-mediated cell death and inflammation after renal ischemia reperfusion injury," *American Journal of Nephrology*, vol. 40, no. 1, pp. 84–95, 2014.

[37] J. Y. Jhun, S. H. Lee, H. Y. Kim et al., "HMGB1/RAGE induces IL-17 expression to exaggerate inflammation in peripheral blood cells of hepatitis B patients," *Journal of Translational Medicine*, 2015.

[38] E. M. Akirav, P. Preston-Hurlburt, J. Garyu et al., "RAGE expression in human T cells: a link between environmental factors and adaptive immune responses," *PLoS ONE*, vol. 7, no. 4, Article ID e34698, 2012.

[39] C.-C. Lee, Y.-T. Lai, H.-T. Chang et al., "Inhibition of high-mobility group box 1 in lung reduced airway inflammation and remodeling in a mouse model of chronic asthma," *Biochemical Pharmacology*, vol. 86, no. 7, pp. 940–949, 2013.

[40] A. Villarreal, R. X. Aviles Reyes, M. F. Angelo, A. G. Reinesf, and A. J. Ramos, "S100B alters neuronal survival and dendrite extension via RAGE-mediated NF-κB signaling," *Journal of Neurochemistry*, vol. 117, no. 2, pp. 321–332, 2011.

[41] Z. Shi, A. Lian, and F. Zhang, "Nuclear factor-κB activation inhibitor attenuates ischemia reperfusion injury and inhibits Hmgb1 expression," *Inflammation Research*, vol. 63, no. 11, pp. 919–925, 2014.

[42] T. M. Wendt, N. Tanji, J. Guo et al., "RAGE drives the development of glomerulosclerosis and implicates podocyte activation in the pathogenesis of diabetic nephropathy," *American Journal of Pathology*, vol. 162, no. 4, pp. 1123–1137, 2003.

[43] A. Simm, G. Münch, F. Seif et al., "Advanced glycation end-products stimulate the MAP-kinase pathway in tubulus cell line LLC-PK1," *FEBS Letters*, vol. 410, no. 2-3, pp. 481–484, 1997.

[44] L. Adhikary, F. Chow, D. J. Nikolic-Paterson et al., "Abnormal p38 mitogen-activated protein kinase signalling in human and experimental diabetic nephropathy," *Diabetologia*, vol. 47, no. 7, pp. 1210–1222, 2004.

[45] C.-H. Wu, C.-M. Huang, C.-H. Lin, Y.-S. Ho, C.-M. Chen, and H.-M. Lee, "Advanced glycosylation end products induce NF-κB dependent iNOS expression in RAW 264.7 cells," *Molecular and Cellular Endocrinology*, vol. 194, no. 1-2, pp. 9–17, 2002.

[46] H. M. Lander, J. M. Tauras, J. S. Ogiste, O. Hori, R. A. Moss, and A. M. Schmidt, "Activation of the receptor for advanced glycation end products triggers a p21(ras)-dependent mitogen-activated protein kinase pathway regulated by oxidant stress," *The Journal of Biological Chemistry*, vol. 272, no. 28, pp. 17810–17814, 1997.

[47] A. Taguchi, D. C. Blood, G. del Toro et al., "Blockade of RAGE-amphoterin signalling suppresses tumour growth and metastases," *Nature*, vol. 405, no. 6784, pp. 354–360, 2000.

[48] E. Y. Park, M. J. Seo, and J. H. Park, "Effects of specific genes activating RAGE on polycystic kidney disease," *American Journal of Nephrology*, vol. 32, no. 2, pp. 169–178, 2010.

[49] R. G. Iannitti, A. Casagrande, A. De Luca et al., "Hypoxia promotes danger-mediated inflammation via receptor for advanced glycation end products in cystic fibrosis," *American Journal of Respiratory and Critical Care Medicine*, vol. 188, no. 11, pp. 1338–1350, 2013.

[50] M. A. H. Bowman and A. M. Schmidt, "The next generation of RAGE modulators: implications for soluble RAGE therapies in vascular inflammation," *Journal of Molecular Medicine*, vol. 91, no. 12, pp. 1329–1331, 2013.

[51] C. Guo, X. Zeng, J. Song et al., "A soluble receptor for advanced glycation end-products inhibits hypoxia/reoxygenation-induced apoptosis in rat cardiomyocytes via the mitochondrial pathway," *International Journal of Molecular Sciences*, vol. 13, no. 9, pp. 11923–11940, 2012.

[52] A. Raucci, S. Cugusi, A. Antonelli et al., "A soluble form of the receptor for advanced glycation endproducts (RAGE) is produced by proteolytic cleavage of the membrane-bound form by the sheddase a disintegrin and metalloprotease 10 (ADAM10)," *The FASEB Journal*, vol. 22, no. 10, pp. 3716–3727, 2008.

[53] G. Gong, L. Xiang, L. Yuan et al., "Protective effect of glycyrrhizin, a direct HMGB1 inhibitor, on focal cerebral

ischemia/reperfusion-induced inflammation, oxidative stress, and apoptosis in rats," *PLoS ONE*, vol. 9, no. 3, Article ID e89450, 2014.

[54] D. Geroldi, C. Falcone, E. Emanuele et al., "Decreased plasma levels of soluble receptor for advanced glycation end-products in patients with essential hypertension," *Journal of Hypertension*, vol. 23, no. 9, pp. 1725–1729, 2005.

[55] K.-H. Chiang, P.-H. Huang, S.-S. Huang, T.-C. Wu, J.-W. Chen, and S.-J. Lin, "Plasma levels of soluble receptor for advanced glycation end products are associated with endothelial function and predict cardiovascular events in nondiabetic patients," *Coronary Artery Disease*, vol. 20, no. 4, pp. 267–273, 2009.

[56] M. Kalousová, M. Jáchymová, M. Oto et al., "Receptor for advanced glycation end products—soluble form and gene polymorphisms in chronic haemodialysis patients," *Nephrology Dialysis Transplantation*, vol. 22, no. 7, pp. 2020–2026, 2007.

[57] B. Liliensiek, M. A. Weigand, A. Bierhaus et al., "Receptor for advanced glycation end products (RAGE) regulates sepsis but not the adaptive immune response," *The Journal of Clinical Investigation*, vol. 113, no. 11, pp. 1641–1650, 2004.

[58] C. Renard, O. Chappey, M.-P. Wautier et al., "Recombinant advanced glycation end product receptor pharmacokinetics in normal and diabetic rats," *Molecular Pharmacology*, vol. 52, no. 1, pp. 54–62, 1997.

[59] G. Daffu, C. H. del Pozo, K. M. O'Shea, R. Ananthakrishnan, R. Ramasamy, and A. M. Schmidt, "Radical roles for RAGE in the pathogenesis of oxidative stress in cardiovascular diseases and beyond," *International Journal of Molecular Sciences*, vol. 14, no. 10, pp. 19891–19910, 2013.

[60] W. Jiang, C. W. Bell, and D. S. Pisetsky, "The relationship between apoptosis and high-mobility group protein 1 release from murine macrophages stimulated with lipopolysaccharide or polyinosinic-polycytidylic acid," *The Journal of Immunology*, vol. 178, no. 10, pp. 6495–6503, 2007.

[61] M. J. Robinson, P. Tessier, R. Poulsom, and N. Hogg, "The S100 family heterodimer, MRP-8/14, binds with high affinity to heparin and heparan sulfate glycosaminoglycans on endothelial cells," *The Journal of Biological Chemistry*, vol. 277, no. 5, pp. 3658–3665, 2002.